Bluetongue Virus Non-Structural Protein 1;

Virus – Host Interactions

Rebecca Ward BSc (Hons)

A Thesis Submitted for the Degree of Doctor of Philosophy

(Faculty of Microbiology) of the University of London

Pathogen Molecular Biology Unit

Department of Infectious and Tropical Diseases

London School of Hygiene and Tropical Medicine

University of London

United Kingdom

January 2006

Abstract

Bluetongue virus (BTV) is an orbivirus of the *Reoviridae* family that infects sheep and other ruminants. BTV has three non-structural proteins, NS1, NS2 and NS3/3A. NS1 forms tubular structures and its function is currently unknown. To investigate the role of NS1 in BTV infection, the interactions of NS1 with mammalian and insect cellular proteins, and BTV viral proteins, were examined. BTV NS1 was identified as interacting with aldolase A, NUBP1, Pyruvate kinase M2, cathespin B, SUMO-1 and peptide TY7 using the yeast two-hybrid system, ELISA and immunofluorescence analysis. TY7 and NS1 caused extensive cell death within 24h of co-expression; this cell death was not apoptosis and reduced BTV yield by 37%. The interaction of NS1 with SUMO-1 and its importance in BTV infection was confirmed using siRNA to knockdown SUMO-1 during BTV-10 infection. Knockdown of SUMO-1 elicited a dramatic reduction in virus yield by 73%. NS1 interactions with proteins of the insect vector *Culicoides* were also examined. A putative interaction between NS1 and the ubiquitin activating enzyme E1 (UBA E1) of *Culicoides* was identified during screening of a phage library, this has not been confirmed by other means. NS1 interactions with other BTV proteins were analysed using immunoprecipitation and a strong interaction between NS1 and VP7 was identified; this was confirmed using the yeast two-hybrid system and immunoflourescence. Two main roles have been hypothesised for NS1 from this data; firstly it is likely that NS1 interaction with SUMO-1 and UBA E1 allows the targeting of specific proteins for sumoylation and ubiquitination allowing NS1 to modify the host response to BTV infection. Secondly it is possible that NS1 serves as an anchor for VP7 and virus cores allowing the build up of cores at the cytoskeleton in close proximity to VP2 for subsequent assembly and release. RNAi against NS1 eliminated tubule formation but did not affect virus yield or VP7 and SUMO-1 distribution and expression. It is therefore likely that the function of NS1 does not rely on tubule formation and that tubules are a form of storage for the active monomer of NS1.

Acknowledgments

I would especially like to thank my supervisor, Prof. Polly Roy for her guidance, patience and support throughout my four years at the London School. I am extremely grateful for the supervision and encouragement I have received, in addition to the novel perspective on life and research she has shared with me.

A big thank you to Dr. Rob Noad, the main driving force behind my project, for his endless knowledge, advice, help and encouragement. Without Rob's sarcastic influence this project would have been less enjoyable and incomplete!

I would also like to thank all of the members of the Roy lab, past and present, in particular Dr. Jo Wehfritz and Dr. Mark Boyce, not only for their help and advice with my work but also for making my time here fun, happy hour will not be the same without you all!

Finally a huge thanks to my family, friends and in particular Paul, without you this would have been much harder. Thank you for helping me to achieve my aspirations.

Abbreviations

293T cells	Human embryonic kidney cells
aa	Amino acid(s)
AcMNPV	*Autographa californica* nucleopolyhedrovirus
ASFV	African swine fever virus
BTV	Bluetongue Virus
BSA	Bovine serum albumin
BSR	Strain of Baby hamster kidney cells.
CBB	Calmodulin binding buffer
CEB	Calmodulin elution buffer
CLP	Core-like particles
CMV	Cytomegalovirus
CPE	Cytopathic effect
C6/36	*Aedes albopictus* cell line
DEN-2	Dengue virus serotype 2 (Flavivirus)
DNA	Deoxyribonucleic acid
DNA-AD	DNA activation domain of GAL4
DNA-BD	DNA binding domain of GAL4
dNTP	Deoxynucleoside triphosphate
dsRNA	Double-stranded RNA
EDTA	Ethylenediamine-tetra-acetic acid
EM	Electron microscope/y

FCS	Foetal calf serum
FITC	Fluorescein isothiocyante isomer 1
FMDV	Foot and mouth disease virus (Apthovirus)
HeLa cells	Human cervical carcinoma cells
HSV-1	Herpes simplex virus 1 (Herpesvirus)
IBDV	Infectious bursal disease virus (Avibirnavirus)
IPTG	Isopropyl β–D-thiogalactopyranoside
JUNV	Junin virus (*Arenaviridae*)
Kc cells	*Culicoides* cell line
KSHV	Karposis sarcoma herpesvirus
LiOAc	Lithium acetate
LLc-MK2 cells	Rhesus monkey kidney cells
LMP agarose	Low melting point agarose
MOI	Multiplicity of infection
mRNA	Messenger RNA
NaOAc	Sodium acetate
NLS	N-Lauryl sarcosine
NP-40	Nonidet P-40
NS1	Non-structural protein 1
OD	Optical density
ORF	Open reading frame
PAGE	Polyacrylamide gel electrophoresis
PBS	Phosphate buffered saline
PCR	Polymerase chain reaction
PEG	Polyethylene glycol

PFU	Plaque forming unit
p.i.	Post infection
PIC	Protease inhibitor cocktail
PtK2 cells	Rat kangaroo kidney epithelium cells
PVX	Potato virus X (Alphavirus)
RDV	Rice dwarf virus (Phytoreovirus)
RNA	Ribonucleic acid
RNase	Ribonuclease
RPM	Revolutions per minute
SBB	Streptavidin binding buffer
SDW	Sterile Distilled Water
SDS	Sodium dodecyl sulphate
SEB	Streptavidin elution buffer
Sf 9/21 cells	*Spodoptera frugiperda* cell lines
siRNA	Small interfering RNA
ssRNA	Single-stranded RNA
SVP cells	Super vero porcine cells
TAP	Tandem affinity purification
TBE	Tick-borne encephalitis virus (Flavivirus)
TRITC	Tetramethylrhodamine
TSWV	Tomato spotted wilt virus (Tospovirus)
VEEV	Venezuelan equine encephalitis virus (Alphavirus)
Vero cells	African green monkey kidney cells
VIB	Virus inclusion body

VLP	Virus-like particle
X-gal	5-bromo-4-chloro-3-indolyl-β-D-galactopyranoside

Table of Contents

Table of Figures

Table of Tables

1: Introduction

1.1: The Reoviridae

The members of the *Reoviridae* family infect an extremely diverse host range including humans, birds, reptiles, fish, insects and plants. There are several notable human viruses within the *Reoviridae* including rotavirus and Colorado tick fever virus. Common characteristics of the *Reoviridae* are a genome of 9 to12 dsRNA segments that usually encode only one major protein per segment (Attoui, Mohd Jaafar *et al.* 2005). Despite the phylogenetic relationship displayed by the genera within the *Reoviridae* little genomic sequence homology exists.

There are currently 12 genera within the *Reoviridae* (Table 1.1), plus 1 proposed genus, that are composed of 75 different virus species; a further 30 virus species are as yet unassigned (Brussaard, Noordeloos *et al.* 2004; Attoui, Mohd Jaafar *et al.* 2005; Fauquet 2005). Many of the plant viruses within this family and mammalian viruses from the Orbivirus, Coltivirus and Seadornavirus genera are transmitted between hosts by arthropod vectors. Viruses from the other genera within the *Reoviridae* are thought to be transmitted horizontally and/or vertically between host organisms (Attoui, Mohd Jaafar *et al.* 2005).

Genus	Number of genome segments	Host range	Example Viruses
Rotavirus	11	Humans & other mammals	Rotavirus A, B & C
Orbivirus	10	Mammals Vector: *Culicoides*, mosquitoes & phlebotomines	Bluetongue virus, African horse sickness virus
Seadornavirus	12	Humans. Vector: Mosquitoes	Banna virus, Kadipiro virus
Coltivirus	12	Humans, cattle & pigs Vector: Mosquitoes & ticks	Colorado tick fever virus, Eyach virus
Phytoreovirus	12	Plants Vector: *Cicadellidae* Leafhoppers	Rice dwarf virus
Oryzavirus	10	Plants Vector: *Fulgoridae* Planthoppers	Rice ragged stunt virus
Fijivirus	10	Plants Vector: Delphacid planthoppers	Nilaparvata lugens virus
Idnoreovirus	10	Insects	Idnoreovirus 2
Cypovirus	10	Insects	Bombyx mori cytoplasmic polyhedrosis virus 1
Aquareovirus	11	Fish & molluscs	Golden shiner reovirus, Grass carp reovirus
Orthoreovirus	10	Mammals & birds	Mammalian orthoreovirus
Mycoreovirus	11 or 12	Fungi	Rosellina anti-rot virus, Cryphonectria parasitica reovirus
Proposed genus: Dinovernavirus	9	Mosquitoes	

Table 1. 1: Genera within the *Reoviridae* family.

In addition to the genomic similarities of the viruses within the *Reoviridae* a number of other structural traits exist. The virions are non-enveloped with concentric protein layers that display icosahedral symmetry and enclose the genome. There are two main types of core structure within this family, those with turreted cores and those with cores lacking

turrets. The turreted core viruses have 12 icosahedrally arranged turrets on the surface of the core and include viruses within the Orthoreovirus and Cypovirus genera (Baker, Olson *et al.* 1999; Hill, Booth *et al.* 1999; Attoui, Mohd Jaafar *et al.* 2005). The non-turreted viruses have no turrets at the 5-fold axis of the icosahedral core giving a smoother, although sometimes bristly, appearance to the core particles and include viruses within the Rotavirus and Orbivirus genera (Grimes, Burroughs *et al.* 1998; Baker, Olson *et al.* 1999; Attoui, Mohd Jaafar *et al.* 2005).

1.2: Orbiviruses

The Orbiviruses are one of the twelve genera within the *Reoviridae* and are non-turreted, arthropod transmitted arboviruses. Orbiviruses are transmitted between their vertebrate hosts by hematophagous arthropods; these include ticks, mosquitoes and *Culicoides* species midges, the precise arthropod varies between the viruses. There are 20 species within the orbivirus genus (Table 1.2) and within many of these are several serotypes (http://www.iah.bbsrc.ac.uk/dsRNA_virus_proteins/ReoID/orbiviruses.htmn November 2005). The host ranges are diverse and include rodents, cattle, kangaroos, birds, primates and humans. The Bluetongue virus group consists of 24 different serotypes all displaying differential prevalence in different areas of the world. Bluetongue Virus (BTV) is the prototypic orbivirus and has been extensively studied, both at the molecular level and epidemiologically.

Virus	Unassigned Viruses
Bluetongue virus	Andasibe virus
African horse sickness virus	Tracambe virus
Palyam virus	Codjas virus
Great Island virus	Ife virus
Saint croix river virus	Itupranga virus
Eubenangee virus	Arkonam virus
Equine encephalosis virus	Chobar Gorge virus
Epizootic haemorrhagic disease virus	Fromede virus
Changuinola virus	Gomoka virus
Corriparta virus	Tracambe virus
Lebombo virus	Japanaut virus
Orungo virus	Kammavanpettal virus
Umatilla virus	Matucare virus
Wallal virus	Tembe virus
Warrego virus	Lake clarendon virus
Kemerovo virus	Ndelle virus
Wongorr virus	Paroo virus
Ieri virus	Picola virus
Peruvian horse sickness virus	
Wad medani virus	

Table 1. 2: Species of virus within the Orbivirus genera and those not yet assigned.

1.3: Bluetongue Virus

BTV is an arbovirus that is vectored by the *Culicoides* genera of biting insects, which are found in many areas of the world and are potentially capable of supporting the spread of BTV infection to new countries. Subsequently BTV already has an economic impact across many areas of the world including Europe, with the most recent outbreak in Spain July 2005 (Purse, Mellor *et al.* 2005).

BTV causes disease in sheep, goats, cattle and wild ruminants, ranging from asymptomatic infection to a disease causing high morbidity and mortality, which is most severe in sheep and deer. Mortality is usually low although in some sheep flocks

mortality may be as high as 50% (http://www.defra.gov.uk/animalh/diseases/notifiable/disease/bluetongue.htm November 2005), with surviving animals displaying a loss of condition and subsequent reduction in meat and wool production.

In sheep the disease is characterised and easily identifiable by changes to the mucous linings of the mouth and nose and the coronary band of the foot. Symptoms of the disease displayed in sheep are a fever lasting for several days in addition to increased respiration and hyperaemia (redness) of the lips, mucous linings of the mouth and nose and eyelids. Swelling and excess salivation and frothing from the mouth with excess nasal discharge are commonly present. In cattle the disease is usually mild or asymptomatic and is therefore difficult to diagnose from disease symptoms; diagnosis is by laboratory confirmation (www.iah.bbsrc.ac.uk/schools/factfiles/BTV.htm, http://www.defra.gov.uk/animalh/diseases/notifiable/disease/bluetongue.htm November 2005).

1.3.1: Virion Structure

BTV particles are non-enveloped with two protein shells comprised of seven viral proteins. The major protein shells are the 'core', consisting of VP3, VP7, VP1, VP4, VP6 and the viral dsRNA genome, and the outer capsid consisting of VP2 and VP5 (Fig 1.1). Ten double-stranded RNA genome segments S1 – S10 each encode one protein which is translated from the first AUG on the mRNA. S10 encodes two proteins from the same frame; NS3 and NS3A which differ by 13 amino acids as a result of translation

initiation from a second initiation codon (Lee and Roy 1986; French, Inumaru *et al.* 1989).

The termini of each segment are conserved and the 5' and 3' termini have partial inverted complementarity and may allow formation of panhandle structures. Cryoelectron microscopy analyses and density mapping of BTV and other dsRNA viruses indicated that the genomic RNA displayed a highly ordered organisation (Prasad, Rothnagel *et al.* 1996; Grimes, Burroughs *et al.* 1998; Gouet, Diprose *et al.* 1999). The RNA is packaged as well-ordered layers surrounding the structural proteins VP1, VP4 and VP6 and appears to be organised by structural features formed by VP3 in the internal surface of the core shell (Gouet, Diprose *et al.* 1999).

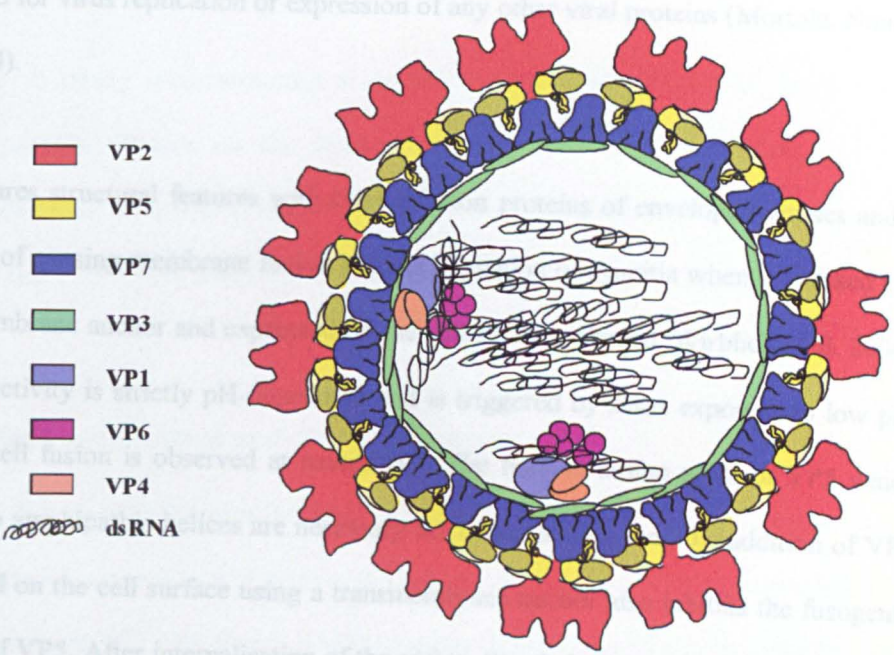

Figure 1. 1: Schematic of Bluetongue virus based on the structure derived from cryoelectron microscopy data.

1.3.2: The Outer capsid and virus entry

VP2 and VP5 form the unique outer capsid of the virion (Fig 1.2) that is different to the T= 13 icosahedral symmetry seen for the reoviruses and rotaviruses within the *Reoviridae*. The outer capsid is an organisation of two distinct shapes the VP2 triskelion and the globular VP5 (Fig 1.2). There are 60 VP2 triskelions and 120 globular VP5 in every outer capsid (Nason, Rothagel *et al.* 2004).

VP2 is a haemaggluttinin that is directly involved with attachment of the virus to the host cell receptor and its subsequent internalisation by receptor mediated endocytosis (Hassan and Roy 1999; Hassan, Wirblich *et al.* 2001). VP2 is the most variable viral protein; it dictates the virus serotype and carries the neutralising epitopes of the virus. VP2, along with VP5, has been shown to trigger apoptosis in mammalian cells without the need for virus replication or expression of any other viral proteins (Mortola, Noad *et al.* 2004).

VP5 shares structural features with class I fusion proteins of enveloped viruses and is capable of causing membrane fusion and the formation of syncitia when it is fused to a transmembrane anchor and expressed on the cell surface (Forzan, Wirblich et al. 2004). Fusion activity is strictly pH-dependent and is triggered by short exposure to low pH; no cell-cell fusion is observed at neutral pH. The first 40 amino acids of VP5 which form two amphipathic helices are necessary for fusion activity and the addition of VP2 expressed on the cell surface using a transmembrane anchor also inhibits the fusogenic activity of VP5. After internalisation of the virion, the clathrin coat of the vesicle is lost resulting in a large endocytic vesicle from which the core particle is released into the cytoplasm. VP5 is likely to mediate membrane fusion within the endocytic entry vesicle

of BTV resulting in the egress of the core particle into the cell cytoplasm (Hassan, Wirblich *et al.* 2001; Forzan, Wirblich *et al.* 2004).

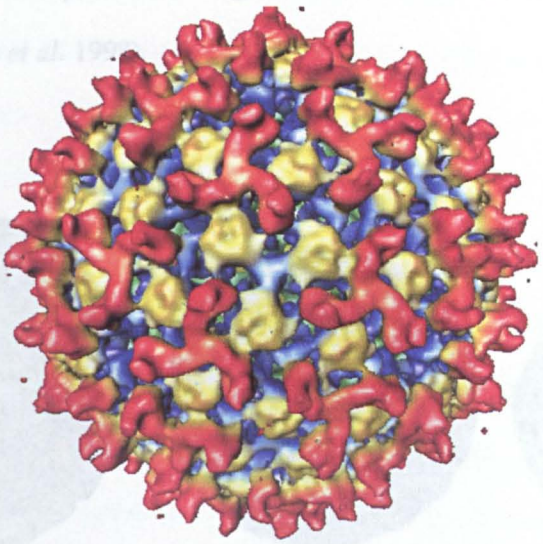

Figure 1. 2: Image reconstruction of the three-dimensional cryo-EM structures of a BTV particle. Visible are the distinctive triskelion VP2 trimers (red) and VP5 trimer globular domains (yellow). The outer core protein VP7 is just visible beneath the VP5 layer (blue) (Nason, Rothagel *et al.* 2004).

1.3.3: The Core Proteins and virus replication

The viral core is released into the cytoplasm from the endosome after entry; the outer capsid proteins are removed at some point during entry and membrane permeablisation of the endosome. The viral core is a highly stable, transcriptionally active particle that is formed from VP3, VP7, VP1, VP4 and VP6 in addition to the viral genome. In contrast to the outer capsid the core particle does show T=13 icosahedral symmetry (Nason,

Rothagel *et al.* 2004). A lattice of sixty VP3 dimers form the scaffold of the core with VP7 trimers arranged on the surface of the VP3 layer (Fig 1.3). The VP3 layer forms an icosahedral lattice that interacts with the dsRNA genome at its five-fold axis. VP7 exists as a trimer which forms pentameric rings around the fivefold axis of the VP3 scaffold (Grimes, Burroughs *et al.* 1998).

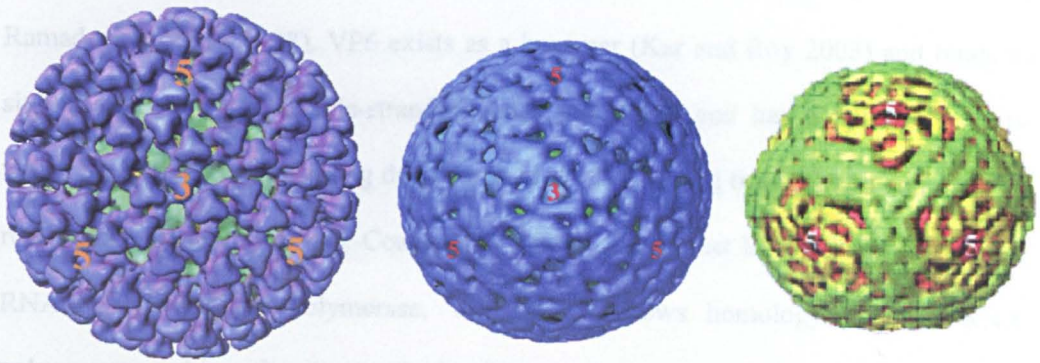

Figure 1. 3: Image reconstruction of the BTV core from three-dimensional cryo-EM studies. (a) The whole BTV core viewed along the icosahedral three-fold axis showing VP7 trimers (purple). (b) The inner lattice of VP3 (blue) along the same axis and (c) The innermost density of the 3 minor core proteins in association with the genome. The red flower shaped densities represent the locations of the structural proteins VP1, VP4 and VP6 lying at the 5 fold axis; represented in green are the ordered strands of genomic RNA (Grimes, Jakana *et al.* 1997).

All viral genomic RNA is found within core particles where both genome replication and production of mRNA occurs. The enclosure of the dsRNA prevents the activation of the interferon pathways and other dsRNA based antiviral mechanisms, preserving the

integrity of the viral genome and the viability of the cells for virus replication. The three core proteins VP1, VP4 and VP6 are the enzymatic proteins necessary for genome replication and transcription.

VP4 exists as a dimer and has all of the enzymatic properties needed for the 5' capping of the viral messenger RNA acting as a guanylyltransferase, methyltransferase and RNA triphosphatase (Martinez-Costas, Sutton *et al.* 1998; Ramadevi, Burroughs *et al.* 1998; Ramadevi and Roy 1998). VP6 exists as a hexamer (Kar and Roy 2003) and binds to single-stranded RNA, double-stranded RNA and DNA, and has a helicase activity which is involved in unwinding double-stranded RNA during transcription and genome replication (Stauber, Martinez-Costas *et al.* 1997). The largest BTV protein is the viral RNA-dependent RNA polymerase, VP1, which shows homology to other RNA polymerases and is active *in vitro* in the absence of other core proteins (Urakawa, Ritter *et al.* 1989; Boyce, Wehrfritz *et al.* 2004). VP1 is responsible for the transcription of mRNA which exits the core to be translated via cellular machinery; in the presence of magnesium ions and NTP substrates the core enzymes are activated causing a conformational change at the five-fold axis opening a pore through the VP3 and VP7 layers through which mRNA molecules pass into the cytosol (Gouet, Diprose *et al.* 1999).

1.3.4: Non-Structural Proteins and virus assembly and egress

In addition to the seven structural proteins BTV has four non-structural proteins NS1, NS2, NS3 and NS3A encoded by segments S6, S8, and S10 (as determined by the migration pattern obtained for the 10 dsRNA segments in acrylamide gel

electrophoresis. NB the segments display a different migration pattern when analysed by agarose gel electrophoresis).

The infecting core particle, released from the endosome into the cytoplasm, is rapidly surrounded by a dense fibrillar network termed the viral inclusion body (VIB). NS2 is a phosphoprotein which is the major component of VIBs that accumulate in infected cells (Fig 1.4); VIBs are also rich in mRNAs (Thomas, Booth *et al.* 1990). NS2 alone is capable of forming inclusion bodies, when expressed using a recombinant baculovirus, in the absence of other viral proteins including core proteins (Thomas, Booth *et al.* 1990). The core structural proteins VP3 and VP7 are also found within the VIB indicating that core particles may assemble within or near to the periphery of the VIB (Hyatt and Eaton 1988).

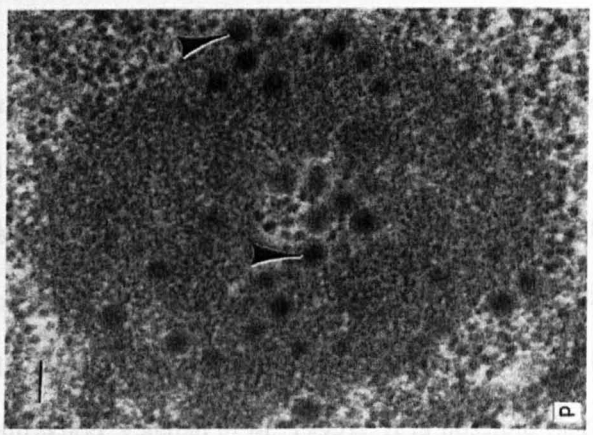

Figure 1. 4: Electron microscopy study of BTV infected mammalian SVP cells. VIBs formed during BTV infection are visible throughout the cell (indicated by the arrows) (Brookes, Hyatt *et al.* 1993). Bar represents 100nm.

NS2 has a high affinity for single-stranded RNA species, with a preference for binding BTV RNA over non-specific RNA species (Thomas, Booth *et al.* 1990; Zhao, Thomas *et al.* 1994; Fillmore, Lin *et al.* 2002; Lymperopoulos, Wirblich *et al.* 2003). It is probable that viral RNA segments have structural or sequence specificities, that are recognised by NS2, that allow recruitment and sorting of genome segments for new core particles which must contain one of each of the 10 segments. It is also possible that NS2 does not sort the RNA segments but recruits and therefore condenses them, which allows selective RNA-RNA interactions to occur between each genome segment followed by packaging of the genome into a new core particle.

BTV has no lipid envelope and egress of the progeny virions from mammalian cells is predominantly via cell lysis. By contrast egress from infected insect cells is via local disruptions in the plasma membrane allowing virions to leave without destroying the cells integrity giving more efficient vectoring of the virus by the insect (Beaton, Rodriguez *et al.* 2002). BTV has not been detected with a lipid envelope indicating that if virus egress occurs via budding through the plasma membrane, rather than through small channels, the envelope is lost extremely quickly afterwards. NS3 and NS3A are BTV glycoproteins which accumulate to low levels in infected mammalian cells; in infected insect cells the levels of NS3 and NS3A are extremely high (French, Inumaru *et al.* 1989; Guirakhoo, Catalan *et al.* 1995). It is possible that the difference in NS3 levels detected within the two cell types may account for the differences in virus egress.

NS3 is transported through the Golgi apparatus to the cell membrane where it has two cytoplasmic domains linked by two membrane spanning domains. Co-expression of NS3 and BTV virus like particles (VLP) from recombinant baculoviruses in *Spodoptera*

frugiperda (*Sf*) cells facilitates the release of VLP from the cells. NS3 is detected in the cell membrane at the site of virus release (Hyatt, Zhao *et al.* 1993). Yeast two-hybrid analysis determined that NS3, but not NS3A, interacts via a putative amphipathic helix at its N-terminus with the calpactin light chain, p11, of the annexin II complex (Beaton, Rodriguez *et al.* 2002). The annexin II complex has been implicated in trafficking of vesicles and other membrane associated events along the endocytic and secretory pathways. p11 is known to interact with phospholipids and cytoskeletal proteins and by undergoing a conformational change may allow the fusion of two membranes leading to exocytosis (Nakata, Sobue *et al.* 1990). Inhibition of NS3-p11 interaction by the use of a small peptide mimicking the p11 binding sequences down-regulated virus release confirming the importance of this interaction in virus egress (Beaton, Rodriguez *et al.* 2002).

NS3 also has late domain motifs located in its N-terminus which have been identified in various viral proteins including HIV Gag and Ebola virus VP40 (Martin-Serrano, Zang *et al.* 2001; Wirblich, Bhattacharya *et al.* 2006). The late domain motifs bind a variety of proteins, including Tsg101 and p11 (Ono and Freed 2004), which are involved in the formation of special endocytic vesicles, multivesicular bodies (MVBs). The formation of MVBs involves invagination of the endosomal membrane away from the cytoplasm, a process which is topologically identical to the formation of many enveloped virus particles (Pornillos, Garrus *et al.* 2002; Raiborg, Rusten *et al.* 2003). Tsg101 interacts with the PTAP late domain motif of HIV (Garrus, von Schwedler *et al.* 2001) facilitating virus egress via budding at the plasma membrane. Both mammalian and insect (*Drosophila*) Tsg101 have been shown to interact with the PSAP late domain motif of BTV NS3, and knockdown of Tsg101 in mammalian cells using siRNA,

inhibited virus release by 65% (Wirblich, Bhattacharya *et al.* 2006). Like many proteins that bind Tsg101 NS3 also binds to NEDD4 and related members of the ubiquitin ligase family.

It is obvious that NS3 plays an important role in virus egress from infected cells but whether or not this results in the differences in release seen in vertebrate and invertebrate cells is still to be confirmed. Since no BTV is detected with envelope, if NS3-Tsg101/p11 interaction is used for virus egress then it can be assumed that there must be an enveloped stage in the BTV life cycle even if this is only transient.

1.3.5: NS1

NS1 is the most abundant viral protein expressed in BTV infected cells and is found throughout the cytoplasm (Fig 1.5) (Huismans 1979). In infected vero cells NS1 is first detected at 5 hours post infection by immunofluorescence staining and flow cytometry (Whetter, Gebhard *et al.* 1990). 552 amino acid NS1 is expressed from genome segment 6 and is 64 kDa; NS1 has a low number of charged amino acids and is high in cysteine residues with several hydrophobic regions (Roy and Gorman 1990). NS1 alone multimerises into large tubule structures; no other viral proteins are required for the formation of tubules when NS1 is expressed in mammalian or insect cell lines (Urakawa and Roy 1988).

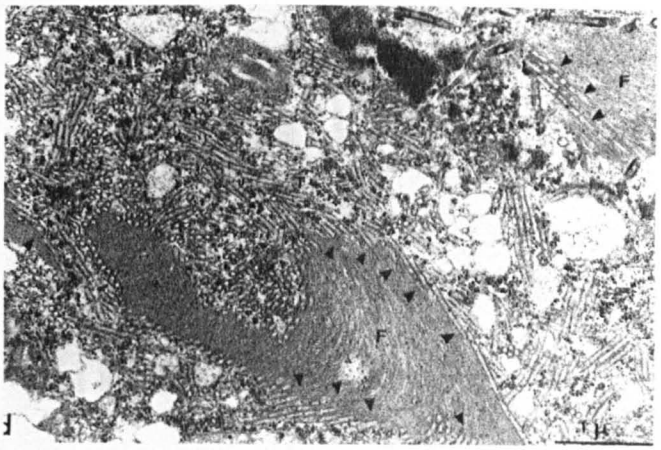

Figure 1. 5: *Sf* insect cell infected with a recombinant baculovirus expressing NS1. NS1 tubules are visible throughout the cytoplasm (Urakawa and Roy 1988). F indicates fibrous structures with the arrow heads indicating tubules lying alongside the fibrous structures.

Cryoelectron microscopy shows that tubules are on average 52.3nm in diameter and up to 1000nm in length with a helical configuration (Fig 1.6) (Hewat, Booth *et al.* 1992; Hewat, Booth *et al.* 1992). The NS1 monomer forms a dimer like structure which is assembled in a helically coiled ribbon with approximately 21 dimers per turn to form the tubule. Mutational analysis of NS1 determined that the amino and carboxy termini, as well as a pair of internal cysteine residues at positions 337 and 340 are essential for tubule formation. If the internal cysteine residues at positions 337 and 340 are mutated into serine, large aggregates of ribbon like structures were identified but no tubules were detected (Monastyrskaya, Booth *et al.* 1994).

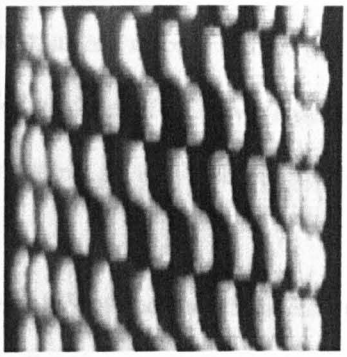

Figure 1. 6: Structural analysis of NS1 tubules showing a distinct ribbon like structure of NS1 dimers forming a helical coil which is the basis of the NS1 tubule. There are approximately 21 dimers per turn and the average tubule has a diameter of 52.3nm and is up to 1000nm in length (Hewat, Booth *et al.* 1992).

The primary antigenic site of NS1 has been localised to the carboxy terminus (Monastyrskaya, Gould *et al.* 1995) and extra peptide sequences can be added to this with no disruption of tubule formation (Mikhailov, Monastyrskaya *et al.* 1996). Foreign sequences representing 44 amino acids (aa) from Clostridium difficile toxin A, 48 aa of the hepatitis B virus preS2 region, and the whole 116 aa of bovine leukaemia virus p15 protein were inserted at the C-terminus of BTV-10 NS1 with no disruption to tubule formation (Mikhailov, Monastyrskaya *et al.* 1996). Furthermore the addition of these sequences lead to their display on the outer surface of the tubule and they were highly immunogenic.

To analyse the immunogenic nature of chimeric tubules, NS1 tubules carrying a single $CD8^+$ T cell epitope from the lymphocytic choriomeningitis virus (LCMV) nucleoprotein were expressed. These chimeric tubules were recognized by MHC class I

restricted T cell hybridoma *in vitro* and induced *in vivo* strong $CD8^+$ class I-restricted CTL responses in immunized mice. Further, the immunized mice were protected when challenged with a lethal dose of LCMV. This finding has allowed novel recombinant vaccines to be made against several diseases (Mikhailov, Monastyrskaya *et al.* 1996).

Amino acids 135-144 of Foot and mouth disease virus (FMDV) VP1 were added to the C-terminus of NS1 eliciting a strong $CD4^+$ T helper cell response and a humoral immune response that was protective in mice subsequently challenged with FMDV (Ghosh, Borca *et al.* 2002; Ghosh, Deriaud *et al.* 2002). Most recently 527 amino acids of the HIV-1 clade A consensus-derived immunogen, HIVA, was expressed fused with NS1 (Larke, Murphy *et al.* 2005). When injected into BALB/c mice by several routes, chimeric NS1.HIVA tubules induced HIV-1-specific major histocompatibility complex class I-restricted T cells. These could be boosted by a modified Ankara vaccine virus, expressing the same immunogen, to generate a memory capable of gamma interferon (IFN-γ) production, proliferation, and lysis of sensitized target cells (Larke, Murphy *et al.* 2005).

The localisation of BTV NS1 has been analysed in virus infected cells by immunofluorescence and electron microscopy. NS1 was detected in high levels throughout the cytoplasm in a punctate pattern, and sometimes within the nucleus (Hyatt, Eaton *et al.* 1987; Eaton, Hyatt *et al.* 1988). Immunogold labelling and visual analysis of NS1 tubules detected NS1 in close proximity to VIB and associated with the cell cytoskeleton. Surprisingly when examined by immunogold electron microscopy virus particles also appeared to label with anti-NS1 gold particles when visualised both in infected cells and when purified and fixed on to electron microscopic grids (Eaton,

Hyatt *et al.* 1987). Core particles purified from virus infected cells also labelled with anti-NS1 gold particles. No NS1 tubules are detected visually when the virus and core particles are examined by electron microscopy indicating that the form of NS1 detected was monomer or was due to cross-reactive antibody. The interaction of NS1 with virus cores, virus particles and the cytoskeleton may indicate that NS1 plays a role in virus morphogenesis and transport from assembly sites to egress sites. No data is available on the interactions of NS1 *in vitro* with other BTV virus proteins to confirm the interaction of NS1 with virus cores and particles.

The role of NS1 in BTV infection was examined using a single chain antibody expressed under the control of a Tet responsive promoter in a clonal mammalian cell line (Owens, Limn *et al.* 2004). The single chain antibody was derived from an NS1 specific monoclonal antibody, 10B1 (Monastyrskaya, Gould *et al.* 1995), and used to knock down the amount of free NS1 in virus infected cells when doxycycline was absent from the growth media. No NS1 tubules could be detected by electron microscopy of cell sections or sucrose gradient purification when the antibody was expressed, although small amounts of NS1 were detected by western blot analysis.

Strikingly less cytopathic effect (CPE) was detected in BTV infected cells where NS1 was knocked down, the mammalian cells appeared comparable to insect cells at the same time post infection. The change in visible CPE was not due to disruption in virus replication as the titre of cell associated virus is comparable to that produced during normal infection. However, a massive increase in the titre of virus released from the cells was observed indicating that production of infectious virus progeny is in fact up-regulated by knock down of NS1. When examined by electron microscopy virions could

be detected budding from the plasma membrane as in insect cell infection rather than exiting via cell lysis, as detected in cells where no antibody was expressed, explaining the change in CPE yet increase in virus yield (Fig 1.7).

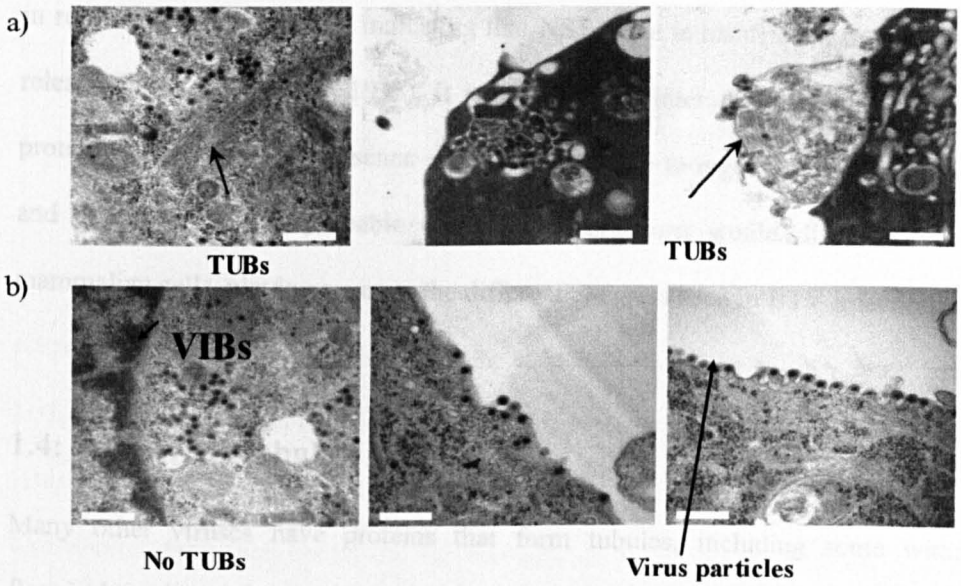

Figure 1. 7: Ultrastructural EM analysis of BTV 10 infection in the presence and absence of an internally expressed single chain antibody against NS1. (a) Typical effects of BTV-10 infection in BSR cells, including cytoplasmic inclusion bodies, tubules, mature virus particles and areas of severe morphological destruction near the plasma membrane consistent with lytic release of the virus. (b) BSR cells expressing the anti-NS1 antibody, no cytoplasmic tubules are detected and virus particles are exiting the cells via budding from the plasma membrane (Owens, Limn *et al.* 2004). Bar represents 500nm.

This data implicates a role for NS1 in virus egress, which is supported in part by the apparent localisation of NS1 with the cytoskeleton and virus and core particles.

However given the strong evidence in support of NS3 involvement in virus egress it is difficult to draw any conclusions as to how the knockdown of NS1 has this effect or the possible mechanisms involved. Unlike co-expression of NS3 and VLP using recombinant baculovirus, co-expression of NS1 and VLP in insect cells does not result in release of virus particles, indicating that NS1 alone is insufficient to trigger particle release (Hyatt, Zhao *et al.* 1993). It is possible that interactions of NS1 with cellular proteins, rather than the presence of NS1 alone, help to regulate virus morphogenesis and egress. It is also probable that those interactions would differ in insect and mammalian cells, playing a part in the differential egress seen in BTV infection.

1.4: Other viral tubules

Many other viruses have proteins that form tubules, including some within the *Reoviridae*. A number of different viruses encode viral tubules for a variety of functions, many of which remain unknown. The variety of viral tubules makes it difficult to identify comparable features between the proteins and functions of the tubules within infected cells. Viral tubules can be assigned to two major types; the movement protein tubules of plant viruses and the storage tubules of excess viral proteins. Several viruses, including BTV, encode tubules that not within either of these categories; a lack of data on the active form of the protein prevents them from being classified as storage tubules, although this may indeed be the case.

The first major type of virus tubules, and the most studied protein tubules, belongs to plant viruses. Plant viruses often encode one or more movement proteins that assemble into tubules and are involved in cell-cell spread of the virus within the plant. Plant cell walls are very rigid and do not allow viral spread from one cell to the next, movement

proteins modify the structure of plasmodesmata (pores in the cell walls allowing transport of nutrients etc) in such a way that viral transport is enabled from one cell to the next by transport of the viral particle through the movement protein tubule (Lazarowitz and Beachy 1999).

Cauliflower mosaic virus (CaMV), a double-stranded DNA virus, belonging to the family *Caulimoviridae* is one such plant virus that uses movement proteins. The movement protein, P1, accumulates in foci at the periphery of transfected protoplasts, and the tubules it forms extend beyond the cell wall (Perbal, Thomas *et al.* 1993; Huang, Han *et al.* 2000). A second viral protein, virion associated protein (VAP) also known as P3, is essential for CaMV movement between plant cells, VAP also mediates virus transmission by aphids through simultaneous interaction with both the aphid transmission factor and the virion. To form tubules P1 oligomerizes as a trimer through a C-terminally located coiled-coil domain. P1 interacts, via its C-terminal coiled-coil domain, with the N-terminal coiled-coil domain of VAP located on the virion surface (Stavolone, Villani *et al.* 2005), this interaction occurs within plasmodesmata that contain virus particles. MP also co-localises with the *Arabidopsis thaliana* MPI7 protein in the cell periphery foci, suggesting the possible involvement of host factors in virus movement (Huang, Andrianov *et al.* 2001).The interactions of VAP with P1 and the virion by the coiled-coil domains, indicate a mechanism for movement in plant cells involving both proteins and possibly P1 interaction with host proteins.

The movement proteins of some plant viruses are efficient enough to allow cell to cell movement in viruses that are normally movement defective. The movement protein of Tomato spotted wilt virus (TSMV), NSm, can complement the movement deficient

Tobacco mosaic virus (TMV) allowing long distance transport to the upper leaves of the plant (Lewandowski and Adkins 2005). The C-terminus of NSm is necessary for its function as a movement protein; NSm does not directly interact with the plasma membrane indicating a possible interaction with a membrane protein for formation and function of tubules.

There are also many plant viruses within the *Reoviridae*, of these some have been identified as expressing movement protein tubules. Rice dwarf virus (RDV) of the Phytoreoviruses, expresses a movement protein, Pns6, from the non-structural genome segment S6; this protein is also capable of complementing the movement deficient potato virus X (PVX) (Li, Bao *et al.* 2004). The S6 genome segment is equivalent to the S6 genome segment of BTV that encodes for NS1; Pns6 is 56kDa which is only slightly smaller than BTV NS1 at 64kDa. When the amino acid sequences of BTV NS1 and RDV Pns6 are aligned they share 12% sequence identity, with a further 22% sequence similarity, i.e. the amino acids are changed to amino acids with similar properties, indicating that the 2 proteins are not particularly similar.

The second major type of virus tubule is those tubules that are a form of storage for excess or misfolded viral proteins. The mammalian Rotavirus, also of the *Reoviridae*, expresses a capsid protein, VP6, which forms tubules that are thought to be either a form of storage for the capsid protein prior to virion assembly or due to misfolding of the protein (Lepault, Petitpas *et al.* 2001). The usual VP6 trimer, the subunit for capsid construction, is disrupted at an increased pH, and the protein assembles helically into tubules of 45nm or 75nm diameter. When VP6 is expressed both forms of tubules plus spherical virus like particles of VP6 are detected.

Infectious bursal disease virus (IBDV) also encodes tubules used for protein storage, in fact it produces two distinct types of viral tubules type I and II. IBDV is an avian virus of the *Birnaviridae* family, possessing a bipartite double-stranded RNA genome (Van Regenmortel 2000; Fauquet 2005), and causes an immunosuppressive disease that affects juvenile chickens. Type I tubules are capsid mulitmers that stack up in a form similar to that seen in the virion subunit and possess the same diameter, 60nm, as the virus particle (Granzow, Birghan *et al.* 1997).

The IBDV type II tubules may also act as storage for excess protein. Type II tubules are smaller, 24 to 26 nm in diameter, found in both cytoplasmic and intranuclear locations and contain the viral structural protein VP4, which is not found in the virus particle (Granzow, Birghan *et al.* 1997). VP4 is a protease responsible for cleavage of the VP2-VP4-VP3 polyprotein encoded by the virus (Kibenge, Qian *et al.* 1997; Lejal, Da Costa *et al.* 2000 Rodriguez-Lecompte, Nino-Fong *et al.* 2005). The role of these virus tubules in unknown, although since VP4 is a protease, aggregation might serve to inactivate excess protease preventing lethal damage to the virus. Surprisingly, although IBDV replicates in the cytoplasm of infected cells, these VP4-containing type II tubules were detected in both the cytoplasm and nucleus although it is unclear how VP4-containing tubules or their immature forms reach the nucleus; no obvious nuclear localization consensus signal has been found (Gorlich and Mattaj 1996).

A different type of tubule entirely, that fits into neither the movement protein tubule or storage tubule groups, is encoded by the insect virus *Autographa californica* nucleopolyhedrovirus (AcMNPV). The very late protein p10 is synthesised in high

levels and forms fibrillar structures that spiral through the nucleus and the cytoplasm of AcMNPV-infected cells (Quant-Russell, Pearson *et al.* 1987; Van Oers, Flipsen *et al.* 1994). The coiled-coil domain within the N-terminus of p10 is responsible for the aggregation of p10 monomers (Van Oers, Flipsen *et al.* 1994; Alaoui-Ismaili and Richardson 1996). p10 and its tubules have no known function although it is thought to be involved in cell lysis due to the failure of cells to lyse when p10 was mutated/absent (Williams, Rohel *et al.* 1989), further evidence suggests that it may be involved in nuclear disintegration and subsequent cell lysis (Patmanidi, Possee *et al.* 2003). The p10 tubules co-localise with cortical microtubules and a depolymersiation of tubulin via treatment with nocodazole leads to an abrogation of p10 tubule formation and a deposition of p10 in cytoplasmic foci (Patmanidi, Possee *et al.* 2003). It is thought that this interaction is ionic via the basic carboxy terminal microtubule binding domain of p10 and the acidic carboxy terminus of tubulin.

Similarly to AcMNPV p10, BTV NS1 does not fit into the movement protein tubule group and may not fit into the storage tubule group either, although this depends if the active form of NS1 is monomers/dimers or tubules. BTV NS1 does however share a number of similarities with the insect virus protein tubules described. The AcMNPV p10 tubules have some structural similarities with NS1 tubules; the amino terminus is required for aggregation of the monomers whilst the carboxy terminus is free to interact with other proteins.

1.5: Viral Non-Structural Proteins and Important Interactions

Virus life cycles can be split into five main stages; entry, replication, trafficking of replication products for assembly, egress and transmission. Throughout their life cycle viruses interact with host cellular proteins at each of the five stages in addition to interacting with host proteins throughout their life cycle to abrogate anti-viral immune responses. Viral interactions range from having no significantly detrimental effects on the host to causing the shut down of protein synthesis and subsequent cell death. The effects of virus-host protein interactions can be localised to the cell that is infected or can have a multi-cellular effect on the host, especially in the case of abrogation of anti-viral immune responses.

1.5.1: Interactions during Virus Entry

Interaction of virus and host proteins during virus entry usually involves viral structural proteins on the outer surface of the virion and cellular surface proteins which the virus uses as receptors. The virus then enters the host cell by receptor mediated endocytocis or membrane fusion in the case of enveloped viruses. As non-structural proteins are not present in virions they rarely have a role in virus entry although several viruses rely on non-structural proteins for inter-cell transmission (chapter 1.5.5).

1.5.2: Interactions during Genome Replication and Protein Translation

Most viruses hijack normal house keeping cellular processes such as the enzymatic machinery for DNA replication and the materials for DNA and RNA replication. All viral transcripts are translated using host cell ribosomes and materials; post translational modifications such as glycosylation are also achieved via normal cellular processing.

Viral non-structural proteins with enzymatic roles sometimes function to allow the virus to use cellular pathways. For example, to utilise the cellular translation machinery Influenza viruses, which lack 5'capped mRNA, have to hijack the 5' m7G caps of cellular mRNAs. The non-structural protein, PB2 endonuclease, of Influenza virus cleaves the 5' m7G cap plus 10-15 nucleotides from the termini (Ulmanen, Broni *et al.* 1981), thus giving heterogeneous 5' termini to the viral RNA segments (Caton and Robertson 1980; Dhar, Chanock *et al.* 1980). By removing the 5' caps from host transcripts the virus has a detrimental effect on the cell reducing/abolishing cellular protein synthesis. Virus replication must therefore be completed rapidly and efficiently before virus induced cell death occurs. Other examples of viral non-structural protein interactions with transcription and translation machinery are detailed in table 1.3.

Virus	Host pathway	Non-structural protein and its Interactions
Poliovirus	Transcription	The viral protease 3C(pro) cleaves and inactivates pol I transcription factors, SL-1 (selectivity factor) and UBF (upstream binding factor), inhibiting RNA polymerase I host cell transcription (Banerjee, Weidman *et al.* 2005).
Poliovirus	Translation	The viral proteases 2A and 3C cleave host factors eukaryotic translation initiation factor (eIF4G) and poly A binding protein (PABP) shutting down host cell protein synthesis (Kuyumcu-Martinez, Van Eden *et al.* 2004).
Murine leukaemia virus	Translation	Viral reverse transcriptase binds to eukaryotic translation release factor inhibiting translation termination and release of polyproteins from the ribosome. This enhances read through of the Gag-Pol polyprotein increasing the amount of reverse transcriptase in the cell (Goff 2004)
Hepatitis C virus	Translation	NS5A inhibits phosphorylation of eIF2alpha and eIF4E exerting counteracting effects on mRNA translation, this might maintain the global mRNA translation rate during early virus infection while favouring cap-independent translation of HCV mRNA during late infection (He, Tan *et al.* 2001).
Encephalomyo -carditis virus	Translation	Viral protein 2A translocates to the nucleus and helps to up-regulate the synthesis of new and modified ribosomes that have an inherent preference for internal ribosomal entry site (IRES)-dependent viral genome translation over cap-dependent host mRNA translation, thus shutting down host protein synthesis (Aminev, Amineva *et al.* 2003; Aminev, Amineva *et al.* 2003).
Poliovirus and Coxsackie's B3 virus	Protein secretion	3A protein inhibits ER-Golgi protein traffic thus inhibiting host protein secretion. This inhibits secretion of various immune response proteins including IFN-β and MHC I and TNF receptors (Choe, Dodd *et al.* 2005).
Dengue virus	Interferon pathway	Viral protein NS4b inhibits activation of STAT1 and blocks ISRE promoter activation in response to IFN-alpha/beta (Munoz-Jordan, Sanchez-Burgos *et al.* 2003).

Table 1. 3: Interactions of viral non-structural proteins with proteins involved in host house keeping pathways.

1.5.3: Interactions during Trafficking of Viral Products to Sites of Assembly

Viruses also make use of the complex trafficking networks within the cell to aid accumulation and movement of specific viral proteins. The golgi body and endocytic vesicles are used to process and traffic viral proteins and particles within the cell. The cytoskeleton network of microtubules, microfilaments and intermediate filaments are also used by many viruses to target viral proteins and virions. The structural proteins of several viruses, including West Nile virus and African swine fever virus, interact with cellular cytoskeletal proteins to traffic proteins and virus particles to egress sites.

The non-structural protein NS3 of Japanese encephalitis virus (JEV), a multifunctional protein with activities of serine protease, triphosphatase and RNA helicase, interacts with microtubules and a Golgi associated protein that associates with microtubules, Tsg101 (Chiou, Hu *et al.* 2003). Infection with JEV causes rearrangement of microtubules within the cell; this is caused by the NS2B-NS3 polyprotein. JEV NS2B or NS3 might induce microtubule reorganization in order to facilitate the transport of other viral proteins from the rER and Golgi apparatus to the CM (virus induced convoluted membrane) during JEV multiplication (Chiou, Hu *et al.* 2003). Furthermore, since tubulin exhibits the functions of a chaperone (Guha, Manna *et al.* 1998; Manna, Sarkar *et al.* 2001), it may help viral proteins to maintain their conformation in the CM.

1.5.4: Interactions during Virus Egress

Other cellular processes that are utilised by viruses include the exocytosis pathway for non-lytic release of virus. Recruitment, by specific viral protein interactions, of cellular protein complexes controlling budding from the plasma membrane are used by retroviruses and BTV (Garrus, von Schwedler *et al.* 2001; Wirblich, Bhattacharya *et al.*

2006). As described in chapter 1.3.4 the BTV non-structural protein NS3 interacts with Tsg101 and the calpactin light chain p11 to aid virus release.

The NS2 protein of Parvovirus minute virus of mice (MVMp) interacts with the nuclear export receptor protein, Crm1, and plays a critical role at a late stage of the parvovirus life cycle involved in release of progeny viruses (Eichwald, Daeffler *et al.* 2002; Miller and Pintel 2002). NS2-Crm1 interactions are essential for egress of the virus particles from the nucleus into the cell cytoplasm, without this interaction egress of progeny virus is severely inhibited.

1.5.5: Interactions during virus transmission

The interaction of viral non-structural proteins with host cellular proteins is vital for the non-circulative transmission of the arbovirus CaMV by aphids. As discussed in chapter 1.4 the VAP non-structural protein, in addition to the non-structural protein ATF (aphid transmission factor), also known as P2, is essential for virus transmission in aphids. ATF is taken up from punctures in plant epidermal and mesophyll cells by the aphid and is retained in the aphid stylet by its interactions with cuticle proteins (Palacios, Drucker *et al.* 2002). Subsequently the viral particles are ingested from the plant phloem and interactions between ATF and VAP, which acts as a bridge between ATF and the virion, retain the virion in the stylets for transmission upon the next plant meal (Leh, Jacquot *et al.* 2001; Palacios, Drucker *et al.* 2002). Furthermore the interaction of VAP with the virion is necessary for the transmission of the virion between plant cells but not for infection of single cells (Kobayashi, Tsuge *et al.* 2002; Stavolone, Villani *et al.* 2005).

1.5.6: Interactions with proteins involved in anti-viral immune responses

The host immune response to virus replication is large and complex and many viruses have developed mechanisms to down-regulate or prevent this response from limiting virus replication. This can be as simple as is seen in BTV replication whereby viral genomic material, double-stranded RNA, is never present in the cell and is always contained within core particles preventing dsRNA activation of the interferon pathway. Table 1.4 gives a summary of some viral non-structural proteins that inhibit host immune responses.

Limitation of the host immune response can also be a more complex process involving protein interactions as is seen in flavivirus replication. The non-structural proteins NS4A, and to some extent NS4B and NS2A, of Dengue virus are known to inhibit interferon induced antiviral activities by interacting with a component of the interferon signalling pathway. Dengue virus and Japanese encephalitis virus (JEV) down-regulate both STAT1 (signal transducer and activator 1), STAT2 and STAT3 expression and activation in addition to disrupting the JAK/STAT pathway further by preventing Tyk2 activation (Munoz-Jordan, Sanchez-Burgos *et al.* 2003; Lin, Liao et al. 2004; Ho, Hung *et al.* 2005).

Simian virus 5 (SV5) links the abrogation of antiviral immune responses to an interaction with the ubiquitin pathway (Precious, Childs *et al.* 2005; Precious, Young *et al.* 2005). SV5 is a rubulavirus of the *Paramyxoviridae*; most viruses within the *Paramyxoviridae* at least partially circumvent the interferon response by blocking interferon signalling and reducing the production of interferon by infected cells. The SV5 V protein does not bind to STAT1 but does bind directly to both STAT2 and

DDB1 mediating degradation of STAT1. The SV5 V protein acts as an adaptor molecule linking a DDB1/Cullin 4a-containing ubiquitin ligase complex to STAT2/STAT1 heterodimers, which leads to the ubiquitination of STAT1 and its subsequent degradation.

Virus	Host pathway	Non-structural protein and its interactions
Influenza A virus	Posttranscriptional inhibition of IFN and TNF induced gene expression	NS1 binds and inhibits the function of the 30-kDa subunit of CPSF, a cellular factor that is required for the 3'-end processing of cellular pre-mRNAs, thus inhibiting posttranscriptional processing of antiviral mRNAs (Wang, Li *et al.* 2000; Noah, Twu *et al.* 2003).
Poliovirus	Protein secretion	3A protein inhibits ER-Golgi protein traffic thus inhibiting host protein secretion. This inhibits secretion of various immune response proteins including IFN-β and MHC I and TNF receptors (Choe, Dodd *et al.* 2005).
Hepatitis C virus	PKR inhibition	NS5A inhibits the cellular interferon (IFN)-induced protein kinase R (PKR) preventing mediation of the IFN induced anti-viral immune response (He, Tan *et al.* 2001).
Poxvirus	Inhibition of NFκB and IRF3 signalling pathways	Secretory protein N1Lmodulates the innate immune response by disrupting signalling to NF-kappaB by Toll/IL-1Rs and TNF superfamily receptors by targeting the IKK complex for inhibition. N1L also inhibits IRF3 signalling (DiPerna, Stack *et al.* 2004).

Table 1. 4: Interactions of viral non-structural proteins with host proteins involved in anti-viral immune responses.

1.6: Insect Transmission of Viruses

In 1902 Yellow fever virus was documented as being transmitted by mosquitoes, since then numerous arboviruses have been identified. Today over 70% of plant and 40% of mammalian viruses are classified as arboviruses with over 100 different pathogens of humans (van den Heuvel, Hogenhout *et al.* 1999). Arboviruses are a diverse collection

of viruses; the best known groups are within the *Togaviridae*, *Flaviviridae*, *Bunyaviridae* and the *Reoviridae*. The host ranges and diseases caused are also diverse ranging from Dengue virus, a human pathogen with a positive ssRNA genome vectored by mosquitoes to Tomato spotted wilt virus, a plant pathogen with a negative ssRNA genome vectored by thrips. BTV is vectored by insects of the *Culicoides* genus and in this respect the orbiviruses are unique to the other viruses within the *Reoviridae* that are not vectored by arthropods.

Arboviruses are often classified within the even broader grouping of emerging infections. As geographic boundaries are disrupted by world travel and transport, vectors and hosts increasingly contact each other in new areas changing the global distribution of disease. Changes in climate, ecological habitats and public health control and perception also add to this burden. BTV is a good example of an emerging infection that has spread from Africa where it was first described in the 18th century across America, Asia, Australasia and more recently Europe. BTV was first detected in Europe in 1956 in an outbreak in Spain and Portugal and, despite efforts to control the disease by vaccination, has since been detected in various European countries including Greece, Italy, Turkey, France and Bulgaria. This continued spread of BTV has been attributed to changes in European climate that have allowed increased virus persistence during winter and a northwards movement of BTVs main vector *Culicoides imicola*. A shift in transmission to new strains of *Culicoides* native to Europe is also an important factor (Purse, Mellor *et al.* 2005).

BTV belongs to the circulative, propagative classification of arboviruses, these viruses are both internalised and actively replicate within the vector species (Gray and Banerjee

1999; van den Heuvel, Hogenhout *et al.* 1999). The arthropod vector is extremely important in the life cycle of BTV as it is necessary for the transmission and long term survival of the virus. The mammalian host is a short term, limiting stage of the BTV life cycle due to the disease it causes. This stage does however provide a high titre source of virus allowing more efficient infection of the insect vectors which are capable of sustaining BTV replication for longer periods. During the BTV life cycle the virus must infect and replicate successfully in both hosts and effectively transmit between both hosts for the cycle to be maintained.

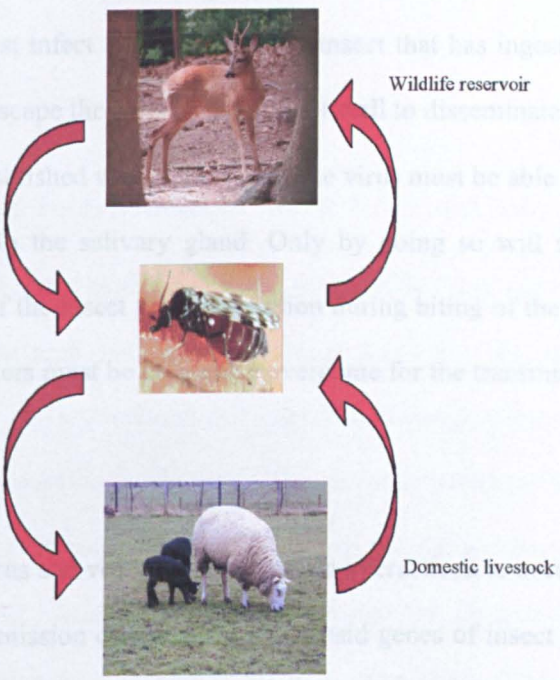

Figure 1.8: Transmission cycle of BTV. The *Culicoides* sp. midge is the BTV vector between the wildlife reservoir and domestic livestock.

Many barriers exist in both the mammalian and arthropod stages of the life cycle which BTV must overcome to replicate and transmit efficiently and sustainably. Whilst a lytic

infection of mammalian cells allows rapid replication and spread of the virus within an organism it does not permit spread from one mammal to another and infection is therefore self-limiting. BTV requires the persistent non-lytic infection of insects for transmission to occur and the disease cycle to be maintained. The relationship between a virus and its insect vector is highly specific; BTV along with many arboviruses can only be transmitted by one or a limited number of closely related species of insect. BTV transmission is sustained by species within the *Culicoides* genus, although BTV is capable of infecting other genera of insect including the sand fly *Lutzomyia longipalpis* (Jennings and Mellor 1987) it is unable to transmit using these insects. For a virus to be transmitted it must first infect the midgut of the insect that has ingested it and then be able to subsequently escape the cells of the midgut wall to disseminate. Once a systemic infection has been established within the insect, the virus must be able to infect and then escape the cells within the salivary gland. Only by doing so will the virus become present in the saliva of the insect for transmission during biting of the next mammalian host. All of these barriers must be efficiently overcome for the transmission cycle of the virus to continue.

Co-evolution of the virus and vector allows specific interactions to occur where by these barriers on virus transmission can be escaped. Capsid genes of insect transmitted plant viruses are subject to greater selective pressure on amino acid sequence than those transmitted by other means (Chare and Holmes 2004). Even greater selective constraints exist for vector-borne animal viruses presumably due to a higher complexity of the hosts involved in circulative transmission of these viruses. Sindbis virus of the Alpha viruses is a well known arbovirus transmitted by mosquitoes, work has identified that the size of the envelope protein transmembrane domain is a key determinate of

infectivity in mammalian cells but has no effect on virus replication and infectivity in insect cells (Hernandez, Ferreira *et al.* 2005).

Despite the huge economic impact of arboviruses little is known about the differences seen between the infections of viruses in insects and mammals. There are obvious biological differences between insects and mammals and yet whilst the interactions of the arboviral proteins with cellular proteins are extensively studied in mammals little work has been done to identify and address these in insects, with few documented results.

1.7: Protein-Protein Interactions between virus and insect cells

BTV protein NS3 interacts with the insect and mammalian homologues of Tsg101, this is an important finding as it confirms that viral proteins may interact with the same proteins in both insect and mammalian cell infection, although it does not confirm that the function of the interaction is identical. The majority of documented research on arbovirus-insect protein interactions is in reference to cellular receptor proteins. A virus protein interaction with insect proteins was identified for Dengue Virus serotype 2 (DEN-2). Virus overlay assays identified 5 C6/36 membrane proteins that interacted with DEN-2, identified by their differing sizes of 19, 65, 67, 79 and 80kDa. DEN-2 binding to two of these proteins, 67KDa and 80KDa, is inhibited by the addition of antibodies specific to the C6/36 membrane indicating that these two proteins are receptors for DEN-2 (Munoz, Cisneros *et al.* 1998). In a different study two proteins of sizes 40 and 45 kDa were identified as putative DEN4 receptors in C6/36 cells (Salas-Benito and del Angel 1997; Reyes-del Valle and del Angel 2004). Unfortunately the

specific interactions and identities of the putative receptor proteins have yet to be determined.

Venezuelan equine encephalitis virus (VEEV), an alphavirus, is different to many arboviruses in that it is transmitted by a broad range of vectors, several genera of mosquitoes and ticks. VEEV binds to a 32-kDa polypeptide present in the C6/36 plasma membrane fraction, which is a laminin binding protein. VEEV binds and competes for binding to this polypeptide with homologous and heterologous alphaviruses, suggesting that this polypeptide binds virus via a receptor-ligand interaction and is a common receptor for alphaviruses. Laminin binding proteins are highly conserved and the broad vector range may be attributed to this (Ludwig, Kondig *et al.* 1996; van den Heuvel, Hogenhout *et al.* 1999). Laminin binding proteins have been identified as receptor proteins for Tick-borne encephalitis virus (TBE) in mammalian cells (Protopopova, Khusainova *et al.* 1996) and other enveloped RNA viruses including Dengue virus and Sindbis virus (Wang, Kuhn *et al.* 1992; Thepparit and Smith 2004) indicating that viral receptors may be common between insect and mammalian cells.

The arbovirus Cucumber Mosaic virus infects over 800 plant species and is vectored by aphids (Palukaitis, Roossinck *et al.* 1992). Like many plant arboviruses it does not replicate inside its insect vector and so the barriers faced are different. Transmissible virus particles acquired from infected plants are retained only on the cuticle lining the food canal in the aphid stylets. From there, Cucumber mosaic virus is released when the vector probes on a new host plant. This interaction does not involve progression of the virus into the insect salivary gland and is therefore much simpler. The betaH-betaI loop of the capsid subunit is a potential key motif responsible for virus interactions with the

insect vector allowing retention and subsequent transmission of the virus (Bowman, Chase *et al.* 2002).

Due to the lack of studies involving arbovirus-insect protein interactions, studies involving insect viruses also allow insight into the interactions that may be necessary for efficient replication and transmission in insects. Members of the *Luteoviridae* are transmitted by aphids in a circulative, non-propagative manner that requires the virus to be acquired through gut tissue into the aphid hemocoel and then exit through salivary tissues. This process is aphid species-specific and involves specific recognition of the virus by unidentified components on the membranes of gut and salivary tissues. Both structural proteins of the virus are involved in the transmission process, with multiple protein domains regulating the movement and survival of the virus in the aphid and plant (Young and Filichkin 1999; Gray and Gildow 2003).

Recent work on a unique relationship between parasitic wasps (*Cotesia congregata*), the caterpillar *Manduca sexta* and a bracovirus, *C. congregata* bracovirus (CcBV), has identified an interaction between the expression of viral cystatins and a change in caterpillar susceptibility to the parasitic wasp infection (Espagne, Douris *et al.* 2005). The parasitoid wasp lays eggs in the caterpillar host and at the same time transmits CcBV into the caterpillar. Expression of viral genes alters the caterpillar's immune defence responses and developmental program, resulting in the creation of a favourable environment for the survival and emergence of adult parasitoid wasps in a bizarre and rare mutualism between viruses and eukaryotes. However the interesting interactions allowing this odd relationship to occur are found at protein level. CcBV encodes three proteins during infection of the caterpillar that have homology to members of the

cystatin superfamily of tightly binding, reversible inhibitors of cysteine proteases. Assays *in vitro* determined that CcBV viral cystatins are functional, having potent inhibitory activity towards the cysteine proteases papain, human cathepsins L and B and Sarcophaga cathespin B. CcBV cystatins are, therefore, likely to play a role in host caterpillar physiological deregulation by interacting with and inhibiting host target proteases in the course of the host-parasite interaction (Espagne, Douris *et al.* 2005).

2: Aims

To investigate the role of NS1 in BTV replication via its interactions with cellular proteins.

To investigate the interactions of NS1 with other BTV proteins to identify a role for NS1 in BTV replication.

3: Materials and Methods

3.1: Cell Culture

293T (Human embryonic kidney) cells were maintained in MEM (Sigma) supplemented with 10% FCS at 37°C, 5% CO_2.

BSR (baby hamster kidney cells), HeLa (Human cervical carcinoma cells) and Vero (African green monkey kidney cells) cells were maintained in DMEM (Sigma) supplemented with 10% FCS at 37°C, 5% CO_2.

Culicoides cells were maintained in Drosophila media-SFM (Invitrogen) supplemented with 10% FCS at room temperature.

C6/36 (*Aedes albopictus* larvae cells) cells were maintained in at Leibovitz media (Sigma) supplemented with 10% FCS at 28°C.

*Sf*9 cells were maintained in SF900 media (Invitrogen) supplemented with 2% FCS at 28°C, 200 RPM shaking.

*Sf*21 cells were maintained in TC100 media (Sigma) supplemented with 10% FCS at 28°C in spinner flasks.

BSR α NS1 cells (Owens, Limn et al. 2004) were maintained in DMEM (Sigma) supplemented with 10% FCS at 37°C, 5% CO_2. These cells contain the single chain

antibody against NS1 under control of a Tet responsive promoter using the Tet off system (BD Clontech). To maintain the cells with no expression of the cassette, media was supplemented with 100μg/ml hygromycin, 100μg/ml G418 and 1μg/ml doxyclycline, to give expression of the cassette, no doxycycline was added.

***Escherichia coli* strains**

Strain	Genotype	Methodologies used for
DH5α	F^-,ϕ80d*lacZ*ΔM15, Δ(*lacZYA-argF*)U169, *deoR*, *recA*1, *endA*1, *hsdR*17(rk^-, mk^+), *phoA*, *supE*44, λ^-, *thi*-1, *gyrA*96, *relA*1	Cloning, propagation and maintenance of all plasmid stocks.
XL1 Blue	*recA1 endA1 gyrA96 thi-1 hsdR17 supE44 relA1 lac* [F'*proAB lacI*^{q}*ZΔM15 Tn10* (Tet^r)]	Construction, propagation and screening of the λ phage libraries
BM25.8	*sup*E44, *thi Δ(lac–proAB)* [F' *tra*D36, *proAB*+, *lacI*$_q$*Z ΔM15*] λ*imm*434 (kan$_R$)*P1* (cam$_R$) *hsdR* (r_{k12}– m_{k12}–)	Cre recombinase mediated recombination of λ phage into plamsids

3.2: Transfection of mammalian cells

293T cells were grown in 24 well plates until 90% confluent, washed in serum free MEM and incubated with 500μl of serum free MEM. 50μl of OPTIMEM (Sigma) was mixed with 2μl of Lipofectamine 2000 transfection reagent (Invitrogen) and incubated at room temperature for 5 minutes. 0.5μg of plasmid DNA or 50-100ng of siRNA was added and incubated for a further 30 minutes (volumes given per well). The media was removed from each well and the transfection mix added drop wise, after 30 minutes at 37°C 400μl of MEM plus 2% FCS was added to each well.

BSR and Vero cells were transfected as above but using the Lipofectamine Plus Transfection reagent (Invitrogen) and DMEM in place of MEM as per cell maintenance.

3.3: Maintenance of BTV Stock

BSR cells were grown to 80% confluency, washed in serum free DMEM and 5ml of serum free DMEM was added. BTV was then added at an MOI of 0.1 and left to adsorb at 35°C for 1 hour. 7ml DMEM 2% FCS was added and cells were incubated at 35°C for 3-4 days. Once 100% CPE was reached cells and virus stock were stored at 4°C.

3.4: Infection with BTV

Cells were grown and maintained in the appropriate media until 80% confluent, washed in serum free media, infected with BTV at the appropriate MOI (MOI of 1 was used for most experiments giving almost synchronous infection of all cells in the culture) and incubated at 35°C for 1 hour. The virus inoculum was removed, cells were washed in serum free media and then maintained until harvest in media supplemented with 2% FCS at 35°C.

3.5: Maintenance of Baculovirus Stock

*Sf*9 cells were grown in suspension to a density of $1x10^6$ cells/ml and infected with recombinant baculovirus at an MOI of 0.01 then incubated with shaking at 200rpm at 28°C for 5-6 days. Virus was harvested by centrifugation at 9500rpm and supernatant was stored at 4°C.

3.6: Infection with Baculovirus

*Sf*9 cells were grown in suspension to a density of $1x10^6$ cells/ml and infected with baculovirus at an MOI of 0.1. Cells were then maintained for the 3-4 days until harvest for protein analysis.

3.7: Virus Titration

BTV

BSR cells were grown, as in chapter 3.1, in 6 well plates to 100% confluency. Cells were washed in serum free DMEM and 1ml of serum free DMEM was added to each well. The virus stock was added in a serial dilution from $1x10^{-1}$ to $1x10^{-6}$ across the wells and incubated at 35°C for 1 hour, with gentle rocking. The virus inoculum was removed and cells were washed gently in serum free DMEM. 2ml of agarose overlay (1.5% LMP agarose and 5% FCS in DMEM (minus phenol red)) was added and set at 4°C for 5 minutes; the plate was then incubated at 35°C for 3 days. Plaques were visualised by incubation with 2ml of 1/20 neutral red (Sigma) in PBS solution for 5 hours.

Baculovirus

*Sf*21 cells were seeded at a concentration of $1x10^6$ cells/well, in a 6 well plate, and left to adhere, at room temperature, for 30 minutes. The cells were washed with serum free TC100 and then 1ml of serum free TC100 was added to each well. The baculovirus stock was added in a serial dilution from $1x10^{-2}$ to $1x10^{-7}$ across the wells and incubated

at 28°C for 1 hour, with gentle rocking. The virus inoculum was removed and cells were washed gently in serum free TC100. 2ml of agarose overlay (1.5% LMP agarose, 5% FCS, and 50% TC100 in SDW) was added and set at 4°C for 5 minutes before the addition of 1ml of TC100 10% FCS to the surface; the plate was then incubated at 28°C for 4 days. Plaques were visualised by incubation with 2ml of 1/20 neutral red (Sigma) in PBS solution for 5 hours.

3.8: RNA Extraction

Total RNA was purified from T-75 flasks of cells (293T, BSR or Kc cells) only or cells infected with BTV-10. Media was removed and centrifuged at 3000rpm for 5 minutes, the supernatant was discarded. The cell pellet and cells in the flask were combined and lysed by incubation with 10mls of TRI reagent (Sigma), a single step RNA isolation reagent, containing phenol and guanidine thiocyanate that immediately inactivates RNase activity, for 30 minutes. 1ml of chloroform was added; using acidic phenol/guanididium extraction, the aqueous phase, containing RNA, was harvested by centrifugation. Total RNA was then precipitated in isopropanol, washed with 70% ethanol and re-suspended in DEPC treated water.

RNA was extracted from live, virgin *Aedes aegypti* mosquitoes by grinding them in TRI reagent using a pestle and mortar and then purifying as above.

3.9: Purification of Poly A^+ RNA

Poly A^+ RNA was purified from total RNA using the Oligotex mini kit (Qiagen). Briefly total RNA was added to the oligotex beads which have $dC_{10}T_{30}$ oligonucleotides

covalently linked to the surface. mRNA hybridises with high efficiency to this matrix, in high salt conditions, by base pairing interactions between its poly A^+ tail and the poly dT tail of the beads. After washing mRNA and can be eluted in pure form, from the beads by disruption of the hydrogen bonds using a low salt solution, without the need for ethanol precipitation.

3.10: cDNA synthesis

The SMART cDNA library construction kit (BD-Clontech) was used to synthesise double-stranded cDNA from Kc cell poly A^+ RNA. The cDNA was synthesised, using a thermal cycler, with the appropriate termini, for use in the construction of a λ library, provided by the sequence of the primers. Briefly the cDNA was amplified using primers that promote the inclusion of full length cDNA, including the 5' termini of the mRNA, giving specific ends with directional *Sfi 1* sites used for ligation with the provided λ phage arms. The cDNA was size fractionated using chromaspin 400 size exclusion columns (BD-Clontech) and the larger and middle size cDNA (approximately 1Kb-7Kb) was collected.

The BD Matchmaker library construction kit was used to synthesise double-stranded cDNA from Kc cell poly A^+ RNA and *A. aegypti* poly A^+ RNA. The cDNA was synthesised as above but with the appropriate termini for use in the construction of a plasmid library that can be expressed in the yeast two-hybrid system, again the sequence was provided by the primers. The termini in this case are used for homologous recombination with the yeast plasmid giving directional inserts for expression in the yeast two-hybrid system.

3.11: cDNA library construction

The HeLa cDNA library was purchased from Clontech. This was generated by directional cloning of HeLa cDNA into the two-hybrid DNA activating domain vector pGADGH.

The Kc λ library was constructed using the SMART cDNA library construction kit (BD-Clontech). cDNA was synthesised as above and the appropriate size fractions were digested with *Sfi 1* and ligated directionally into the λ phage arms which are pre-digested with *Sfi 1*. This produces a λ phage with a cDNA insert within the multiple cloning site situated between the two arms of the phage. The library was then tested using blue/white plaque screens to calculate the percentage of λ phage with cDNA inserts, blue colouration of plaques identifies non-recombinant λ phages, and then the resulting library was amplified before use. In this library the cDNA insert was expressed from a triple reading frame cassette that allowed all cDNA inserts to be expressed in the frame normally used by the host, in addition to the remaining two frames.

A Kc cDNA library was constructed using the BD matchmaker library and screening kit (BD Clontech). Kc cDNA was produced as in chapter 3.10 and cloned into the two-hybrid DNA activating domain vector pGADT7-Rec by recombination of homologous sites in the primer sequences. Recombination was carried out in the yeast strain AH109 by co-transformation of the cDNA and linearised plasmid; recombination repaired the linearised plasmid and allowed expression of the transcription factors necessary for complementation of the yeast auxotrophisms. Successful recombination was selected

for on solid yeast media (see chapter 3.13) minus leucine, and positive colonies were amplified and washed off the media before use. The library in this procedure is present in yeast and screening is done via mating to limit amplification of the library. In contrast to the λ phage library, the cDNA insert is only expressed in one frame which decreases the chance of it producing the same peptide as is produced from within the normal host.

The BD matchmaker kit was also used to construct an *A. aegypti* cDNA library in the yeast strain AH109.

3.12: λ Library Screening

The λ library was screened using the plaque lift technique (Stratagene Picoblue immunoscreening kit). A plaque assay was performed with the λ library in a lawn of XL1 blue *E. coli* in NZY agar (5g NaCl, 2g $MgSO_4$, 5g yeast extract and 10g NZ amine per litre, pH 7.5. For bottom agar add 15g agar/l, for top agar add agarose to 0.7% w/v). Once small plaques were visible, approximately 8 hours post plating; cDNA expression was induced with IPTG, by overlaying the agar with a nitrocellulose filter and subsequent incubation for 4 hours at 37°C. The filters were first soaked in 10mM IPTG for 1 minute and then dried. The expressed cDNA proteins were bound to nitrocellulose filters, as they were released by lytic λ phage replication. The filters were washed in TBS-T (20 mM Tris-HCl, pH 7.6, 137 mM NaCl, and 0.1% Tween-20) and then blocked with TBS-T 5% milk powder for 1 hour. After blocking the filters were then incubated for 2 hours with [^{35}S-methionine] labelled NS1 expressed from a recombinant baculovirus. The filters were washed 5 times in TBS-T, dried on blotting paper and viewed via radiography to identify positive plaques that bound NS1; the corresponding

plaques were then purified with 3 rounds of plaque assays. BM25.8, an E. coli strain that expresses Cre recombinase, was infected with the purified phage λTripl Ex2 which contains *loxP* sites flanking the embedded plasmid pTripl Ex2 (containing the cDNA insert). The plasmid was excised using Cre-mediated site specific recombination at 31°C, for 1.5 hours, and the resulting colonies containing the plasmid were selected for using ampicillin selection. The plasmids were then amplified and purified by normal DNA purification protocols. Any further studies with the purified plasmids were performed in DH5α strain *E. coli* to prevent further recombination.

3' sequencing primer: TAATACGACTCACTATAGGGC

5' sequencing primer: CTCCGAGATCTGGACGAGC

3.13: Yeast Two-Hybrid System

3.13.1: Yeast strains

The yeast strains of *Saccaromyces cerevisiae* routinely used for yeast two-hybrid analysis were propagated on complete nutrient media, YPDA (10g yeast extract, 10g bactopeptone and 20g dextrose per litre, pH 5.6. For solid YPDA add 15g agar), and kept at 4°C. AH109 and Y187 were used for the mating screen (AH109 being the A strain and Y187 being the α strain), PJ694A was used for the HeLa cDNA screen. These yeast strains are defective in various nutritional pathways which are complemented by the plasmids used in this system; without the plasmids these yeast strains can only be propagated on YPDA.

Yeast strain	Auxotrophic requirements	Plasmid complementing the mutation
AH109, Y187 and PJ694A	trp1-901 genotype, requires tryptophan for growth	pAS2-1 and recombinant plasmids e.g. pAS-NS1 and pAS-VP7
	leu2-3, 112 genotype, requires leucine for growth	pACT2 and pGADT7-Rec plasmids e.g. library plasmids and pACT-VP7
AH109 and pJ694A	ADE2	Interaction of the GAL4 transcription factor domains, as a result of interaction of the recombinant proteins fused to them, gives complementation.
	HIS3	

Table 3. 1: Table of all the auxotrophic properties of the yeast strains used and the plasmids that complement each mutation (for further information on complementation of Ade2 and His3 mutations see figure 3.1).

3.13.2: Yeast transformation

Yeast were grown in YPDA liquid culture over night and grown to an OD_{600} of 1.0. Yeast were pelleted and washed in 100mM LiOAc before re-suspension in 100mM LiOAc. Approximately 5.0 x 10^7 yeast were combined with 33% PEG 3350, 100mM LiOAc, 300μM ssDNA (from salmon testes) and 1μg of plasmid in a final volume of 180μl and incubated for 30 minutes at 30°C. After a further 30 minute incubation at 42°C yeast were centrifuged and re-suspended in SDW before plating on minimal media minus the appropriate amino acids to allow plasmid selection, see table 3.1 (SM minimal media (6.7g yeast nitrogen base, 20g dextrose and dried amino acid mix that does not contain adenine (A), tryptophan (W), histidine (H) and leucine (L)) with H, A, L and W added to the appropriate concentrations when needed).

3.13.3: Yeast mating

Approximately 1 x 10^{10} Y187 yeast containing the bait DNA-BD plasmid were combined with 1 x 10^{8} AH109 yeast containing the prey DNA-AD plasmid on a 15cm plate of complete YPDA agar. This was incubated at 30°C for 12 hours before the yeast were washed off using PBS and sterile glass beads. Yeast were centrifuged and resuspended in SDW before plating on SM media minus the appropriate amino acids to select for the plasmid or the plasmid and protein interactions.

3.13.4: Plasmid isolation

Yeast were grown in liquid culture overnight, centrifuged and resuspended in lysis buffer (25mM Tris pH8, 10mM EDTA pH 8, 1% SDS, 1% NLS and 0.3M NaOAc). Phenol: chloroform was added to 20% with sterile glass beads and the solution was vortexed for 3 minutes. The aqueous phase was recovered and isopropanol precipitated. The pellet was re-suspended in SDW and RNA was precipitated in 3M NaOAc on ice for 30 minutes, the resulting supernatant was isopropanol precipitated. Chromosomal DNA was removed from the pellet in 6.5% PEG 8000, 0.8M NaCl on ice for 10 minutes. After centrifugation the resulting pellet of plasmid DNA was resuspended in SDW.

3.13.5: Library Screening

The HeLa yeast two-hybrid library was screened following the protocol supplied with the library by co-transfection of the bait plasmid (NS1-DNABD) and the library plasmids. Yeast (PJ694A) containing pAS-NS1 was transformed with the library plasmid and plated on SM media minus leucine and tryptophan, selecting for the

presence of both plasmids which complement the auxotrophic requirements of the yeast parent. Interacting bait and prey proteins were identified by replica plating onto a further selection of SM media minus histidine and adenine, in addition to leucine and tryptophan, on this media the yeast will only grow if the 2 proteins interact bringing together the GAL4 DNA binding and activation domains (Fig 3.1). This step was repeated to minimise the number of false positives. The library plasmids were extracted and re-transformed in parallel into yeast containing either pAS-NS1 to confirm the interaction or pAS-VP7 to isolate non-specific interactions. The cDNA inserts identified as putative positives by interacting with pAS-NS1 but not pAS-VP7, were sequenced using primers specific to the 3' and 5' flanking regions of the cDNA insert.

3' sequencing plasmid: 5'------GAA GAT ACC CCA CCA AAC CC---------3'

5' sequencing plasmid: 5'------GA AGG CCT GAA TTC AGA TCT GCC---3'

The Kc and *A. aegypti* cDNA libraries were screened as above with the exception that the plasmids were not co-transformed. The library plasmid was constructed by recombination, in the yeast strain AH109, of the cDNA insert and linearised plasmid, and then mated on YPD agar overnight with yeast strainY187 pre-transformed with pAS-NS1. Yeast containing both plasmids was selected for as above and then replica plated to select for interaction as above. The positives were sequenced using the primers, 3' sequencing plasmid and 5' sequencing plasmid, as described for sequencing of the HeLa cDNA library.

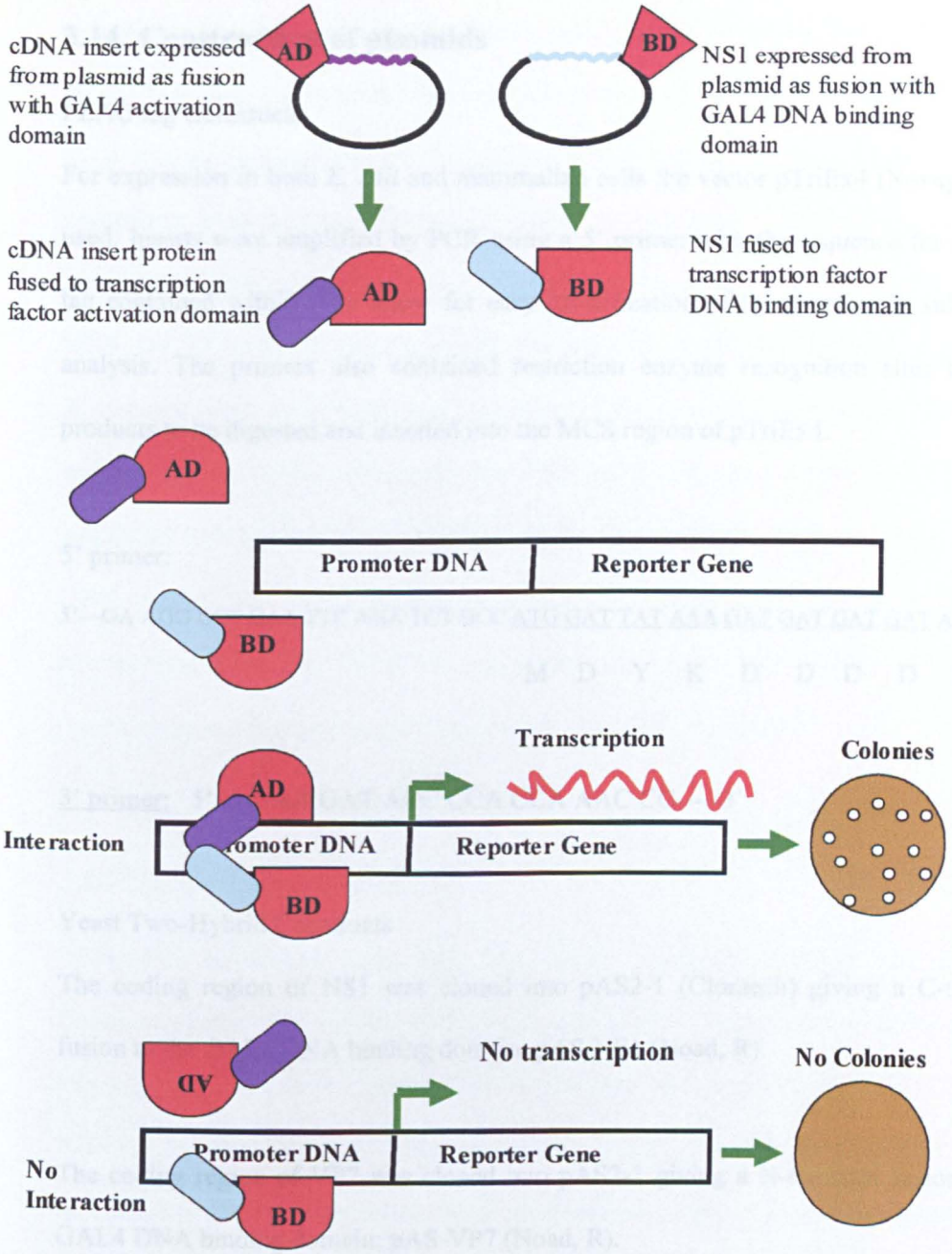

Figure 3. 2: Schematic of the yeast two-hybrid system screening process, detailing the interactions of the GAL4 domains necessary for identification of the cDNA interactions to occur.

3.14: Construction of plasmids

FLAG tag Constructs

For expression in both *E. coli* and mammalian cells the vector pTriEx4 (Novagen) was used. Inserts were amplified by PCR using a 5' primer with the sequence for a FLAG tag contained within it to allow for easy identification of the proteins in subsequent analysis. The primers also contained restriction enzyme recognition sites to allow products to be digested and inserted into the MCS region of pTriEx4.

5' primer:

5'---GA AGG CCT GAA TTC AGA TCT GCC ATG GAT TAT AAA GAT GAT GAT GAT AAA----3'

M D Y K D D D D K

3' primer: 5'----GAA GAT ACC CCA CCA AAC CC-----3'

Yeast Two-Hybrid Constructs

The coding region of NS1 was cloned into pAS2-1 (Clontech) giving a C-terminal fusion to the GAL4 DNA binding domain; pAS-NS1 (Noad, R).

The coding region of VP7 was cloned into pAS2-1 giving a N-terminal fusion to the GAL4 DNA binding domain; pAS-VP7 (Noad, R).

3.15: Plasmid DNA Purification

Plasmids were transformed into competent *E. coli* DH5α by heat shock at 42°C and then grown in 50ml liquid culture for approximately16 hours. *E. coli* was harvested via

centrifugation and re-suspended in 6ml 25mM Tris, 10mM EDTA. 9ml 0.2M NaOH , 1% SDS to lyse the bacterial cells and denature DNA, the protein and chromosomal DNA was then precipitated by the addition of 7ml 4M KOAc and centrifugation. The supernatant was strained through 2 layers of wet muslin and nucleic acid was precipitated using isopropanol and centrifugation. The pellet was re-suspended in 185μl SDW, and 555μl of 4M NaOAc pH 6.0 was added; the RNA was precipitated on ice for 30 minutes. After centrifugation at 13000 rpm the supernatant was harvested and DNA was precipitated with isopropanol. The DNA pellet was re-suspended in 600μl SDW and 600μl 13% PEG 8000 1.6M NaCl was added; the centrifugation was repeated. This DNA pellet was re-suspended thoroughly in 700μl of SDW and 200μl of phenol/chloroform was added. The supernatant was clarified by centrifugation and the purified plasmid was precipitated by NaOAc/ethanol precipitation.

3.16: Sequencing of DNA

DNA was sequenced using Big Dye chain terminator reaction mix (Applied Biosystems) in a total volume of 10μl (4.4μl of DNA (50ng/μl), 4μl of ABI version 3 mix and 1.6μl of primer (1pmol/μl)). The reaction was heated to 96°C for 2 minutes followed by 35 cycles of 96°C for 30 seconds, 50-58°C for 15 seconds and 60°C for 4 minutes. The DNA was prepared for gel sequencing by NaOAc/ethanol precipitation (to the 10μl reaction add 3μl NaOAc pH5.2 and 86μl 70% ethanol, incubate at room temperature for 15 minutes and centrifuge at 13000 rpm for 20 minutes. Wash the pellet twice in 500μl 70% ethanol to remove the excess salt and dry) and analysed on an ABI prism 337 DNA sequencer.

3.17: SDS PAGE and Western Blot Analysis

Protein samples were analysed on 10% polyacrylamide SDS gels and then either visualised by coomassie staining or western blotting. To stain gels with coomassie blue, gels were fixed in destain buffer (450ml methanol, 100ml acetic acid and 450ml water per litre) for 20 minutes and then stained in coomassie blue buffer (450ml methanol, 100ml acetic acid, 450ml water and 2.5g coomassie brilliant blue per litre) overnight. The excess staining was removed by washing in destain buffer until only the proteins were stained.

For analysis by western blot proteins were transferred by western blotting at 100mAmp for 1 hour to nitrocellulose membranes. The membranes were blocked in PBS-T 5% milk powder (0.05% tween 20 in PBS (0.01 M phosphate buffer, 0.0027 M potassium chloride and 0.137 M sodium chloride) pH 7.4,) for 1 hour before being probed with primary antibodies at a 1/1000 dilution, in PBS-T milk, against the desired proteins over night. The membranes were washed then re-probed with secondary antibodies conjugated with alkaline phosphatase diluted at 1/10000 in PBS-T milk, and the protein bands were visualised using Lumiphos (Pierce) and chemiluminescence detection by film, or Sigma fast tablets (Sigma).

3.18: Antibodies

Antibody	Protein detected	Techniques used for
Rabbit anti-BTV-10 (R)	BTV-10 proteins	Western blot
Mouse anti-VP2	VP2	Western blot
Rabbit anti-VP3	VP3	Immunofluorescence
Guinea pig anti-VP5 (GP)	VP5	IImmunofluorescence, immunoprecipitation,
Mouse anti-VP7 (MAb 11A10)	VP7	Immunofluorescence, immunoprecipitation, western blot
Rabbit anti-NS1 (R633)	NS1	Western blot
Guinea pig anti-NS1 (GP 791)	NS1	Immunofluorescence, immunoprecipitation
Guinea pig anti-NS2 (GP 373)	NS2	Immunofluorescence, immunoprecipitation
Mouse anti-NS3 (AF 434)	NS3	Immunofluorescence, western blot
Rabbit anti-CBP (Upstate)	Calmodulin binding protein	Western blot
Mouse anti- α tubulin (Sc 5286, Santa Cruz Biotechnology)	α tubulin	Immunofluorescence
Goat anti-actin (Sc 1616, Santa Cruz Biotechnology)	Actin	Immunofluorescence, western blot
Goat anti-vimentin (Sc 7557, Santa Cruz Biotechnology)	Vimentin	Immunofluorescence, western blot
mouse anti-Caspase 3 (eBioscience, San Diego, CA)	Caspase 3	Western blot
Rabbit anti-SUMO-1 (Sc 5308, Santa Cruz Biotechnology)	SUMO-1	Immunofluorescence, western blot, immunoprecipitation
Mouse anti-FLAG (Sigma)	FLAG peptide	Immunofluorescence, western blot, immunoprecipitation

Table 3. 2: Antibodies used in methods described in this thesis.

3.19: Confocal Immunofluorescence Microscopy

Cells (BSR, 293T or *Sf*21) were cultured on glass cover slips in 24 well tissue culture plates and where necessary infected with BTV-10 and/or transfected with plasmids expressing various proteins (BTV-10 NS1, FLAG tagged cDNA inserts or SUMO-1). Cells were washed with PBS and fixed using cold PBS 4% paraformaldehyde at room temperature for 30 minutes, the washes were repeated. Cells were permeablised with PBS 1% Triton X-100 for 10 minutes and then washed. Cells were incubated with primary antibody at a dilution of 1/100 to 1/300 for 20 minutes, washed and then incubated with secondary antibody conjugated to FITC or TRITC stains for 30 minutes. During staining with the secondary antibody the nuclei were also stained using Hoesch stain (Sigma-Aldrich), at a concentration of 10μg/ml. Cover slips were washed and mounted in 5μl of mountant on slides, the edges were sealed with clear nail varnish and slides were examined using a Zeiss LSH 510 confocal microscope and images were elaborated using LSH 510 image browser software.

3.20: Radio-labelling of Proteins

Proteins under the control of the T7 promoter (cloned into plasmid pOcus or pTriEx4, both Novagen,) were transcribed and translated *in vitro* using the TNT T7 quick coupled transcription/translation kit (Promega). The plasmid was incubated with the rabbit reticulocyte lysate mix and [^{35}S] methionine at 30°C for 90 minutes and the labelled proteins were then analysed by SDS PAGE. The TNT kit combines T7 RNA polymerase to transcribe RNA from the T7 promoter, and rabbit reticulocytes, which provide the tRNA, ribosomes, amino acids, initiation, elongation and termination

factors needed for translation. The labelled methionine is incorporated into the proteins as they are translated as it is the only source of methionine in the mix.

Proteins expressed in the baculovirus system can also be labelled. *Sf*9 cells were grown in tissue culture plates and infected as described in chapter 3.7; 24 hours post infection cells were washed in SF900 II minus L-methionine (Invitrogen), and then incubated for 30 minutes in this media. After this starvation period the media was supplemented with 0.6MBq ^{35}S labelled L- methionine and incubated at 28°C for 2 hours, proteins made during this time incorporated the labelled methionine as the non-labelled methionine was limited by the previous starvation step. Labelled proteins were harvested via cell lysis.

3.21: Co-immunoprecipitation

Test proteins were co-expressed and radio-labelled using co-infection of recombinant baculoviruses (*Sf*9 cells lysed using freeze thaw in 25mM$NaHCO_3$) or the *in vitro* TNT system (chapter 3.20). Protein A sepharose beads were prepared in IP buffer (50mM Tris pH 7.4, 150mM NaCl, 1mM EDTA, 0.025% NP40) and incubated at 4°C, with rolling, for 1 hour with primary antibody (against one of the proteins being isolated e.g. anti-NS1 antibody). The beads were then washed 4 times in IP buffer and a further twice in Native IP buffer (50mM Tris pH 7.4, 150mM NaCl, 1mM EDTA, 0.5% NP40, 0.05% deoxycholate). The beads were re-suspended in Native IP buffer (0.05% deoxycholate for medium stringency) and the labelled proteins were added. After 1 hour incubation at 4°C, with rolling, the beads were washed three times and the samples were re-suspended in SDS PAGE loading buffer (removes any proteins from the beads for analysis as normal) and analysed by SDS PAGE and autoradiography.

3.22: TAP tag Construct and Purification

NS1 was cloned into pNTAP B (Stratagene) for expression of N-terminal TAP tagged NS1 in mammalian cells. NS1 was amplified by PCR from PNSS (a plasmid containing full length NS1 already analysed for tubule production) to give Bam HI and Eco RI sites for directional cloning (primers NS1 fwd and NS1 rev below). NS1 was digested and inserted into pNTAP B, which was digested with the same enzymes, giving pTAPBNS1.

NS1 fwd: 5'----CTG GAA TTC GGA TCC TCT AGT TGG CAA CCA CCA------3'

Eco RI Bam HI

NS1 rev: 5'----CTG CTC GAG GAA TTC ATA CTC CAT CCA CAT CTG AG--3'

Xho I Eco RI

The TAP tag of pTAPBNS1 contains a streptavidin binding site and a calmodulin binding site. NS1 can be purified via both tags yielding NS1 plus any proteins that interact with NS1 in the mammalian cell culture system.

Tandem affinity purification of TAPBNS1 was performed by joining two well known purification procedures together. The streptavidin purification protocol from the Stratagene Interplay mammalian TAP system was followed using buffers, SBB and SEB, and the calmodulin binding protein purification protocol from the Stratagene Interplay mammalian TAP system was followed using buffers, CBB and CEB.

SBB: 40mM Tris pH 8.0, 300mM KCl, 2mM EDTA, 0.1% Triton X 100, 5mM βME, 100μg/ml BSA, 20μl/ml PIC (protease inhibitor cocktail, Sigma) and 1mM pefabloc (Sigma).

SEB: SBB plus 2mM biotin

CBB: 10mM tris pH 8.0, 150mM NaCl, 0.1% imidazole, 2mM $CaCl_2$, 5mM βME, 20μl/ml PIC and 1mM pefabloc (Sigma).

CEB: 10mM Tris pH 8.0, 2mM EGTA, 0.1% NP40, 1mM imidazole and 10mM βME.

Streptavidin beads were washed 5 times in SBB and then re-suspended in SBB. TAPBNS1 was expressed in 293T cells which were then lysed by dounce homogenisation in PBS 0.5% Triton X 100. Cell lysate was clarified by centrifugation and the supernatant was added to the streptavidin beads and incubated at 4°C for 2 hours, with rolling. The beads were washed 3 times in SBB and then re-suspended in SEB (contains 2mM biotin which competes for the streptavidin, displacing the protein from the beads and into the eluate) and incubated at 4°C for 2 hours, with rolling. The supernatant was collected and $CaCl_2$ (Ca^{2+} is needed for binding of the CBP tag to the calmodulin beads) was added to a final concentration of 2mM, the supernatant was then added to the calmodulin beads in CBB (washed and re-suspended in CBB) and incubated at 4°C for 2 hours, with rolling. The beads were washed 3 times and re-suspended in CEB (contains 2mM EGTA to chelate the Ca^{2+} ions dissociating the tagged protein from the calmodulin beads) and incubated at 4°C for 2 hours, with rolling. The eluate and beads were harvested and analysed via SDS PAGE and western blot alongside samples from each step of the protocol.

3.23: Caspase 3 Assay

293T cells were transfected with plasmids expressing the yeast positive TY7 and NS1 protein under the cytomegalovirus promoter (CMV), a pol II based promoter, and incubated for 20 hours. Cells were harvested by centrifugation and re-suspended in lysis buffer (PBS 0.5% Triton X 100) containing protease inhibitors (PIC Sigma). After 4 cycles of freeze-thaw, cell debris was pelleted by centrifugation and the supernatant harvested. The supernatant was analysed by western blot using mouse Ig G anti-Caspase 3 (eBioscience, San Diego, CA) and lumiphos (PIERCE). The blot was visualised using hyperfilm (Amersham-Pharmecia Biotech).

3.24: DNA Fragmentation Assay

293T cells were transfected with plasmids expressing the yeast positive TY7 and NS1 protein under the CMV promoter and incubated for 20 hours. Cells were harvested by centrifugation and re-suspended in lysis buffer (PBS 0.5% Triton X 100) containing protease inhibitors (PIC Sigma). After 4 cycles of freeze-thaw, cell debris was pelleted by centrifugation and the supernatant harvested. The supernatant was incubated for 1 hour at 50°C with RNase A at 50μg/ml to remove RNA from the sample which affects the results when visualised by UV. The cell supernatant was then clarified by phenol/chloroform precipitation and the aqueous phase containing total cellular DNA was harvested. The DNA was precipitated in 3M NaOAc pH7.4 and 70% ethanol to concentrate it and washed twice in 70% ethanol to remove excess salt. The DNA pellet was air dried, re-suspended in SDW and analysed on a 2% agarose gel.

3.25: ELISA

ELISA (enzyme linked immunosorbent assay) assays were performed by coating 96 well plates with purified NS1 tubules over night at room temperature. Wells were washed 3 times with PBS and blocked with either PBS 5% milk or PBS 5% BSA for 2 hours at 37°C; washes were repeated. The test FLAG tagged protein was added to the wells and incubated for 90 minutes at room temperature; wells were washed 3 times with PBS and then primary antibody, mouse anti-FLAG antibody (Sigma), was added and incubated at room temperature for 2 hours. After washing a further 3 times secondary anti-mouse-HRP conjugate (Sigma) was added and incubated for 2 hours at room temperature. The wells were washed extensively (6 times) and 100μl of TMB liquid for ELISA (Sigma) was added, this produced a blue colour in wells that contained the FLAG tagged product binding both primary and secondary antibodies (this indicated an interaction between the FLAG tagged protein and NS1). Once the blue coloured product appeared the reaction was stopped immediately by the addition of 50μl 1/10 HCl. The colour change product was read on a plate scanner, stronger signals indicated more binding of the FLAG tagged proteins to NS1.

3.26: NS1 Tubule Purification

NS1 expressed by baculovirus produces large amounts of tubules that can be purified by sucrose gradient. Cells expressing NS1 (mammalian cells infected with virus or transfected with plasmid, or *Sf*9 cells infected with recombinant baculovirus) were lysed in STE buffer (150mM NaCl, 1mM EDTA, 10mM Tris pH 7.5) with 0.5% Triton X-100 (Sigma) and dounce homogenisation. The cell lysate was clarified by centrifugation and the supernatant was loaded onto a 2ml 40% sucrose cushion in STE buffer. Tubules

accumulate in a pellet having passed through the sucrose cushion, leaving smaller cellular material above the sucrose cushion, by ultra-centrifugation at 35 000rpm for 2 hours. The sucrose cushion was then diluted with STE buffer to a volume of 5ml and loaded onto a continuous sucrose gradient of 10-40% before ultra-centrifugation at 20 000rpm for 1 hour. The gradient is collected in 1ml samples and each sample is analysed by SDS PAGE and/or western blot, tubules are large and vary in length so should be present in middle to bottom fractions of the gradient.

3.27: Disruption of Intermediate Filaments

293T or BSR cells were grown in 6 well plates, or on cover slips as for confocal immunofluorescence microscopy, in MEM 10% FCS or DMEM 10% FCS respectively. Cells were infected with BTV-10 at an MOI of 1, and left to adsorb at 4°C for 1 hour. The inoculum was removed and fresh media was added. Cells were maintained until harvest in MEM/DMEM media supplemented with 2% FCS, containing 0mM acrylamide as a negative control or 2mM acrylamide at 35°C, 5% CO_2. Cells were harvested or fixed and the effects of acrylamide on virus replication and protein expression/distribution were examined by immunofluorescence, western blot and virus titre analysis.

3.28: siRNA design and optimisation

siRNA against NS1 was designed as an RNA molecule, to be transfected directly into cells, using the design tool, siMAX™, supplied on the MWG website (http://www.mwg-biotech.com/html/s_synthetic_acids/s_rna.shtml). The tool ranks

potential siRNA according to their ability to fulfil 12 criteria including GC content, secondary structure and critical positioning of specific nucleotide bases in the siRNA sequence. The siRNA that achieved the highest rank for potential knockdown in the modelling design tool is aimed at region 347 – 365 of NS1.

NS1 siRNA; Sense strand 5'--- UGA UGG AGG CUA UUA ATT---3'

siRNA against SUMO-1 was pre-designed by Ambion (http://www.ambion.com), two siRNA were used with the following sequences:

siRNA 138970: 5'--- GGU GAG AGU AAU GAC UAA Ctt----3'

3'--tt CCA CUC UCA UUA CUG AUU G------5'

siRNA 13183: 5'--- GGA AGA AGA UGU GAU UGA Att----3'

3'--ct CCU UCU UCU ACA CUA ACU U -----5'

Fluorescein labelled scramble siRNA (NEB) was used as a transfection efficiency control. The double-stranded siRNA is 21 bases in length (19 of these are complementary and base pair, the remaining 2 bases overhang at the 3' terminus) and has a fluorescein molecule linked to the 5' termini of both strands. This control has no sequence identity to any mammalian sequences in the database and has the following sequence:

Fluorescein-5'----AGG UCG AAC UAC GGG UCA AUC----3'

Fluorescein-5'----UUG ACC CGU AGU UCG ACC UAG----3'

3.29: siRNA transfection in mammalian cells

siRNA was transfected into 293T cells twice, once at 24 hours prior to infection and a second time 12 hours prior to infection with BTV-10. 100ng of siRNA was used per well on a 24 well plate and either Lipofectamine 2000 (Invitrogen) or simporter (Upstate) transfection reagent was used.

293T cells were grown in 24 well plates until 90% confluent, washed in serum free MEM and incubated with 500μl of serum free MEM. 100μl of serum free OPTIMEM was mixed with 1μl of transfection reagent and incubated at room temperature for 5 minutes. In a separate tube 100μl of serum free OPTIMEM was mixed with 100ng siRNA (volumes given per well). The 2 tubes were mixed and incubated at room temperature for 30 minutes then added to one well of cells. FCS was not added to the wells after the first transfection but was added after the second transfection to a final concentration of 2%. Cells were not washed prior to the second transfection or prior to infection with BTV-10 as better transfection efficiencies were obtained if the transfection mix remained on the cells.

Transfection efficiency was highly variable dependant upon cell condition, confluency of the monolayer and amount of siRNA used; some cell death was detected after the second transfection in every experiment performed. Cells were always transfected for

the first time, 24 hours prior to infection, at a confluency of approximately 90%; only fresh cells seeded the day prior to transfection were used.

3.30: Preparation of Cells for Electron Microscopy

293T and BSR α NS1 cells were grown as in Chapter 3.1 in T-75 flasks. 293T cells were transfected with the appropriate siRNA, specific to NS1 or control scramble siRNA, or left un-transfected as positive control. The flasks were infected with BTV-10 at an MOI of 1, except for the negative control which was neither transfected nor infected, and incubated for 18 hours at 35°C, 5% CO_2. The monolayer was washed with serum free DMEM pre-warmed to 37°C and then fixative 1 (3% gluteraldehyde in serum free DMEM pH 7.4) pre-warmed to 37°C was added. Cells were immediately scraped off the flask in large sheets and incubated for 15 minutes. Cell sheets were pelleted gently at room temperature for 5 minutes, 3000rpm and re-suspended in fixative 2 (3% gluteraldehyde in 0.2M sodium cacodylate buffer pH 7.4), pre-warmed to room temperature, and subsequently incubated at 4°C for 2 hours.

The cells were washed in 0.2M sodium cacodylate buffer for 15 minutes, this step was repeated 4 times. Cells were then osmicated in 1% OsO_4 for 90 minutes and the washes were repeated as above and then again using SDW. Cells were added to 2% LMP agarose in SDW and incubated at 45°C for 2 hours. The cell samples were then dehydrated, for 10 minutes in each solution, in ever increasing concentrations of methanol starting at 30% and continuing to 100%. The dehydrated cells were treated with propylene oxide at a 1:1 ratio with 100% methanol for 10 minutes before treatment with propylene oxide only for 10 minutes. The propylene oxide was replaced with propylene oxide at a 1:1 ratio with TAAB resin for 10 minutes and then incubated

overnight at room temperature with TAAB resin only. Fresh TAAB resin was added before the samples were embedded and polymerised at 60°C for 24-48 hours.

Cell samples were fixed, sectioned and examined by Maria McCrossan and Dr David Ellis using transmission electron microscopy before digital capturing of the images.

4: Identification of Interactions between NS1 and Mammalian Cellular Proteins

4.1 Introduction

Viruses encode few proteins in comparison to their complex mammalian hosts and therefore use host macromolecular machinery and materials to replicate successfully. This dependence means that viruses have adapted a variety of mechanisms for exploiting host cell functions. Since this is often detrimental to the cell, the virus must either replicate fast enough for this to be negligible or must evolve mechanisms of limiting damage and evading host immune responses until its replication cycle is complete.

During virus infection there are continuous interactions between the virus and the host, some interactions are the use of housekeeping cellular processes such as DNA replication, RNA translation and protein maturation pathways. Other interactions are an interference of cellular functions providing more favourable conditions for virus replication, for example the interference of the interferon and related pathways by viruses with single-stranded RNA genomes allowing evasion of this cellular antiviral pathway (Diamond 2003).

BTV has 4 non-structural proteins which do not have any enzymatic function assigned; it is therefore likely that they perform some other role in virus replication. NS2 is known to bind ssRNA and is present in large amounts at the site of virus replication

(Thomas, Booth et al. 1990); it is probable that NS2 is involved in recruiting and packaging of ssRNA before encapsidation, potentially using specific RNA structures or sequences to ensure that 10 different RNAs are packaged in each virion. NS3 has a role in virus egress from the cells which it achieves via interactions with several cellular proteins including the calpactin light chain (p11) and TSG101 (Beaton, Rodriguez et al. 2002; Wirblich, Bhattacharya et al. 2006).

NS1 has no known role in BTV replication, although given that it is the most highly expressed viral protein it is likely to have an important role. It has been linked to virus egress although given that NS3 also has a role in this it can be assumed that NS1 will have more than one function. There is no current explanation for the differences in pathogenesis and virus egress between insect and mammalian cells and little is known of the cellular proteins that BTV interacts with.

The yeast two-hybrid system is well known for its use in identifying protein-protein interactions using a specified bait protein. Large numbers of potential interactions can be screened as the interaction is based on a powerful growth selection from the conditional expression of the yeast HIS3 reporter gene. A second conditional reporter gene ADE2 increases the stringency of this screening method. Using the specified protein fused to the GAL-4 DNA binding domain as bait, interacting clones fused to the GAL-4 activation domain can be quickly identified and processed for use in subsequent analysis.

Another useful method for identifying protein-protein interactions is the TAP tag tandem affinity purification system. This method identifies proteins that interact *in vivo*

and therefore produces less false positives than the yeast two-hybrid system. The protein of interest is cloned with a TAP tag consisting of the streptavidin binding protein and the calmodulin binding protein. This dual tag is used for a double purification of the tagged protein without the use of harsh buffers; this ensures that any proteins that have a strong interaction with the tagged protein are co-purified. Co-purifying proteins are identified by mass spectrometry and further analysis can be completed.

Previous work on NS1 interactions identified a putative interaction between SUMO-1 and NS1, by yeast two-hybrid analysis using NS1 with an N-terminal tag to the GAL4 DNA binding domain (pAS2-NS1) as bait (Noad, R and Roy, P; personal communication). SUMO-1 was isolated from this screen on 5 separate occasions and confirmed as a positive by retransformation into yeast containing pAS2-NS1. Further confirmation of this interaction was provided by confocal immunofluorescence microscopy analysis indicating co-localisation between SUMO-1 and plasmid expressed, or BTV-10 expressed, NS1 in mammalian cells.

Basal levels of SUMO-1 were not detectable by western blot or confocal analysis in uninfected cells. However BTV-10 infection readily induced SUMO-1 expression within 293T and BSR cells; sumoylated proteins were detected as early as 1 hour post infection. A variety of sumoylated products were detected by western blot analysis, these were 30, 43, 58, 70 and 80 kDa in size (Fig 4.1); none of these proteins were identified as BTV proteins. Confocal analysis of BTV-10 infected cells detected SUMO-1 localising in distinct foci within the cell, not all of which co-localised with NS1. Further analysis showed SUMO-1 induction to be a specific response to BTV-10

infection as no SUMO-1 could be detected by subjecting 293T or BSR cells to infection by Fowl pox virus or heat shock stress (Fig 4.1).

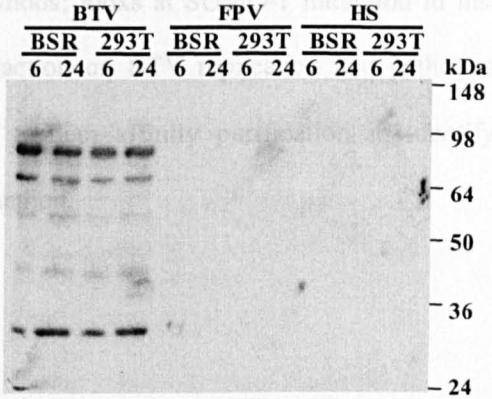

Figure 4. 1: Western blot comparison of sumoylation patterns following a variety of 'stresses' in 293T and BSR cells. Cells were treated with BTV-10, Fowl pox virus (FPV) or heat shock at 42°C (HS) and harvested at 6 and 24 hours. Note the identical patterns of sumoylated proteins in BTV-10 infected 293T and BSR cells (Noad, R and Roy, P; personal communication).

NS1 alone was insufficient to induce expression of SUMO-1 within mammalian cells and interaction *in vitro* was not proved as immunoprecipitation could not be achieved with either anti-NS1 or anti-SUMO-1 antibodies. It was hypothesised from this data that SUMO-1 may be induced due to specific stresses caused by BTV-10 infection, and that since there is no covalent modification of NS1 by SUMO-1, NS1 may be binding sumoylated transcription factors and retarding their translocation to the nucleus. Thus NS1 would be modulating the host response to BTV infection in a way that was advantageous for the virus.

This chapter describes the identification of mammalian proteins that interact with NS1 using the yeast two-hybrid system and the subsequent verification of the results by biochemical methods. This chapter also confirms the interaction of NS1 with SUMO-1 by biochemical methods; looks at SUMO-1 induction in insect cells and analyses the impact of the interaction on BTV replication and pathogenesis. Finally this chapter studies the use of tandem affinity purification in identifying interactions and the drawbacks of this method.

4.2: Results

Several approaches were employed to identify mammalian proteins that interact with NS1. The main method used was a yeast two-hybrid screen using the coding region of NS1 with the GAL4 DNA binding domain tagged to the C- terminus (pAS-NS1) as bait and a human HeLa cDNA library expressed with the DNA activation domain tagged to the N-terminus as prey.

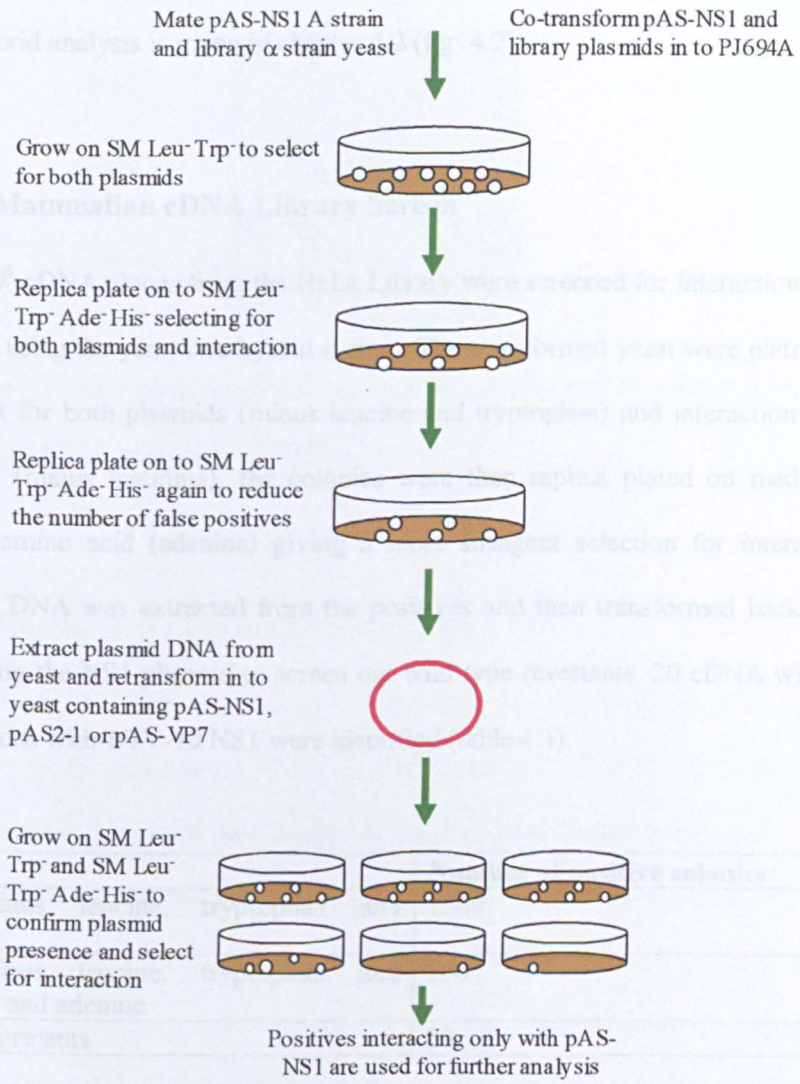

Figure 4.2: Overview of the procedure used to identify putative positives in the yeast two-hybrid screen, indicating selective media at each stage.

Although humans are not the mammalian host for BTV, human cell lines are permissive to BTV infection *in vitro*. Many of the house keeping genes in human cells will show some homology to sheep genes, thus proteins identified in this screen, despite being human, may be extrapolated to sheep and other mammalian hosts. However it worth considering the strict host range displayed by BTV when extrapolating data between species where one is infected and one is not. A description of the yeast two-hybrid system is given in chapter 3.13, figure 3.1; an overview of the procedure used for yeast two-hybrid analysis is given in chapter 4.2 (fig: 4.2).

4.2.1: Mammalian cDNA Library Screen

1.3 x 10^6 cDNA clones from the HeLa Library were screened for interaction with BTV-10 NS1 using the yeast two hybrid system. The transformed yeast were plated on media to select for both plasmids (minus leucine and tryptophan) and interaction of the two proteins (minus histidine), the colonies were then replica plated on media minus a further amino acid (adenine) giving a more stringent selection for interaction. The plasmid DNA was extracted from the positives and then transformed back into yeast containing the NS1 plasmid to screen out wild type revertants. 20 cDNA with putative interactions with BTV-10 NS1 were identified (table 4.1).

	Number of positive colonies
SM minus leucine, tryptophan and histidine	1500
SM minus leucine, tryptophan and histidine and adenine	300
Retransformants	20

Table 4. 1: Number of yeast colonies after each step in the screening procedure.

The 20 positives were verified as interacting in yeast with three bait constructs; pAS-NS1 to confirm the interaction, pAS2-NS1 (N-terminal fusion to the DNA binding domain) to see if the position of the tag affected interaction and AS2-VP7 to screen out non-specific interactions. All of the yeast positives screened in this way interacted only with pAS-NS1, data for 3 separate positives is shown in figure 4.3.

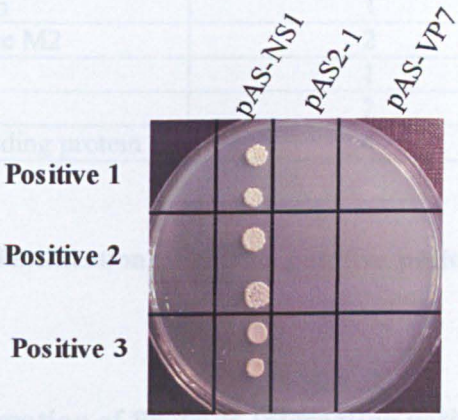

Figure 4.3: Yeast re-transformation analysis of 3 putative positives with (a) pAS-NS1, (b) pAS2-1 and (c) pAS-VP7.

4.2.2: Proteins and Peptides interacting with NS1

Many of the 20 cDNAs isolated encode for short peptides from out of frame truncated proteins e.g. 15 amino acids of out of frame translated BAF155, peptide TY7 (Table 4.2). Four of the positives gave longer in-frame peptides from human genes, Nucleotide binding protein 1 (NUBP1), aldolase A, cathespin B and pyruvate kinase M2 (PKM2). Cathespin B is a proteolytic protein found in cellular lysosomes and is unlikely to represent a real partner for NS1; it was therefore dismissed as a yeast two-hybrid artefact. PKM2 was not studied further as I was unable to produce a plasmid with this cDNA product fused to a FLAG tag. One of the two-hybrid positives that interacted

with NS1, the peptide TY7, was found to induce cell death only on co-expression with NS1 in mammalian cells.

Positive	Number of times isolated	Number of amino acids translated
Out of frame truncation (various)	10	6-20
TY7 truncation	1	15
Pyruvate kinase M2	2	238 (aa 191- 429)
Aldolase A	1	233 (aa 121- 354)
Cathespin B	2	198 (aa 142- 340)
Nucleotide binding protein 1	4	218 (aa 2- 220)

Table 4. 2: Identification of the 20 putative positives from the yeast two-hybrid screen.

4.2.3: Confirmation of Proteins Interacting with NS1

Further confirmation of the interactions was necessary; an overview of the steps taken to achieve this is shown in figure 4.4.

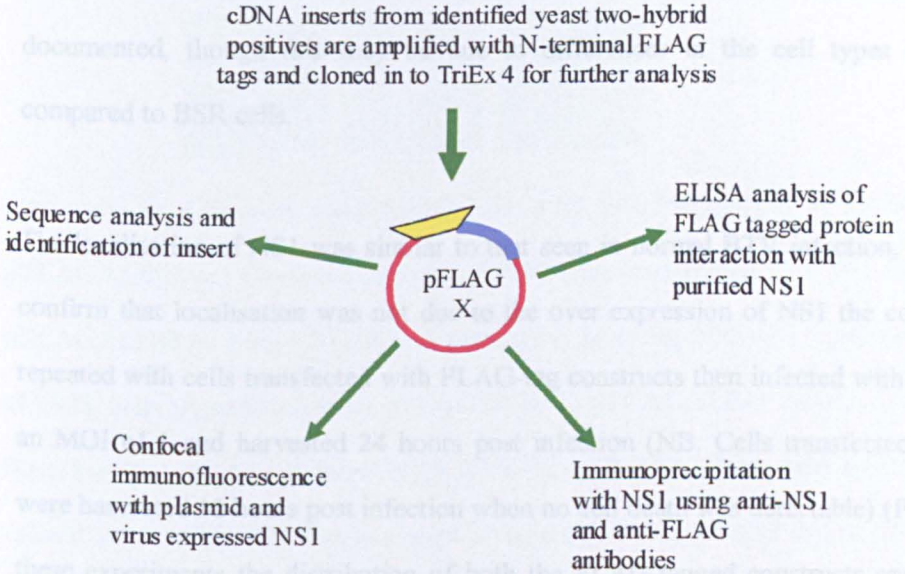

Figure 4. 4: Overview of the biochemical procedures used to confirm putative positives.

To further confirm the interaction of NUBP1 and aldolase A with NS1 the cDNA inserts were amplified by PCR from the cDNA library plasmid to give an N-terminal FLAG tag and then cloned into pTriex-4. The resulting plasmids (pFLAGNUBP1 and pFLAGALDO) were co-transfected into 293T cells with a plasmid expressing NS1 under the control of the CMV promoter and analysed 24 hours later by immunofluorescence. NS1 was detected with polyclonal antisera GP691 and anti-guinea pig IgG FITC conjugate (Sigma), the test positives were detected with mouse monoclonal anti-FLAG antisera and anti-mouse IgG TRITC conjugate (both Sigma). Peptide TY7 was also analysed for further interaction with NS1 as it was the first to be cloned with a FLAG tag (pFLAGTY7) due to its smaller size of 267 bp, however due to the induction of cell death on co-expression of NS1, samples were harvested at 12 hours post-transfection. NUBP1, aldolase A and TY7 all show some co-localisation with NS1, which displayed a punctate localisation (Fig 4.5a). When examined by performing a Z-stack of sections throughout the cell the proteins appeared to be localised towards the outer membrane of the cell. NS1 displays denser staining in this data than previously documented, though this may be due to differences in the cell types used, 293T compared to BSR cells.

The localisation of NS1 was similar to that seen in normal BTV infection, however to confirm that localisation was not due to the over expression of NS1 the confocal was repeated with cells transfected with FLAG-tag constructs then infected with BTV-10 at an MOI of 1 and harvested 24 hours post infection (NB. Cells transfected with TY7 were harvested 12 hours post infection when no cell death was detectable) (Fig 4.5c). In these experiments the distribution of both the FLAG-tagged constructs and NS1 was similar to that detected with plasmid expressed NS1 and co-localisation was retained.

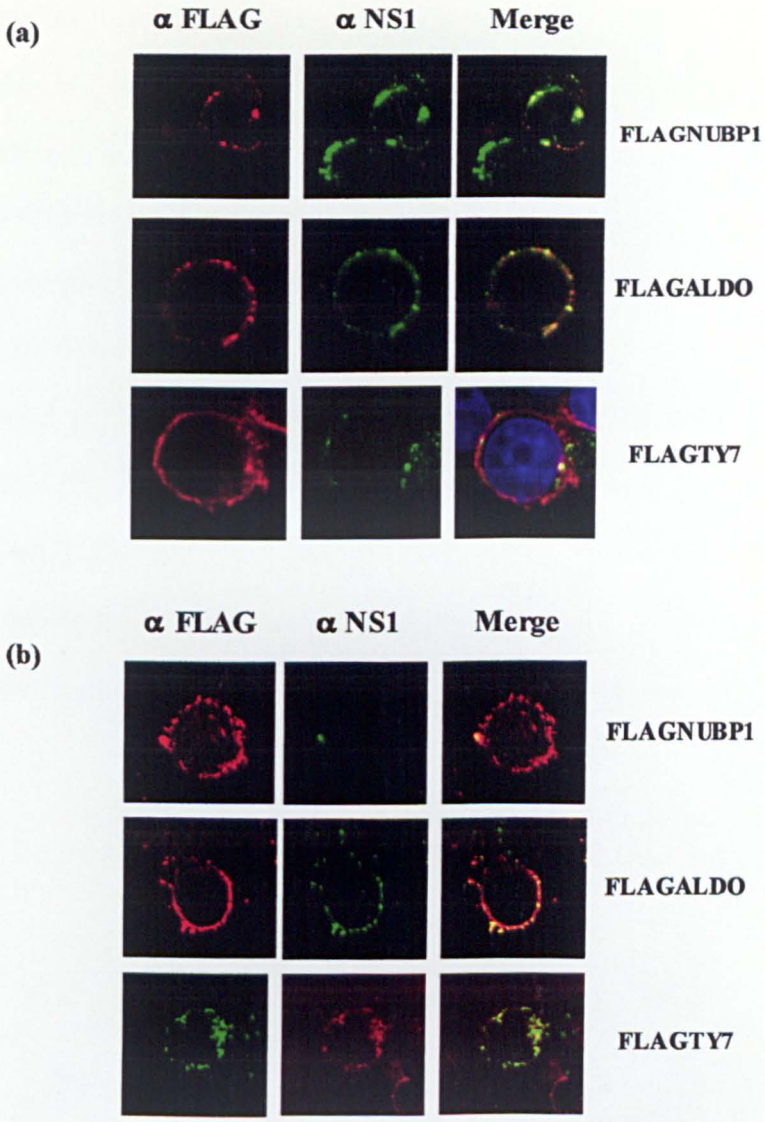

Figure 4. 5: Confocal analysis of NS1 and pFLAGNUBP1, pFLAGTY7 and pFLAGALDO. (a) Confocal analysis of 293T cells transfected with pFLAGNUBP1, pFLAGALDO or pFLAGTY7 and plasmid expressing NS1. (b) Confocal analysis of 293T cells transfected with pFLAGNUBP1, pFLAGALDO or pFLAGTY7 and then infected 24 hours later with BTV-10. pFLAGNUBP1 and pFLAGALDO colocalisation with NS1 was analysed 24 hours post infection as in (a); pFLAGTY7 colocalisation with NS1 was analysed 12 h post infection.

BTV NS1 and the FLAG-tagged positives, pFLAGNUBP1 and pFLAGALDO, were transcribed and translated *in vitro* and an immunoprecipitation assay was then performed using sepharose beads conjugated to either Guinea Pig anti-NS1 or mouse anti-FLAG monoclonal antibody. Many non-specific bands were present in the transcription/translation products (lanes 1 and 6 Fig 4.6), and the two main bands for the FLAG tagged products, at approximately 58 and 45 kDa, were weaker than expected. αFLAG precipitation gave no visible bands for FLAGNUBP1 and NS1 (lane 3) but a weak band of NS1 was visible for FLAGALDO and NS1 precipitation, although no FLAGALDO was visible (lane 8). αNS1 precipitates NS1 for both reactions but no FLAGNUBP1 or FLAGALDO was present (lanes 4 and 9 respectively). The unlabelled negative control beads did not precipitate any protein (lanes 5 and 10).

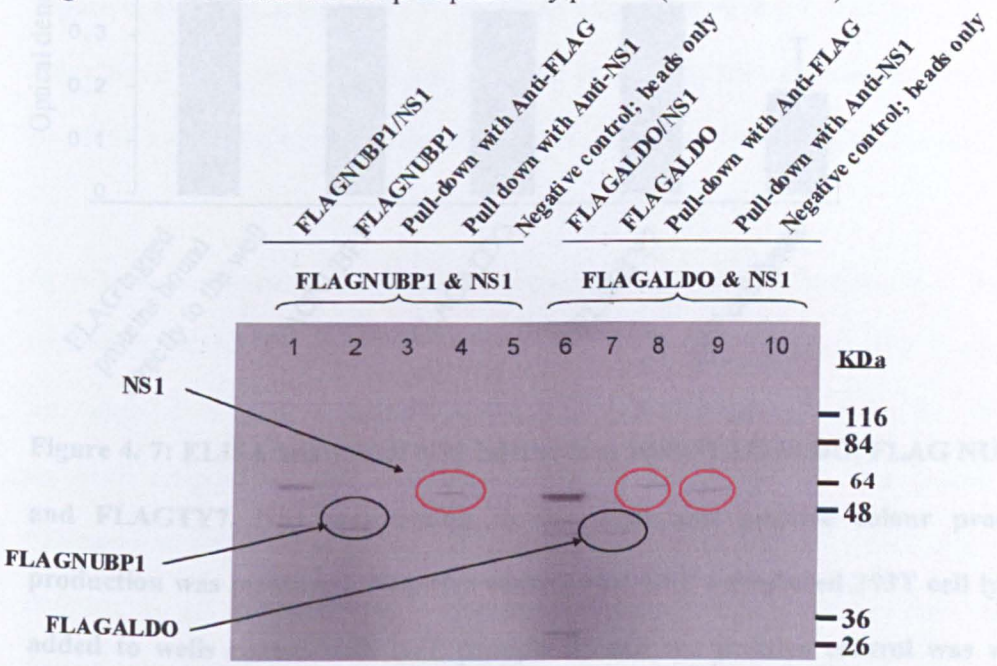

Figure 4. 6: Immunoprecipitation of NS1 and FLAGNUBP1 and NS1 and FLAGALDO. Lanes 1, 2, 6 and 7 are samples of the protein mix used in the pull-down; the negative controls are unlabelled beads used for pull-down.

To confirm this data and further analyse the interactions of these proteins ELISA analysis was performed. NS1 was bound to the wells and FLAG-tagged proteins (mammalian cell lysates of transfected cells) were added, positive interactions were identified by the presence of the FLAG-tag bound to the NS1 within the well giving a colour change product above that identified in the negative control. Positive results were obtained for aldolase A, NUBP1 and TY7 (Fig 4.7) confirming an interaction *in vitro* with NS1.

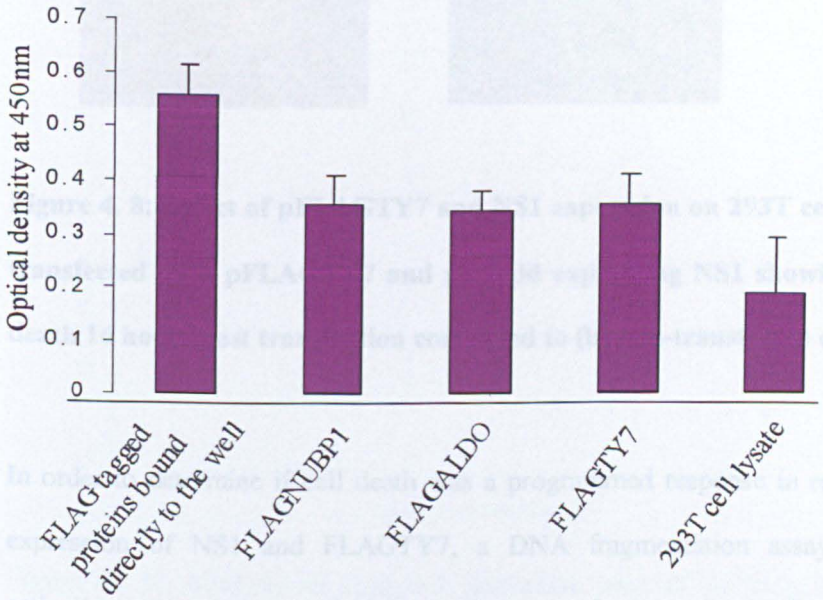

Figure 4. 7: ELISA analysis of NS1 interactions with FLAGALDO, FLAG NUBP1 and FLAGTY7. NS1 was bound to the wells and positive colour product production was measured. Negative control was GFP transfected 293T cell lysate added to wells coated with NS1 (sample 5) and the positive control was wells coated directly with FLAG-tagged protein (sample 1). Error bars represent standard deviation where n=5.

4.2.4: Examination of TY7 and NS1 Induced Cell Death

Surprisingly when 293T cells were transfected with both NS1 and TY7 for immunofluorescence analysis (Fig 4.3, immunofluorescence performed at 12 hours post transfection), extensive cell death was observed within 24 hours (Fig 4.8). This cell death was not seen in cells transfected with either TY7 or NS1 (data not shown).

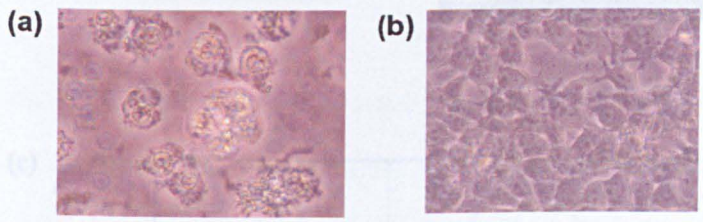

Figure 4. 8: Effect of pFLAGTY7 and NS1 expression on 293T cells. (a) 293T cells transfected with pFLAGTY7 and plasmid expressing NS1 showing extensive cell death 16 hours post transfection compared to (b) non-transfected control cells.

In order to determine if cell death was a programmed response in reaction to the co-expression of NS1 and FLAGTY7, a DNA fragmentation assay and Caspase-3 activation assay were performed as these are both markers of apoptosis. During apoptosis Caspase-3 is activated from a 32 kDa protein to a 17 kDa protein and chromosomal DNA is fragmented and degraded into a ladder of DNA visible as a smear or ladder by gel electrophoresis. In cells exhibiting cell death the inactivated form of Caspase-3 is present at 32 kDa, and no band is seen at 17 kDa, indicating that Caspase-3 has not been activated (Fig 4.9a). All of the DNA remains in the wells indicating that chromosomal DNA has not started to fragment and is too large to run through the gel (Fig 4.9b) compared to the positive control of BTV infected cells (sample supplied by Eduardo Mortola, Roy lab).

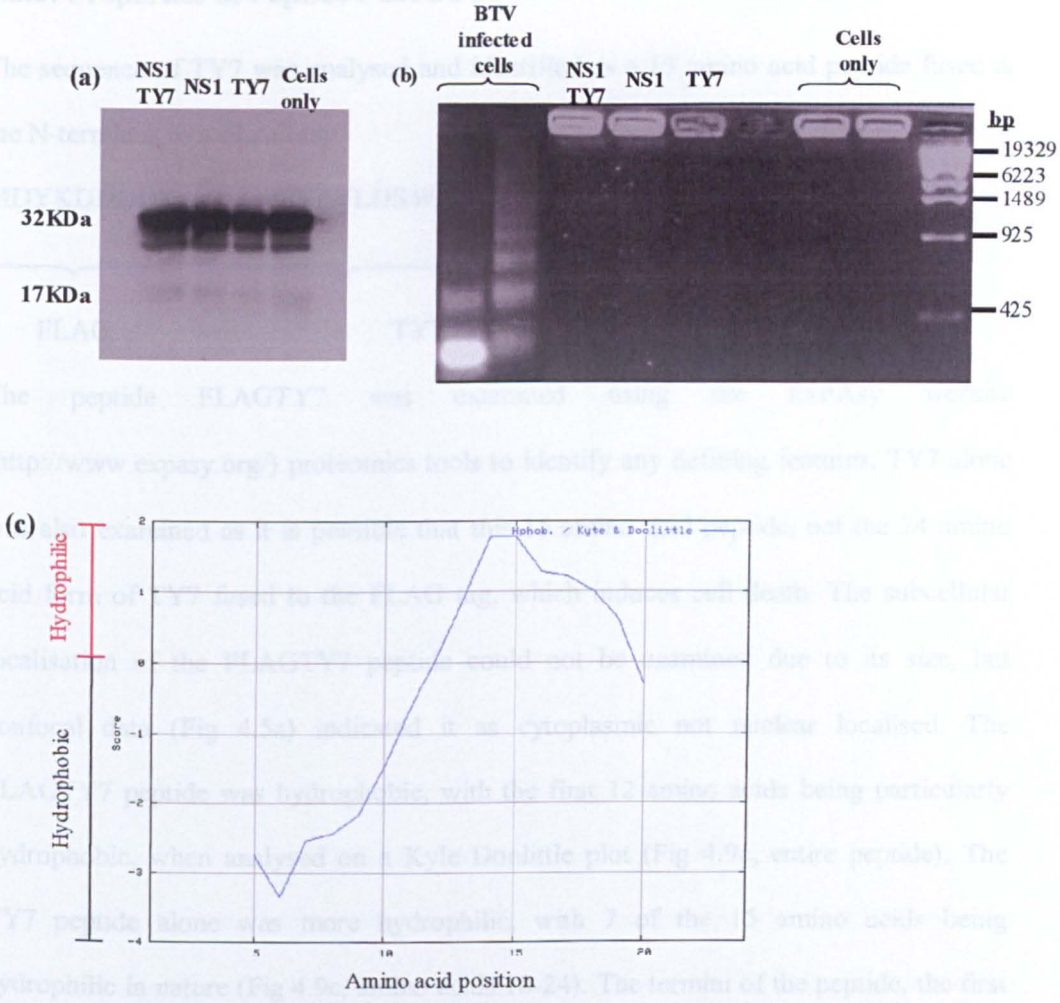

Figure 4. 9: Analysis of capase-3 activation and DNA fragmentation in cells expressing pFLAGTY7 and NS1. (a) Western blot analysis of Caspase-3 activation in cells undergoing pFLAGTY7 and plasmid expressed NS1 induced cell death. No band of activated Caspase 3 is visible at 17 kDa. (b) DNA fragmentation assay of cells undergoing pFLAGTY7 and plasmid expressed NS1 induced cell death. DNA fragmentation is detected in the BTV infected cell lysates but not in the pFLAGTY7/NS1 transfected cell lysates. (c) Kyle and Doolittle hydrophobicity plot of the peptide FLAGTY7.

4.2.5: Properties of Peptide FLAGTY7

The sequence of TY7 was analysed and identified as a 15 amino acid peptide fused at the N-terminus to a FLAG tag:

MDYKDDDDK - DLGPFVFVLDSWEWK

FLAG TY7

The peptide FLAGTY7 was examined using the ExPAsy website (http://www.expasy.org/) proteomics tools to identify any defining features; TY7 alone was also examined as it is possible that this 15 amino acid peptide, not the 24 amino acid form of TY7 fused to the FLAG tag, which induces cell death. The subcellular localisation of the FLAGTY7 peptide could not be examined due to its size, but confocal data (Fig 4.5a) indicated it as cytoplasmic not nuclear localised. The FLAGTY7 peptide was hydrophobic, with the first 12 amino acids being particularly hydrophobic, when analysed on a Kyle Doolittle plot (Fig 4.9c, entire peptide). The TY7 peptide alone was more hydrophilic, with 7 of the 15 amino acids being hydrophilic in nature (Fig 4.9c, amino acids 10-24). The termini of the peptide, the first 3 and last 5 amino acids, were hydrophobic in nature. The secondary structure of peptide FLAGTY7 was analysed and found to be generally unstructured, consisting of coiled loop areas (C) and extended β sheets (E) (Fig 4.10). No α helices or structures of interest were located, though given the small size of this peptide it is not surprising. Peptide TY7 alone gave the same data as for the last 15 amino acids of FLAGTY7.

MDYKDDDDKDLGPFVFVLDSWEWK

CCCCCCCCCCCCCEEEEECCCCCC

Figure 4. 10: Predicted secondary structure of peptide FLAGTY7.

4.2.6: Effects of FLAGTY7 on BTV-10 Infection

To identify the effects of this interaction on virus infection 293T cells were transfected with TY7 then infected with BTV-10 which expresses NS1. The rapid cell death occurring in the transfected cells was not easily distinguishable from CPE; cells treated with pFLAGTY7 prior to infection with BTV-10 showed CPE and cell death comparable to that in untreated BTV infected cells. To investigate if there was an effect on virus replication, and identify if the CPE seen was due to virus infection or pFLAGTY7/NS1 induced cell death, titres of virus produced in cells transfected with pFLAGTY7 were assessed across a 24 hour period and compared to those of cells transfected with pFLAGNUBP1 (control for the possible effect of transfection and the FLAG tag on BTV replication) or non-transfected cells.

pFLAGNUBP1 expression had no effect on BTV replication with percentages, 94% and 102% at 12 and 24 hours post infection, comparable to that of untreated cells (Fig 4.11). At 12 hours post infection the yield of virus in cells treated with pFLAGTY7 was 81% of that for untreated cells (Fig 4.11). At 24 hours post infection the difference was even more marked at 63% of normal virus yield. Treatment of cells with pFLAGTY7 greatly reduced the yield of virus, by approximately one third, despite no extra cell death being visible, thus indicating that the CPE, seen at 24 hours post infection, was potentially attributed to lesser levels of virus induced CPE in addition to FLAGTY7/NS1 induced cell death.

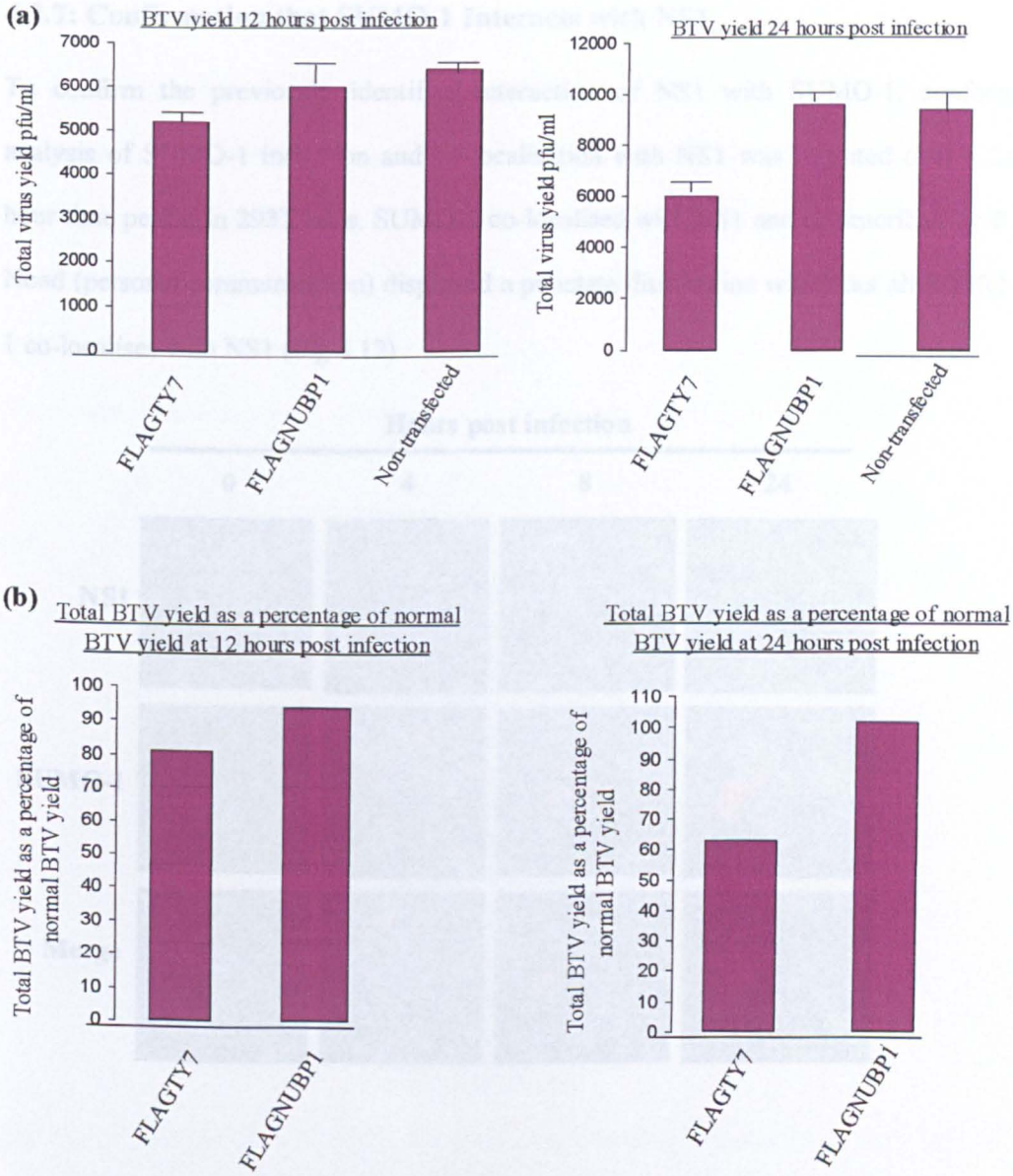

Figure 4. 11: Analysis of the effect of pFLAGTY7 on BTV-10 replication and virus yield. (a) Yield of BTV-10 at 12 and 24 hours post infection from cells transfected with pFLAGTY7, pFLAGNUBP1 or non-transfected cell control. (b) Percentage yield of virus progeny produced in cells treated with pFLAGTY7 or pFLAGNUBP1, where normal virus yield is taken as 100%. Error bars represent standard deviation where n=3.

4.2.7: Confirmation that SUMO-1 Interacts with NS1

To confirm the previously identified interaction of NS1 with SUMO-1, confocal analysis of SUMO-1 induction and co-localisation with NS1 was repeated over a 24 hour time period in 293T cells. SUMO-1 co-localised with NS1 and as described by R. Noad (personal communication) displayed a punctate distribution where not all SUMO-1 co-localises with NS1 (Fig 4.12).

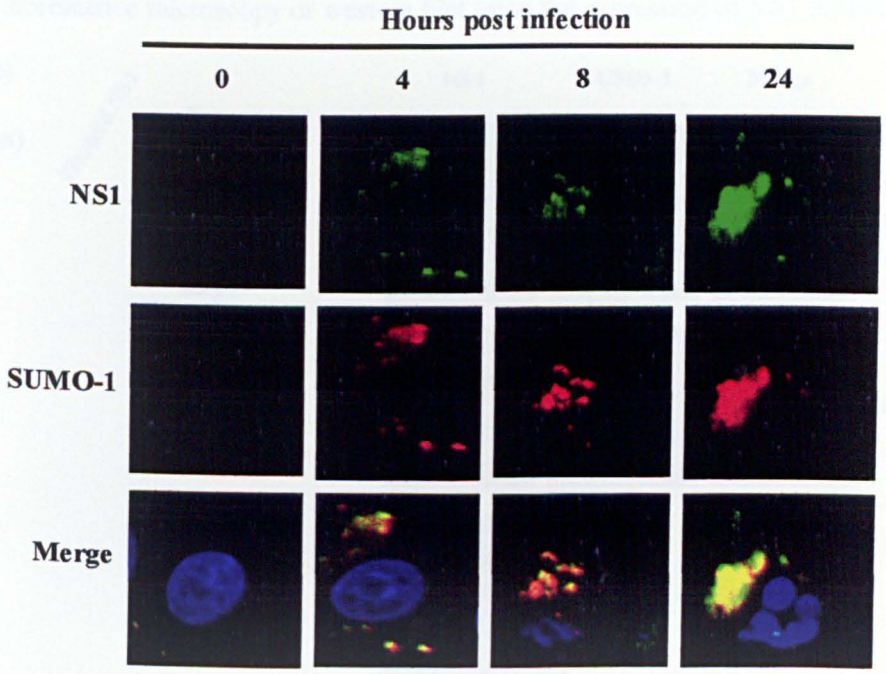

Figure 4. 12: Confocal analysis of native SUMO-1 and NS1 in BTV 10 infected 293T cells. Guinea pig polyclonal and rabbit polyclonal antisera were used to detect NS1 and hSUMO 1 expression respectively over a 24 hour period.

4.2.8: NS1 does not induce SUMO-1 Expression

To confirm previous data indicating that NS1 itself was not sufficient to trigger the sumoylation seen in BTV infected cells (Noad, R and Roy, P personal communication), 293T cells were transfected with a plasmid expressing NS1 under the control on the CMV promoter and harvested at 24 hours post transfection for confocal and western blot analysis. As identified previously SUMO-1 is not detectable by confocal fluorescence microscopy or western blot upon the expression of NS1 only (Fig 4.13a & b).

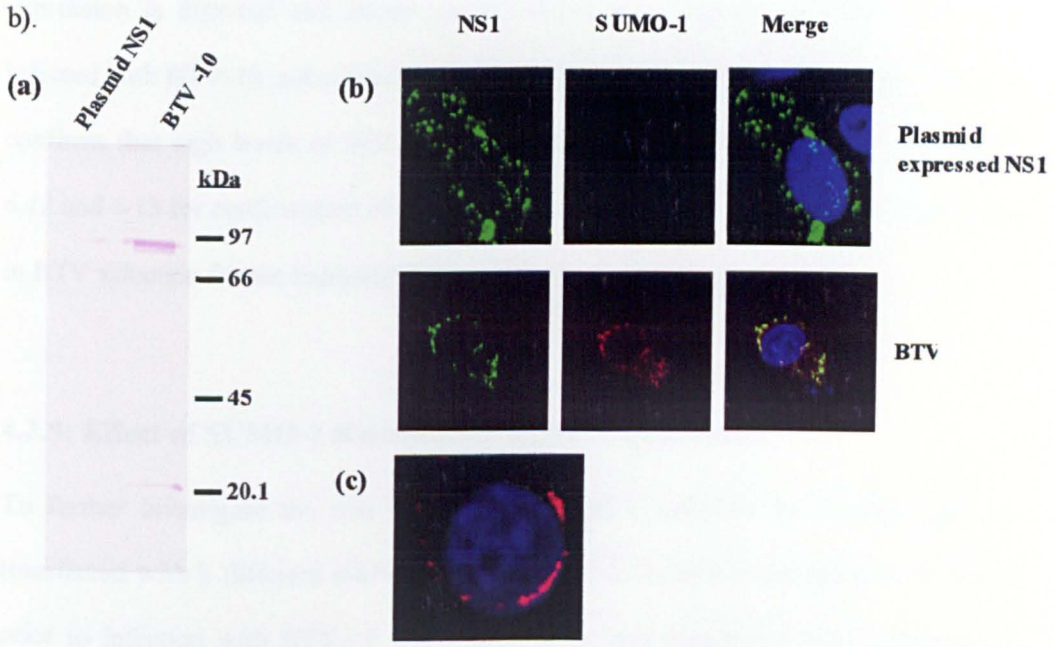

Figure 4. 13: Analysis of SUMO-1 expression following expression of BTv NS1 in the absence of BTV-10 infection. (a) Western blot analysis of SUMO-1 expression after transfection of 293T cells with a plasmid expressing NS1 or infection with BTV-10. (b) Confocal analysis of SUMO-1 expression after transfection of 293T cells with a plasmid expressing NS1, control showing SUMO-1 expression 24 hours after BTV infection of 293T cells. (c) Confocal analysis of SUMO-1 expression in BSR NS1 α cells after infection with BTV-10. SUMO-1 was detected with rabbit polyclonal antisera.

In addition the expression of SUMO-1 in BTV-10 infected cells where NS1 expression levels have been reduced was studied. Confocal analysis of SUMO-1 expression was carried out 24 hours post infection, in BSR α NS1 cells infected with BTV-10 at an MOI of 1. BSR α NS1 cells expressing an antibody against NS1 also express GFP to confirm expression from the promoter, therefore GFP expression within a cell corresponds to knockdown of NS1 (see figure 6.2 for evidence of GFP expression and figures 6.12 and 6.14 for confirmation of NS1 knockdown in this cell line). SUMO-1 expression is detected and shows normal distribution patterns in BSR α NS1 cells infected with BTV-10 and exhibiting GFP expression (not shown) (Fig 4.13c). This data confirms that high levels of NS1, and NS1 tubules (See Owens *et al* 2004 and figures 6.12 and 6.13 for confirmation of tubule absence in BSR α NS1 cells), are not necessary in BTV infection for the induction of SUMO-1.

4.2.9: Effect of SUMO-1 Knockdown on BTV Replication

To further investigate the role of SUMO-1 in BTV infection 293T cells were co-transfected with 2 different siRNA against SUMO-1, 12 hours and again at 24 hours, prior to infection with BTV-10. 293T cells were also transfected with a fluorescein linked scramble siRNA as a control. A transfection efficiency of 66% was achieved in 293T cells and gave approximately 50% knockdown of SUMO-1 in BTV infected cells (Fig 4.14). A slight knockdown was achieved with the scramble siRNA; this may be due to a lower infection rate in the transfected cells.

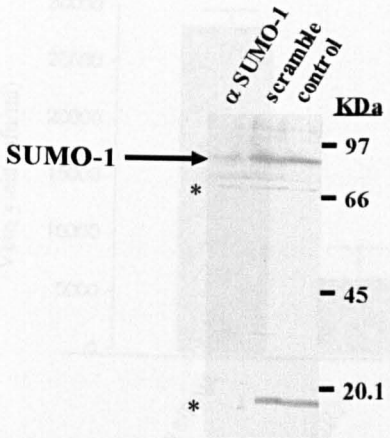

Figure 4. 14. Western blot analysis of SUMO-1 expression in 293T cells and knockdown with SUMO-1 specific siRNA or scramble siRNA in comparison to un-treated cells infected with BTV-10. * Represents sumoylated proteins that are often detected by western blot with antibody against SUMO-1 in BTV-10 infected cells.

Virus yield in scramble transfected cells was lower than that in non-transfected cells confirming that transfection of siRNA lowers the production of BTV infection, probably due to a change in cell fitness, indicating that levels of NS1 can not be compared between cells transfected with siRNA and untransfected cells. To analyse the effects of SUMO-1 reduction on BTV-10 replication, virus was harvested from siRNA transfected, BTV infected cells and the yield was compared to that of cells transfected with the fluorescein linked scramble siRNA control (Fig 4.15). Released virus and cell associated virus were harvested and titrated separately. Total yield of virus in cells where SUMO-1 levels were knocked down was drastically reduced to 27% of the yield produced in cells transfected with scramble siRNA. Ratios of cell associated virus to released virus were comparable in both SUMO-1 and scramble siRNA transfected cells.

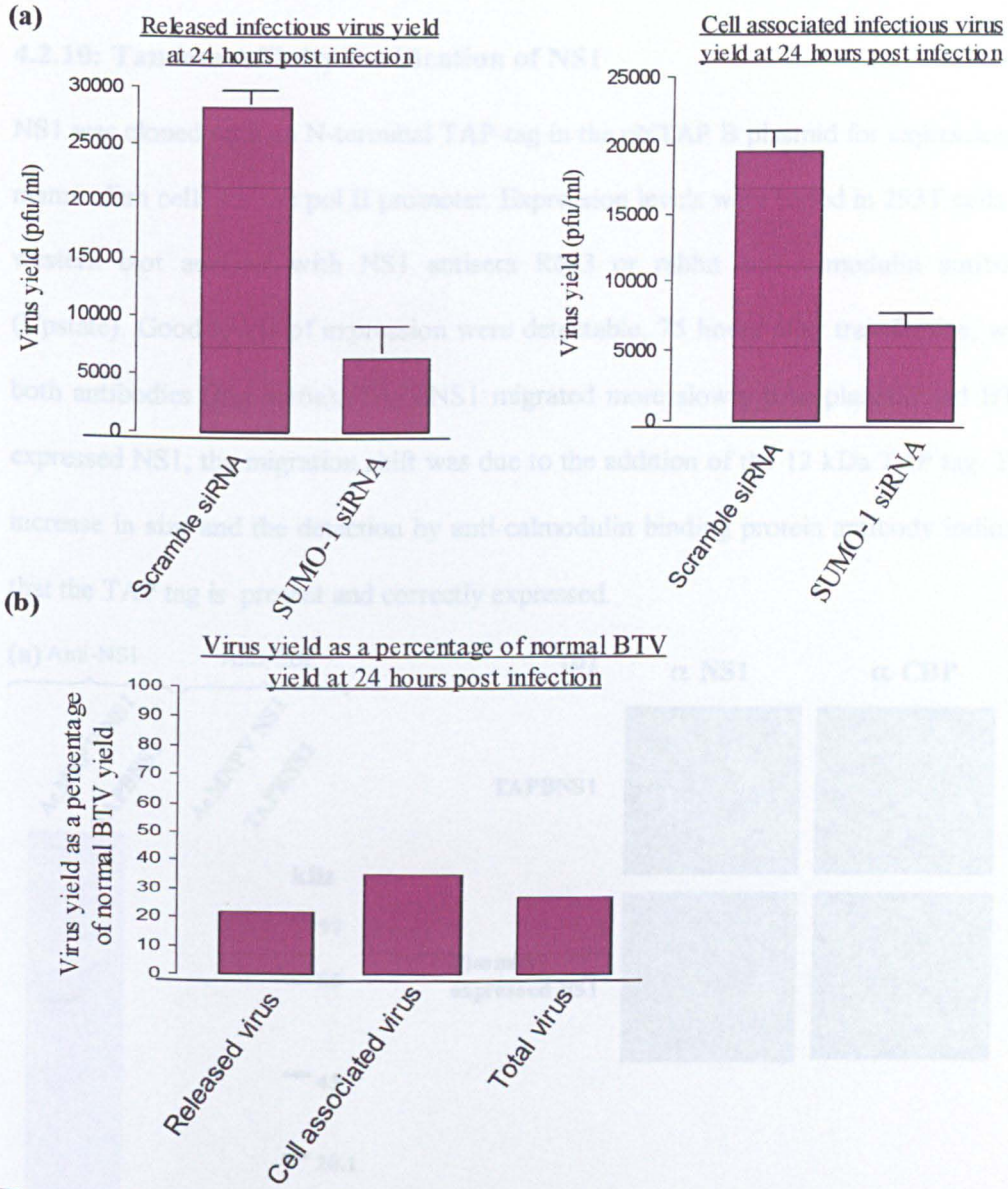

Figure 4.15: Effect of SUMO-1 knockdown on BTV-10 replication and yield. (a) Yield of released and cell associated BTV-10 in cells where SUMO-1 is knocked down with siRNA, in comparison to the yield obtained in scramble siRNA transfected cells. (b) Yield of virus in cells with reduced levels of SUMO-1 expressed as a percentage of virus yield in scramble transfected cells. Yield given for released, cell associated and total virus. Error bars represent standard deviation where n= 3.

4.2.10: Tandem Affinity Purification of NS1

NS1 was cloned with an N-terminal TAP-tag in the pNTAP B plasmid for expression in mammalian cells via the pol II promoter. Expression levels were tested in 293T cells by western blot analysis with NS1 antisera R633 or rabbit anti-calmodulin antibody (Upstate). Good levels of expression were detectable, 75 hours after transfection, with both antibodies (Fig 4.16a); TAPBNS1 migrated more slowly than plasmid and BTV expressed NS1, the migration shift was due to the addition of the 12 kDa TAP tag. The increase in size and the detection by anti-calmodulin binding protein antibody indicate that the TAP tag is present and correctly expressed.

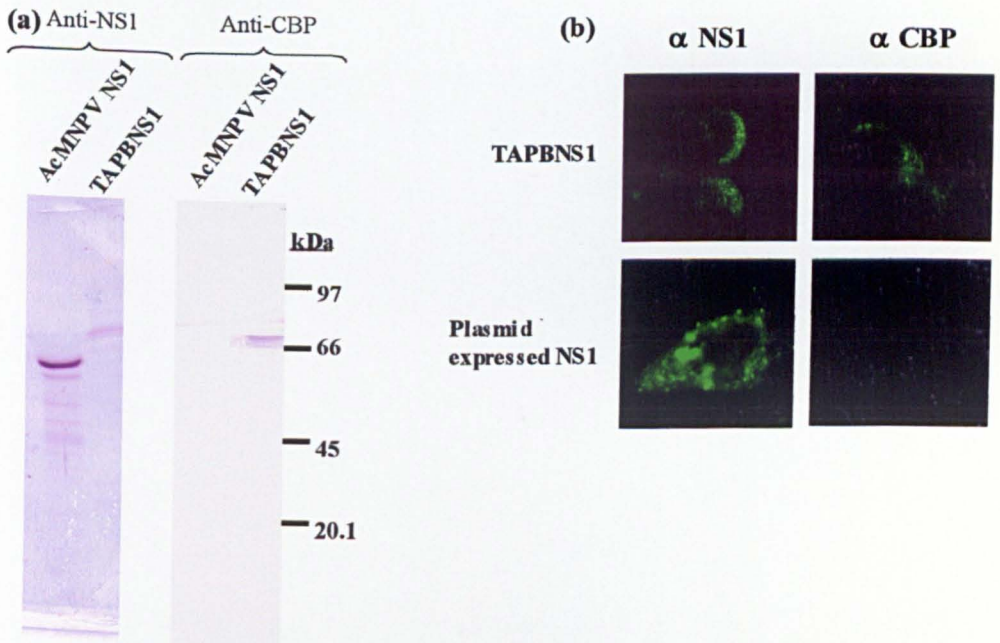

Figure 4. 16: Confocal and western blot analysis of TAPBNS1 expression and distribution. (a) Western blot analysis of TAPBNS1 expression in 293T cells 75 hours after transfection, detected by both α NS1 and polyclonal α calmodulin binding protein antibody. (b) Confocal analysis of TAPBNS1 expression in 293T cells 75 hours after transfection, detected by polyclonal α NS1. Note the differences in NS1 localisation with and without the N-terminal TAP tag.

Expression and cellular localisation of TAPBNS1 was assessed by immunofluorescence using polyclonal antisera GP691 and anti-guinea pig IgG FITC conjugate (Sigma). NS1 expression is moderate (Fig 4.16b) but more diffuse than the normal punctate staining seen with BTV infected cells or plasmid expressed NS1.

The TAP tag was placed at the N-terminus of NS1 and it was not known if this would effect tubule formation, given the slightly different distribution of TAPBNS1 tubule formation was analysed by purification of tubules on a sucrose gradient followed by western blot analysis. This was performed in tandem with plasmid expressed NS1 and baculovirus expressed NS1. Baculovirus expressed NS1 is present throughout the gradient sufficiently purified in high enough concentrations to be detected by coomassie staining (Fig 4.17a). Neither plasmid expressed NS1 nor TAPBNS1 was detected in the gradient by coomassie staining. When these samples were analysed by western blot (Fig 4.17b) only a little NS1 is detected in the cell lysate, once distributed in the sucrose gradient it is possible that the levels of NS1 would no longer be detectable.

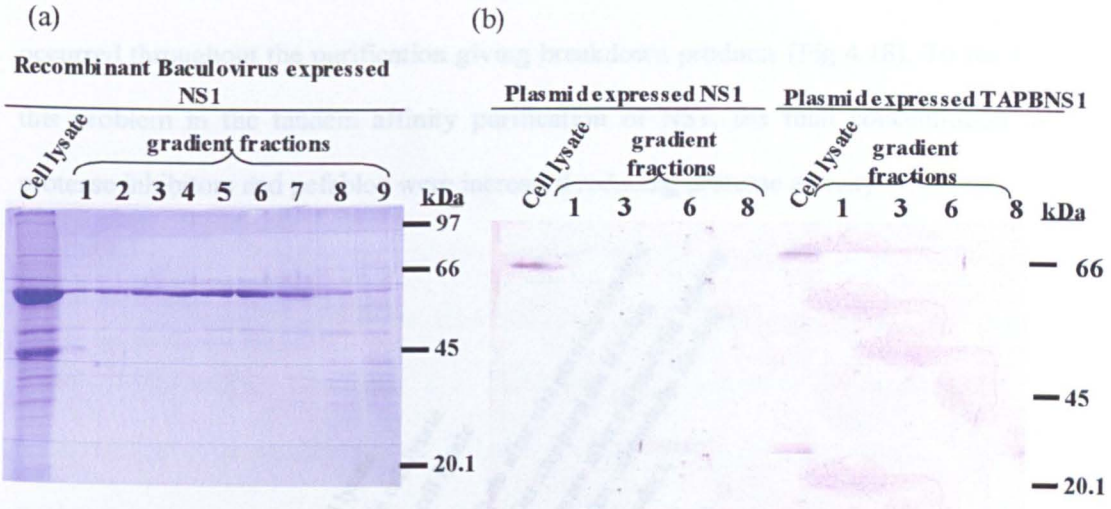

Figure 4. 17: Sucrose gradient purification of NS1 tubules. (a) Continuous sucrose gradient purification of baculovirus expressed NS1 tubules visualised by coomassie staining, (b) Continuous sucrose gradient purification of plasmid expressed NS1 in 293T cells and TAPBNS1 expressed in 293T cells visualised by western blot and R633 anti-NS1 antisera.

TAPBNS1 was purified using two purification steps based on its two tags; Streptavidin purification followed by calmodulin binding protein purification. This purification protocol was first tested on 2 control proteins supplied with the Interplay TAP system; Tag 2 MEF 2c and TAP MEF 2a. These 2 proteins are known to interact strongly and the TAP tag on TAP MEF 2a was used to co-purify Tag 2 MEF 2c which was detected on western blot via its FLAG tag. Very little Tag 2 MEF 2c was detected in the insoluble fraction of cell lysate, the SN removed from the streptavidin beads after binding or the supernatant removed from the calmodulin beads after binding indicating that binding to both types of bead was successful (Fig 4.18). Less of the Tag 2 MEF 2c was present at the end of the procedure than was initially present and some degradation

occurred throughout the purification giving breakdown products (Fig 4.18). To resolve this problem in the tandem affinity purification of NS1, the final concentration of protease inhibitors and pefabloc were increased reducing protease activity.

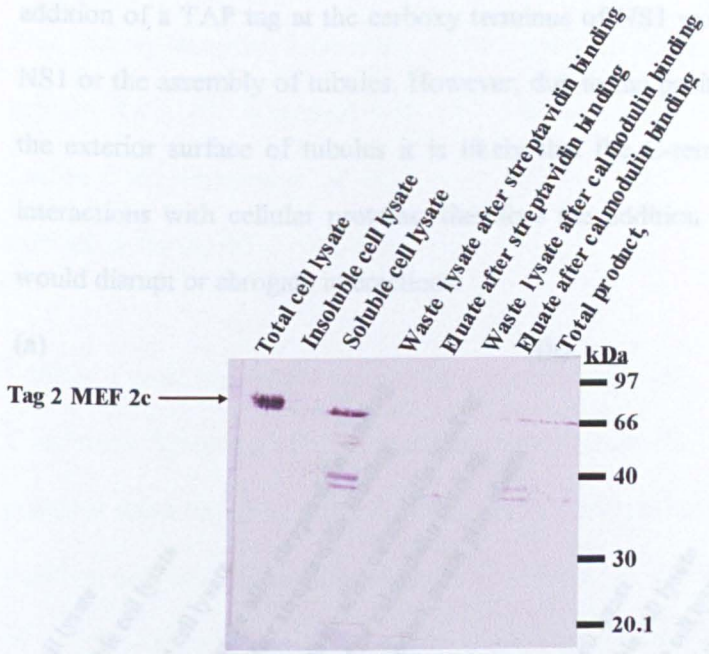

Figure 4. 18: Western blot analysis of tandem affinity purification of the control protein Tag 2 MEF 2c, detected by α FLAG antibody, co-purified by TAP MEF 2a. Samples were taken throughout the purification to assess the efficiency of the protocol.

Very little NS1 was present in the cell lysate compared to the insoluble pellet fraction indicating only partial cell lysis or the presence of an insoluble TAPBNS1 protein. Of the small amount detected in the cell lysate a similar amount was detected in the supernatant removed from the streptavidin beads after binding indicating that binding was ineffective (Fig 4.19). No NS1 was detected in the samples from the later stages of the purification. The protocol was repeated a second time to improve binding but again

much of the TAPBNS1 was detected in the insoluble fraction of cell lysate. It is likely that the addition of a tag at the N-terminus of NS1 causes the protein to become insoluble, probably due to misfolding, and hence purification can not be achieved. The addition of a TAP tag at the carboxy terminus of NS1 would not affect the folding of NS1 or the assembly of tubules. However, due to the positioning of the C-terminus on the exterior surface of tubules it is likely that the C-terminus is necessary for NS1 interactions with cellular proteins; therefore the addition of a tag on the C-terminus would disrupt or abrogate interactions.

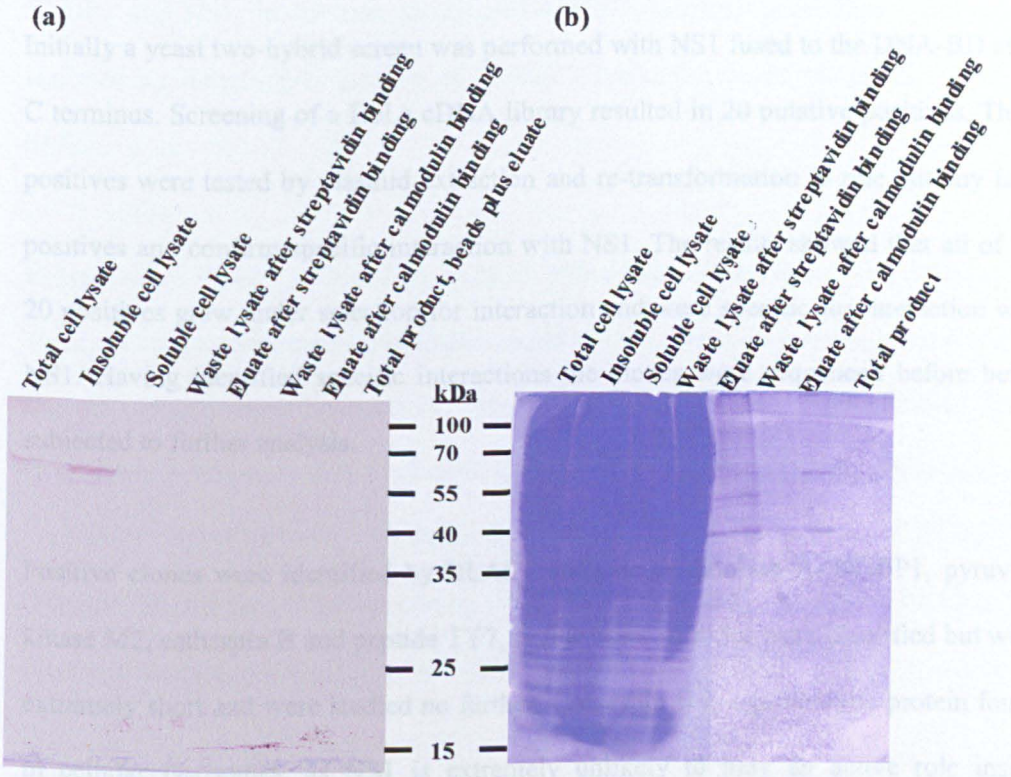

Figure 4. 19: Tandem affinity purification of TAPBNS1. (a) Western blot and (b) SDS PAGE analysis of tandem affinity purification of TAPBNS1. Cell lysates were harvested 75 hours post transfection and purified immediately by streptavidin beads and calmodulin beads.

4.3: Discussion

The work in this chapter was undertaken to identify a possible role for BTV NS1 in virus replication and pathogenesis via its interactions with mammalian cellular proteins. This chapter identifies 3 proteins; NUBP1, pyruvate kinase M2 and aldolase A, and 1 peptide, TY7, which interact with NS1 both *in vitro* and *in vivo*. This chapter also confirms the interaction of NS1 with SUMO-1 and the importance of SUMO-1 expression during BTV virus replication.

Initially a yeast two-hybrid screen was performed with NS1 fused to the DNA-BD at its C terminus. Screening of a HeLa cDNA library resulted in 20 putative positives. These positives were tested by plasmid extraction and re-transformation to rule out any false positives and confirm specific interaction with NS1. The results showed that all of the 20 positives grew under selection for interaction and were specific for interaction with NS1. Having identified specific interactions the clones were sequenced before being subjected to further analysis.

Positive clones were identified by BLAST analysis as aldolase A, NUBP1, pyruvate kinase M2, cathespin B and peptide TY7. A few other peptides were identified but were extremely short and were studied no further. Cathespin B is a proteolytic protein found in cellular lysosomes, as NS1 is extremely unlikely to play an active role inside lysosomes; this result was discarded as a yeast two-hybrid artefact. PKM2 was also not studied further due to being unable to produce a plasmid containing a FLAG tagged version of this gene.

NUBP1, Aldolase A and TY7 were cloned from the yeast two-hybrid plasmid using PCR to give a FLAG tag at the N terminus. Interactions *in vivo* were studied by expressing both NS1 and the tagged positive in 293T cells and studying their co-localisation. Results show that all proteins co-localised well with both plasmid and BTV expressed NS1 indicating that an interaction could occur as both proteins were found localised in the same places at the same times. ELISA analysis confirmed an interaction *in vitro* between NUBP1, aldolase A and TY7 with NS1; pull-down analysis was less conclusive indicating an interaction for aldolase A and NS1 but no interaction for NUBP1 and NS1. In addition to this pFLAGTY7 and NS1 interaction could not be analysed by immunoprecipitation as FLAGTY7 was too small to visualise by SDS PAGE.

Expression of FLAGTY7 and NS1 in 293T cells resulted in extensive cell death within 16 hours of plasmid transfection. The mode of cell death was analysed and results showed that it was not due to programmed cell death. Chromosomal DNA fragmentation and activation of Caspase 3 are markers characteristic of cells undergoing apoptosis, neither of these indicators were present. Proteomic analysis of FLAGTY7 detected a high level of hydrophobicity (reading of less than 0) within the first 12 amino acids and the last 3 amino acids, an overall hydrophobicity of -0.9.

When FLAGTY7 was expressed in cells infected with BTV-10 the amount of CPE was comparable to that in untransfected cells infected with BTV-10. The virus yield of cells treated with FLAGTY7/NS1 before infection with BTV-10 was 63% of normal virus yield, a 3-fold reduction. The decrease in BTV yield is almost certainly due to the increased speed of cell death meaning less virus progeny are formed. The lack of

apparent increased CPE in FLAGTY7/NS1 treated cells 24 hours post infection, may be attributed to less CPE caused by virus replication in addition to extra cell death caused by FLAGTY7/NS1, overall this would appear comparable to normal CPE at 24 hours post infection, where many cells are dead. Given the data it can be assumed that if no programmed response is occurring upon the co-expression of NS1 and FLAGTY7 from either plasmid or virus expressed NS1 the cell death may be caused by a toxic effect of a complex formed by the two proteins and not due to a specific effect on part of the BTV replication cycle or cellular response to infection.

Specific polyclonal antibodies against SUMO-1 allowed further studies to be carried out against native SUMO-1 in BTV infected cells. Data had already identified and confirmed a putative interaction between NS1 and SUMO-1, by both yeast two-hybrid and confocal immunofluorescence microscopy analysis (Noad, R and Roy, P; personal communication). Repetition of aspects of this work confirmed co-localisation of SUMO-1 and NS1 in BTV infected cells.

NS1 alone was insufficient to stimulate SUMO-1 expression and down regulation of NS1 using Tet-off α NS1 BSR cells did not effect the distribution of SUMO-1 in BTV infected cells. This data further confirms that BTV infection, but not the expression of NS1, can induce SUMO-1 in mammalian cells.

The interaction of SUMO-1 with NS1 was of great interest and two different siRNA were used to knockdown SUMO-1 in BTV infected mammalian cells to examine if any of the characteristics of BTV infection were modified. Results indicated a dramatic reduction in virus yield to 27% of the yield produced in cells transfected with scramble

siRNA. Ratios of cell associated virus to released virus were comparable in both SUMO-1 siRNA, and scramble siRNA transfected cells. The mechanisms by which this occurs require further investigation.

SUMO-1 is a small ubiquitin related modifier that post-translationally modifies cellular proteins. It has diverse roles within the cell including regulation of transcription, chromatin structure, DNA repair and differential protein localisation. SUMO-1 can covalently modify proteins with distinct functional consequences; this modification can be reversible and in some cases is necessary for the cyclic activity of individual proteins. SUMO-1 is well known for its role in Herpes virus infections and is used to regulate the function of many herpesvirus encoded proteins; such as enhancing the transactivation activity of the Rta protein encoded by Epstein Barr virus (Chang, Lee *et al.* 2004; Izumiya, Ellison *et al.* 2005).

Recently SUMO-1 has been identified as a partner in interactions where the protein is not covalently modified but interacts transiently with SUMO-1. One such interaction is that of SUMO-1 with the GTP binding protein dynamin. Dynamin mediates endocytosis by assembling around the necks of lipid vesicles and controlling the pinching off step of endocytosis. When SUMO-1 was up-regulated in mammalian cells there was a down regulation in dynamin mediated endocytosis (Mishra, Jatiani *et al.* 2004) by inhibition of the lipid dependant oligomerisation of dynamin necessary for its role in pinching off vesicles. Data suggests that dynamin may act as scaffold that concentrates sumoylation machinery thereby facilitating the sumoylation of other proteins.

SUMO-1 has been identified as interacting with viral proteins previously via non-covalent modifications; the best example is that of Hantaan virus (HTNV) nucleocapsid protein (NP). SUMO-1 and its conjugating enzyme Ubc9 interact with NP via a specific region of NP, residues 101-125, the MKAE motif within this region is a putative SUMO-1 binding site. The interaction of Ubc9 is necessary for the peri-nuclear localisation of NP and subsequent assembly of HTNV-NP (Lee, Yoshimatsu *et al.* 2003; Maeda, Lee *et al.* 2003).

NS1 has two putative sumoylation sites at residues 194-198 (IKRE) and 370-374 (VKIE). However this does not confirm the interaction of NS1 with SUMO-1 as it is possible that these residues are not positioned in an accessible conformation once NS1 is folded.

One proposed role of NS1 interaction with SUMO-1 is that NS1 is a virus response to the up-regulation of SUMO-1 in infected cells. NS1 could act as an inhibitor of SUMO-1 interaction with dynamin with subsequent consequences for virus trafficking and egress. If this is the case it is expected that interference of the ratios of dynamin and SUMO-1 in BTV infected cells would elicit a change in virus yield and potentially in virus sub-cellular distribution. Therefore it is also likely that alteration of the ratios of dynamin and SUMO-1 in cells where NS1 is knocked down should elicit an attenuated difference in virus yield.

Another possible role of NS1 is that NS1 may be binding sumoylated transcription factors and retarding their translocation to the nucleus. Thus NS1 would be modulating the host response to BTV infection in a way that was advantageous for the virus. It is

also possible that NS1, like many other viral proteins, forms part of an E3 ligation complex and is involved in the targeting of SUMO-1 onto specific cellular targets. This would also allow modification and control of host responses to BTV infection. Continuing studies within this area are needed to further elucidate the importance of NS1 and SUMO-1 in BTV replication.

In conclusion whilst it is difficult to draw direct conclusions from the work carried out I believe that the interaction of NS1 with pFLAGTY7 produces an extremely interesting effect during BTV-10 infection and requires further study. It is unlikely that this interaction occurs during BTV-10 infection since peptide FLAGTY7 is not a naturally expressed protein, however further study in this area may elucidate how the addition of a peptide with no defining characteristics has such a large impact on cellular health when expressed in conjunction with NS1.

The interaction of SUMO-1 with NS1 needs further characterisation. This is the most promising interaction identified in this study and data on the role of SUMO-1 in BTV infection may help identify differences/similarities between BTV and other viruses that interact with this protein. Analysis of the mechanism of this interaction and the affects it causes may also help to define a role for NS1 in BTV infection and increase understanding of virus interactions and hijacking of host pathways.

Aldolase A is a cellular house keeping protein and is therefore difficult to study with siRNA technology. It has not been possible to identify any importance in this interaction from literature regarding other virus interactions with this protein and it is therefore likely that this interaction may be an artefact of the yeast two-hybrid system.

NUBP1 is a hypothesised open reading frame discovered during human genome sequence analysis. The lack of information on this protein makes it difficult to assess the possible importance of an interaction with NS1 in virus infected cells and therefore further study of this protein is unlikely.

5: Identification of Interactions between NS1 and Insect Cellular Proteins

5.1: Introduction

As described in chapter 1.5, the interactions of a virus with its insect vector may help to determine transmissibility and aspects of viral replication. BTV replicates in its insect vector, *Culicoides*, and its mammalian host to high titres. It is likely that BTV proteins, in particular NS1, may interact with both insect and mammalian proteins to create a more advantageous environment for BTV replication.

The balance between BTV and its insect and mammalian hosts is critical, if it causes too severe a disease in either one the virus would no longer be transmitted, but if too little virus replication occurs transmission would be severely limited. BTV replication in its insect vectors of the *Culicoides* genus, causes little damage to the insect allowing continuing virus replication and excellent transmission of the virus. In contrast BTV replication in its mammalian host causes significant amounts cellular damage and overall disease. This infection is self limiting, limited by either death or clearance of the virus by the immune system; however it is enough to maintain a reservoir of BTV for insect transmission.

Several differences exist between BTV infection in insect cells and mammalian cells including the varying amounts of NS3/NS3A expression, the varying levels of virus

induced CPE and the different methods of virion egress (budding and cell lysis) displayed in the two cell types. Recent work has identified that NS3 interacts with both the insect and mammalian homologues of certain cellular proteins, including Tsg101, indicating that viral proteins may play comparable roles within the two host systems (Wirblich, Bhattacharya *et al.* 2006). No data is currently available for interactions of other BTV proteins with insect cell proteins.

There are few reagents with which to study insect protein interactions and yet an approach similar to that taken in chapter 4 is possible with the synthesis of insect cDNA libraries. Unfortunately many insect proteins are uncharacterised although genetic databases do exist for several insects including *Aedes aegypti* and *Drosophila melanogasta*, and although these are not complete genomic sequences many protein homologues are already identified.

This chapter discusses the construction of several insect cDNA libraries and identifies, by use of λ phage plaque screening and yeast two-hybrid analysis, insect proteins that interact with BTV NS1 *in vitro*.

5.2: Results

Given the lack of reagents available to screen protein-protein interactions involving insect proteins it was necessary to first construct cDNA libraries for such analysis. Several insect cell lines were available within the lab including the Kc cell line derived from the BTV vector *Culicoides sonorensis*. It is highly likely that different cellular genes will be switched on during virus infection and this is an important consideration for studying the interactions of BTV with its vector. Given the wide variety of barriers within the insect vector that the virus must overcome it was important to represent as many different mRNA species as possible, no live *Culicoides* were available within our laboratory but live mosquitoes were. Though *A. aegypti* is evolutionary distinct from *C. variipennis* it is likely that most house keeping genes and many other genes will possess homology between the two genera. Also with the published *A. aegypti* genome database, analysis of positives would be more conclusive.

5.2.1: Insect cDNA Library Construction

Two cDNA libraries were constructed to generate two independent methods of screening. The benefits of the yeast two-hybrid system were discussed in the previous chapter; however the major drawback of this method is the lengthy screening process and high number of false positives. A λ phage library is quicker to screen since it relies on expression within *E. coli* which is inducible using the *Lac* operon in 4 hours, allowing more cDNA to be screened and more rounds of screening to be performed, thus minimising the number of false positives.

To address the issues regarding virus induced gene expression and to ensure that all potential protein interactions were examined, poly A^+ RNA was harvested from both uninfected and infected Kc cells. Total RNA was harvested at early, mid and late time points of virus infection; 0, 2, 27 and 72 hours post infection with BTV-10 at an MOI of 1.

In addition to addressing virus induced gene expression it was vital to ensure that poly A^+ RNA species from as many representative cell types as possible were represented within the screen. Live virgin *A. aegypti* mosquitoes were used for RNA extraction providing poly A^+ RNA from all tissue types.

cDNA was synthesised from the poly A^+ RNA using primers that promote the inclusion of full length cDNA, including the 5' termini of the mRNA. Different primers were used to construct the two-hybrid library and λ library (as described in chapter 3) giving either specific ends with directional *Sfi 1* sites used for ligation with the provided λ phage arms or giving sites for homologous recombination with linearised yeast plasmid. The cDNA was size fractionated and the larger and middle size cDNA (approximately 1Kb-7Kb) was collected to represent poly A^+ RNA species.

Two Kc cDNA libraries were constructed, one for use in the yeast two-hybrid system and one for use in the λ phage system. The *A. aegypti* cDNA was used to construct a library for use in the yeast two-hybrid system.

Inserts from 10 random Kc cDNA library yeast two-hybrid plasmids were amplified using PCR and primers targeted to the termini of the plasmid outside the region of

homologous recombination (5' and 3' primers used in FLAG tag construct synthesis chapter 3). 8 out of 10 positives analysed had strong bands from PCR when visualised by electrophoresis; insert sizes ranged from 300 to 900 base pairs and were different in all 8 samples (Fig 5.1).

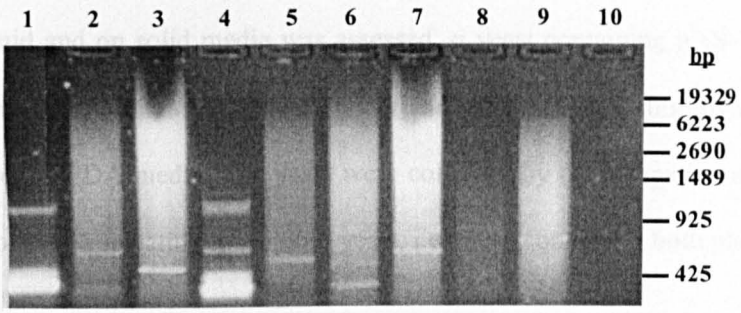

Figure 5. 1: PCR amplification of inserts from 10 random Kc cDNA library plasmids. Inserts are present in 8 of the library plasmids and range from 300-900b in length. All of the inserts visualised are different in length suggesting that each plasmid contains a different cDNA species.

5.2.2: Yeast two-hybrid cDNA Library Screen

The yeast two-hybrid Kc library was screened using pAS-NS1 as in chapter 4 with the exception that α strain yeast containing pAS-NS1 were mated with A strain yeast containing the library to give co-expression of the bait and prey plasmids in diploid yeast. Co-transformation of pAS-NS1 and library plasmids could not be performed as the library was constructed within the A strain yeast. Amplification and purification of the library plasmids from the yeast would result in amplification of the library and disproportionate levels of some cDNA species.

Initially I used the mating procedure described in the library manual (BD-Clontech). However, this gave a very low mating efficiency of less than 2% resulting in very little diploid yeast colonies; this meant only 2.1 x 10^4 cDNA had been screened. Therefore a different, more efficient approach for yeast mating was required. The mating efficiency of yeast in liquid and on solid media was assessed. α yeast containing pAS-NS1 were combined with library containing A strain yeast and subjected to mating over night in liquid or on solid YPDA media. The yeast were collected by centrifugation and plated on SM Leu^-Trp^- media selecting for diploid yeast, i.e. those containing both plasmids.

Mating on solid media gave a higher percentage of diploid yeast, 5%, and was therefore more effective allowing 4.68 x 10^5 cDNA to be screened. However, a comprehensive screen of cDNA species requires the screening of at least 5 x 10^6 cDNA, therefore the current mating efficiency was insufficient. The ratio of bait to prey yeast was analysed as it is possible that this may affect the mating efficiency of the yeast on solid media. The optimal ratio of bait: prey yeast was very low at 0.01:1 giving a mating efficiency of just under 40% (Fig 5.2). The mating efficiency decreased rapidly as the ratio was increased, dropping to just 5% for a ratio of 0.1:1 bait: prey yeast.

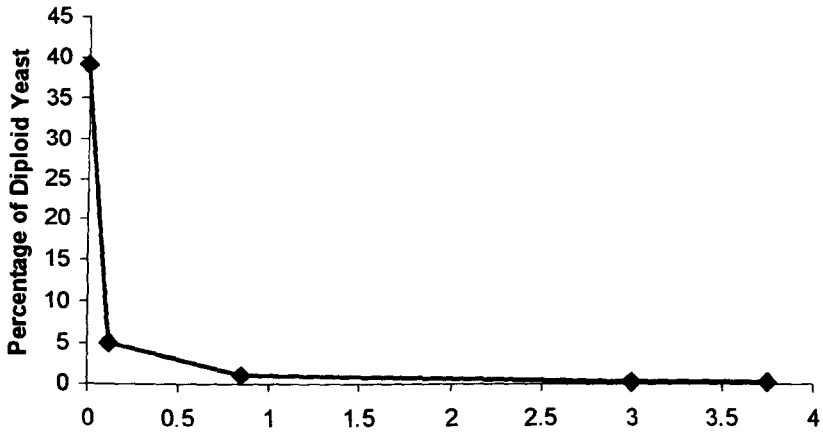

Figure 5. 2: The ratio of bait Y187 yeast: prey AH109 library yeast required for the formation of diploid yeast colonies possessing both plasmids. Yeast were counted with a haemocytometer and combined at the appropriate ratios on YPDA agar plates over night.

The yeast two-hybrid screen (see fig 4.1 for overview of process) yielded 23 putative positives displaying strong interactions with NS1 i.e. growth on SM $Leu^{-}Trp^{-}His^{-}Ade^{-}$ media. These were isolated and analysis for strong interactions was repeated; 3 positives were identified. After plasmid purification and retransformation analysis to limit the number of false positives, one cDNA plasmid was confirmed as positive, this was termed pLib-A.

5.2.3: Analysis of Yeast Two-Hybrid Positives

The positive pLib-A, plasmid DNA was extracted from yeast liquid culture and purified. The insert was amplified by PCR as above (5.2.1) and the resulting insert was

approximately 200bp long. The insert was sequenced using primers described in chapter 3.12 and sequence data (Fig 5.3) was analysed by BLAST software (http://www.ncbi.nlm.nih.gov/BLAST/). The insert showed little homology to any sequences within the database. When the BLAST search was rerun with specificity for identity to *Drosophila melanogaster* genes, there were many matches but each section of homology was a maximum of 40bp; it is likely that none of these represents true sequence identities. *D. melanogaster* may be too distantly related to *C. sonorensis* for the BLAST analysis to identify full length sections of homologous DNA sequence.

TTTTCGTAATCTTCCTAATGATCACATTTTATTACATAATCAAAGAATCGTACGAATATTATA
AAACAATTGATTTGTTATTTTAAAAACTATTCATTTACTTGGAACTGCGTTTACCACGACGAG
CGTCTGAAAATATAACATAAATTATTAAATTAAGGGAATCGGCATTACGGCCGGGTAAATTA
TTAAA

Figure 5. 3: Sequence data for the 193bp cDNA insert of pLib-A.

The predicted protein sequence of pLib-A was generated using SIXFRAME software (SDSC Biology workbench, http://workbench.sdsc.edu/) (NB this plasmid expresses the cDNA in one frame only as a read through from the GAL4 AD). pLib-A encodes a 27 amino acid peptide fused at the amino terminus to the carboxy terminus of the GAL4 activation domain (Fig 5.4).

GAL4 DNA AD----FVIFLMITFYYIIKESYEYYKTIDLLF

Figure 5.4: Amino acid sequence of pLib-A insert that encodes for a 27 amino acid peptide fused at the amino terminus to the GAL4 DNA activation domain.

No amino acid sequence identity could be detected for peptide Lib-A when sequence alignment was performed using the *D. melanogaster* protein database. The properties of this peptide were analysed using the ExPAsy website (http://www.expasy.org/) proteomics tools to identify any defining features. The peptide was mainly hydrophilic with hydrophilic termini and a short hydrophobic area in the centre (amino acids 14-22) when analysed on a Kyle Doolittle plot (Fig 5.5). No other features of interest were detected for this peptide; cellular localisation and secondary structure analyses were inconclusive due to the small size of the peptide.

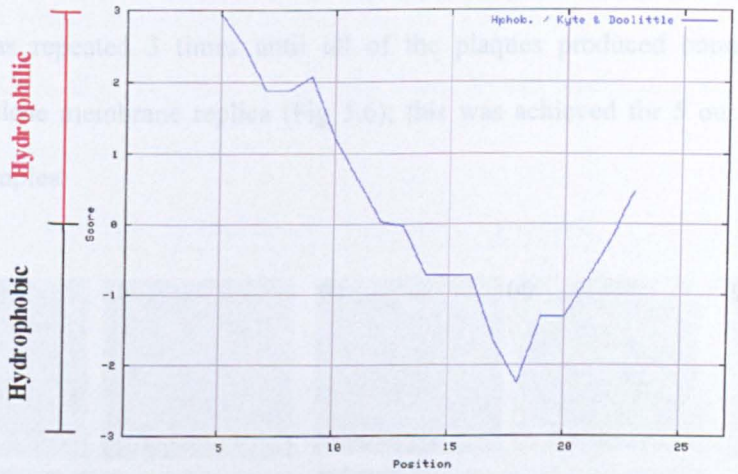

Figure 5.5: Kyle and Doolittle hydrophobicity plot of the peptide Lib-A.

5.2.4: λ cDNA Library Screen

The Kc cDNA λ library was screened using a method based around the plaque lift technique. The library was expressed after IPTG induction during lytic replication of the λ phage; the proteins expressed were released by bacterial cell lysis and bound to nitrocellulose filters for subsequent interaction analysis.

Approximately 1 x 10^7 pfu were screened giving a screen of 1 x 10^7 individual clones. In the first round of screening approximately 70% of plaques showed binding of NS1 to the nitrocellulose membrane, these were identified by formation of radiolabelled spots, corresponding to the position of a plaque, when the filters were examined by autoradiography or phosphoscreen analysis. By comparison the control plate, where expression of the inserts was not induced, had few plaques that displayed interaction and binding with NS1. 10 plaques that showed greater levels of binding to NS1 (identified by the formation of more intense radiolabelled spots) were purified by isolating the phage from an individual plaque and repetition of the screening stage. This phase was repeated 3 times until all of the plaques produced bound NS1 on the nitrocellulose membrane replica (Fig 5.6); this was achieved for 5 out of 10 purified phage samples.

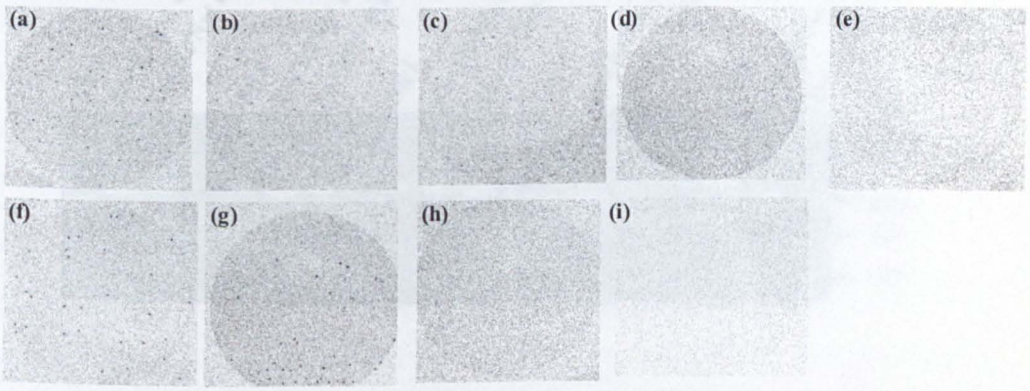

Figure 5.6: Interaction of ^{35}S met labelled NS1 to plaques after 3 rounds of plaque purification. 5 of the filters show binding of NS1 to every plaque, a, b, c, f and g, the remaining 5 show binding of NS1 to very few plaques.

Once purified a single plaque was picked from each plate and subjected to *Cre* mediated site-specific recombination. Plasmid was recovered for all 5 phage positives that underwent excision; pTripl Ex2 A, B, C, D and E.

5.2.5: Analysis of λ screen positives

The 5 positive plasmids pTripl Ex2 A-E were analysed by restriction digest to determine the insert sizes of the cDNA in each. Each plasmid was digested with Sfi I, Eco R1/Sac I and Eco R1/Not I; the resulting fragments were analysed by electrophoresis and UV visualisation. The restriction sites are positioned either side of the insert within the multiple cloning site of pTripl Ex2. No insert was detected for pTripl Ex2 A, C or E, whilst pTripl Ex2 B and D had inserts of approximately 350b, and 300b respectively (Fig 5.7).

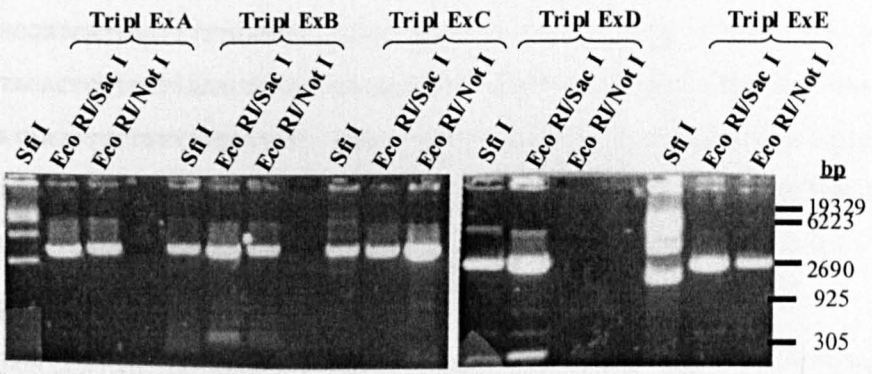

Figure 5. 7 : Restriction enzyme analysis of the 5 putative positive cDNA plasmids, pTripl Ex2 A-E. Each plasmid was digested with *Sfi I*, *Eco R1/Sac I* and Eco *R1/Not I* and fragments were visualised by electrophoresis. Inserts of 350bp and 300bp were detected for pTripl Ex2 B and D respectively, the other 3 plasmids had no inserts.

The plasmids were sequenced using primers described in chapter 3.12 and the results were subjected to BLAST analysis. All cDNA inserts are expressed in the frame used by the host, in addition to the remaining two frames, due to the presence of a triple reading frame cassette in the plasmid. Sequence data confirmed the absence of inserts in pTripl Ex2 A, C and E. Sequence data was obtained for pTripl Ex2 B and D covering the entire length of the inserts, 335bp and 216bp respectively (Fig 5.8). Very little of the insert sequence for pTripl Ex2 B and D showed homology to any sequences in the BLAST database. Small sections of sequence, 25 and 40 bases, showed homology to *Drosophila* proteins but these were not arranged in the same consecutive order as the comparative sequence in the *Drosophila* genome, thus it is likely that none of these represents true sequence identities.

pTripl Ex2 B:

GGGAACGGTCATTAGTTTTTGAAATTTGCTGTAATGATGAAGAAGGCGAAGATGTTGAAGTTCCATATGT

GCAGTACACTCTTCCTTAAACGAAATCAGAAAATTAAAGGATGTCCCTAAGCTTGATTTAATGATGATTA

TATGATAATGTTTTTTTTTTCATCATCAAACTTTTTTTTATGTTAATCGCGCCGTAATTAACTGTATTTA

TTTTATAAAACACTCGCCTCTCACTCAATTTTTTCAAATGTGTAGACAATTATCCGTACTTTTAAAATAA

TAAGAATTTCAATCATGACAAAAAAAAAAAAAAAAAAAAAAAAAAAAAACATGTC

pTripl Ex2 D:

TCGGGACCGCATGTGTGGTCCGGGAATCGGCATTACGGCCGGGTATAATGTAGTAAAAATTTTTTTCTCG

TAAAAGTTAAAGTAGATGATTTTATATTAAATTTAAAAAAAAAAATACCCAATATAACATAAATTATTAA

ATTAAATAACAAAACAAGGGATTGCTTAAGGTCTCTCAGAAAAAAAAAAAAAAAAAAAAAAAAAAAAA

CATGTC

Figure 5. 8: DNA sequence data for the 335bp and 216bp inserts of plasmids pTripl Ex2 B and D respectively.

5.2.6: NS1 putatively interacts with the C-terminus of UBA-1 (E1)

The open reading frames for each insert were studied and translation products for each identified using SIXFRAME software (SDSC Biology workbench). pTripl Ex2 B has no long ORF, the longest is 28 amino acids long, and the longest ORF for pTripl Ex2 D is 23 amino acids long.

pTripl Ex2 B longest ORF	ERSLVFEICCNDEEGEDVEVPYVQYTLP
pTripl Ex2 D longest ORF:	RDRMCGPGIGITAGYNVVKIFFS

The inserts were analysed for any sequence identities to known protein finger prints, which may help define their functions and properties, using Interproscan (EMBL, http://www.ebi.ac.uk/InterProScan/). pTripl Ex2 B showed similarity to the finger print of the UAB1 gene from the ubiquitin ligase activating family, no finger prints were found in pTripl Ex2 D. BLAST analysis of pTripl Ex2 B using the protein databases showed that the peptide had 89% homology to the 28 C-terminal amino acids of *Drosophila melanogaster* ubiquitin activating enzyme 1 (UBA-1 or E1). The properties of the three amino acids that do not share homology, positions 13, 14 and 24, were compared. The D to E (aspartate to glutamate) change at position 14 does not greatly change the overall properties of the peptide, changing from one acidic amino acid to another, whilst the change from R to Q (arginine to glutamine) at position 24 confers some changes; both R and Q are hydrophilic amino acids but R is a basic amino acid whilst Q is acidic. The V to E change at position 13 confers the largest difference, this swaps an uncharged aliphatic amino acid for an acidic amino acid; a change from hydrophobic to hydrophilic.

pTripl Ex2 B	ERSLVFEICCNDEEGEDVEVPYVQYTLP
981–1008 of *D. melanogaster* UBA1	ERSLVFEICCNDVDGEDVEVPYVRYTLP

Figure 5. 9: Sequence alignment of the longest ORF of pTripl Ex2 B with C-terminal amino acids 981–1008 *D. melanogaster* UBA1. Amino acids highlighted in pink are those that are not identical but possess similar properties, the amino acids high lighted in blue are those which are not identical and do not have similar properties.

The insert sequences were examined further for any defining features that may help to characterise them, using the ExPAsy website proteomics tools (http://www.expasy.org/). Neither sequence was long enough to predict the subcellular localisation; pTripl Ex2 B has no predicted transmembrane domains whilst pTripl Ex2 D has 1 predicted transmembrane domain in the centre of the sequence. There is a hydrophobic region in the centre of pTripl Ex2 B; pTripl Ex2 D has a small hydrophobic region at the N terminus with the rest of the peptide being hydrophilic.

5.3: Discussion

The work in this chapter was undertaken to provide reagents to study the interactions of NS1 with insect cellular proteins and to identify and characterise these interactions with the aim of elucidating the role of NS1 in BTV replication and pathogenesis. This work identifies 2 peptides that putatively interact with NS1, one of which displays homology to the E1 ubiquitin acitivating enzyme (UAB1) of *Drosophila melanogaster.*

Initially cDNA was synthesised from two sources of RNA, RNA extracted from Kc cells infected with BTV-10 over a 72 hour time course and RNA from live virgin *A. aegypti* mosquitoes. The sources of RNA were chosen to give a representative population of mRNA providing as many cellular proteins as possible that may be present during BTV infection. The cDNA was synthesised using two different sets of primers to yield cDNA compatible with two different library plasmids, one for use in the yeast two-hybrid system and one for use in phage display.

The phage display library was quicker and more efficient at generating positives than the yeast two-hybrid screen. Subsequent analysis of the positives was also more efficient when using the phage display library due to the fast process of plasmid isolation. Of the two systems used for cDNA screening the phage display library gave more reproducible results and allowed more data to be generated in a set time period.

A yeast two-hybrid screen was performed with NS1 fused to the DNA-BD at its C terminus. Screening of 1.52×10^6 independent clones from the Kc cDNA library resulted in 3 putative positives. One of the positives, pLib-A, was specific for interaction with NS1 and was sequenced before being subjected to further analysis.

The DNA sequence of the 193b cDNA insert of pLib-A showed little homology to any sequences within the BLAST database. The peptide encoded by the insert is 27 amino acids in length and mainly hydrophilic, except for a small patch of hydrophobic amino acids in the centre of the peptide. The Lib-A peptide has no other defining characteristics or sequence homology that indicate possible roles or identities of the cDNA insert. Although *Drosophila* and *Culicoides* are not closely related it can be expected that they would share some sequence similarity. The lack of sequence data for the *Culicoides* genus makes positive identification difficult, and the *A. aegypti* cDNA library may be of more use, despite the fact that this insect does not vector BTV.

A screen of the phage Kc cDNA library was performed using plaque lift technology and subsequent interaction analysis with radio labelled NS1. After the first round of screening many plaques were positive, after 3 rounds of plaque purification 5 of the clones produced plaques that showed complete binding with NS1. *Cre* recombination allowed excision of a plasmid containing the insert from the λ phage particle, this was used to analyse the size and identity of the insert.

Three of the five plasmids, pTripl Ex2 A, C and E, had no insert, this is unexpected as it is unlikely that the plaques would show such extensive binding to NS1 if they were empty. It is likely that the inserts were lost during *Cre* recombination due to continued recombination between *loxP* sites. This is supported by the observation that approximately 10% of the original library consists of empty phage vector. If the three positive plasmids were empty during screening and NS1 was therefore interacting with proteins from either the λ phage or *E. coli* almost one tenth of the plaques screened

would have shown the increased levels of binding detected for these 3 plaques. Also when comparing the plaque lifts for induced and none induced expression of the cDNA insert, many more plaques showed binding when the inserts were expressed. This indicates that though there is a high a level of background much of the binding detected for NS1 is with insect cDNA expressed proteins not proteins found in normal lytic phage replication.

pTripl Ex2 B and D had inserts of approximately 335bp and 216bp respectively. These were sequenced using primers at either side of the multiple cloning sites giving read across the entire insert and 5' and 3' ends of the plasmid DNA. As with pLib-A, the yeast two-hybrid positive, very little sequence homology was detected for the inserts in these plasmids.

Despite the length of each insert sequence and the presence of a triple reading frame cassette the longest open reading frames for each clone are very small giving maximum reads of 28 amino acids and 23 amino acids for pTripl Ex2 B and D respectively. Analysis of the peptides using proteomics software did not detect anything of interest for the peptide encoded by pTripl Ex2 D; however the finger print study of pTripl Ex2 B was extremely interesting. The peptide sequence was identified as having similarity to the finger print of the UAB1 mouse gene from the ubiquitin ligase activating family. When the sequence was analysed in BLAST using protein databases the peptide showed 89% sequence homology to UBA1 of *D. melanogaster*. No confirmation of the interaction between NS1 and UBA-1 has been carried out *in vitro* due to the time restrictions of this project; though future work within the laboratory is expected to analyse this interaction further. If this putative interaction is confirmed it is also

necessary to carry out studies of the effects of this interaction on virus replication and pathogenicity by over expression studies and siRNA analysis.

Ubiquitin activating enzyme 1, E1, is one of three essential genes necessary for the activation of ubiquitin for ubiquitination of proteins in the cell cycle and degradation pathways. UBA1 is thought to consist of an adenylation domain, a catalytic cysteine domain, a four-helix bundle, and possibly, an ubiquitin-like domain (Szczepanowski, Filipek *et al.* 2005). The adenylation domain of UBA1 is homologous to the adenylation domains of the activating enzymes for the small ubiquitin-like modifier (SUMO) (Szczepanowski, Filipek *et al.* 2005). The E1 enzyme hydrolyses ATP and forms a complex with the resulting ubiquitin adenylate; this is followed by transfer of ubiquitin to the active site cysteine of E1 to form a thiol ester between the C-terminus of ubiquitin and the thiol group of the E1. The ubiquitin is transferred from E1 to one of the ubiquitin ligase family enzymes, E2 and from there is conjugated to the protein targeted for ubiquitination via interaction with E3; this marks the protein for degradation by the 26S proteasome (Fig 5.10).

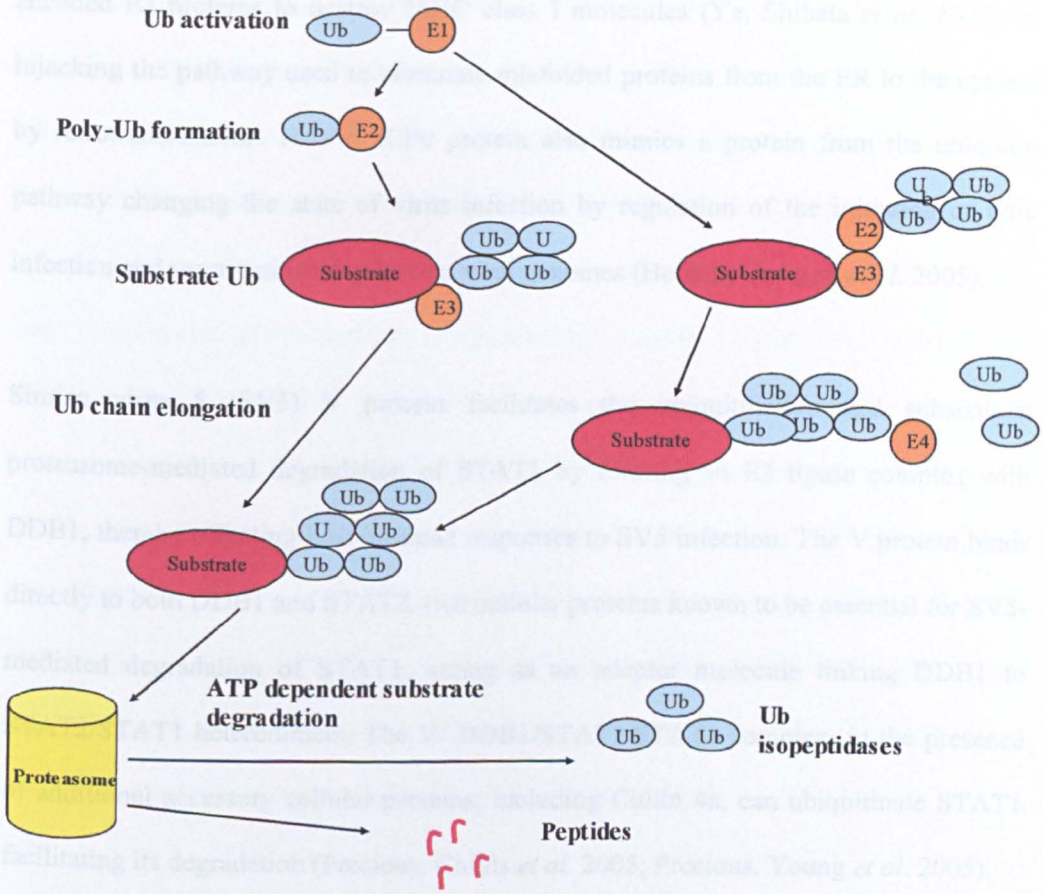

Figure 5. 10: Overview of the role ubiquitin (Ub) and enzymes E1, E2 and E3 play in protein degradation. Adapted from a schematic produced by Sigma Aldrich.

Many viruses use the ubiquitin pathway during replication to their advantage, whether by mimicry of proteins or interaction with proteins involved in the ubiquitination pathway. The majority of these interactions are used to degrade cellular proteins that interfere with virus replication such as factors of the immune response or to affect the

cell cycle in a way which is advantageous for virus replication. KSHV uses two viral encoded E3 proteins to destroy MHC class I molecules (Ye, Shibata *et al.* 2005) by hijacking the pathway used to eliminate misfolded proteins from the ER to the cytosol by retrotranslocation. HSV-1 ICP0 protein also mimics a protein from the ubiquitin pathway changing the state of virus infection by regulation of the initiation of lytic infection and reactivation of quiescent viral genomes (Boutell, Canning *et al.* 2005).

Simian virus 5 (SV5) V protein facilitates the ubiquitination and subsequent proteasome-mediated degradation of STAT1 by forming an E3 ligase complex with DDB1, thereby effecting host immune responses to SV5 infection. The V protein binds directly to both DDB1 and STAT2, two cellular proteins known to be essential for SV5-mediated degradation of STAT1, acting as an adaptor molecule linking DDB1 to STAT2/STAT1 heterodimers. The V/ DDB1/STAT2/STAT1 complex, in the presence of additional accessory cellular proteins, including Cullin 4a, can ubiquitinate STAT1 facilitating its degradation (Precious, Childs *et al.* 2005; Precious, Young *et al.* 2005).

The L domain of Rous sarcoma virus interacts with proteins from the Nedd4 family of E3 ubiquitin protein ligases, these selectively interact with specific E2 ubiquitin conjugating enzymes involved in the ubiquitin pathway, to carry out ubiquitin dependent modification of cellular proteins. The interactions of the L domain with proteins from the Nedd4 family are necessary for Gag budding of particles from the cell (Kikonyogo, Bouamr *et al.* 2001). Interestingly BTV-10 NS3 also interacts with a protein from the Nedd 4 like family of ubiquitin ligases (Wirblich *et al.* 2006) to aid virus particle release in addition to its interaction with Tsg101 (see chapter 1.7). Data identified that the knockdown of Tsg101 in cells infected with BTV reduced the virus

yield though did not completely abolish virus replication and release indicating that other pathways are involved in BTV release. The interaction of BTV NS1 with proteins involved in the ubiquitin pathway and sumoylation pathway, and the interaction of BTV NS3 with Nedd4 like ubiquitin ligases, gives rise to a number of interesting possibilities for virus release and perceived pathogenicity. Since NS3 has a proven role in virus release and interactions with Tsg101, that is involved in controlling virus budding, it is easy to speculate the importance of this in virus egress (Hyatt, Zhao *et al.* 1993; Wirblich, Bhattacharya *et al.* 2006). However given the apparent involvement of NS1 in non-lytic virus egress (Owens, Limn *et al.* 2004) and its interaction with both SUMO-1 and possibly UBA 1 it is possible that NS1 and NS3 function together, either dependently or independently, to regulate virus egress. Further more, given the differences in the ratio of NS1: NS3 between insect and mammalian cell infections it is possible that more budding is seen during insect cell infection due to a differential balance of interactions with cellular proteins via NS1 and NS3.

A study of the localisation and possible interaction of NS1 with NS3 and other BTV proteins may help to elucidate the role both proteins play in BTV egress in addition to other roles of NS1 in virus replication.

6: Identification of Interactions between NS1 and BTV Proteins and analysis of the role of NS1 in virus infection

6.1: Introduction

BTV NS1 is identified in BTV infected mammalian and insect cells as tubules; purification of NS1 from infected cells or recombinant baculovirus expression favours the purification of tubules as opposed to monomers/dimmers. Nevertheless, smaller material that is confirmed as NS1 is always present at the top of the sucrose gradient. It is possible that tubules are a storage state for NS1 and that the active form is the NS1 monomer or dimer as is seen with Infectious Bursal disease virus (IBDV) tubules. Conversely it is also possible that NS1 tubules are the active form of NS1 and play an important role in virus infection, this may be related to their distinctive structure as seen with AcMNPV p10 tubules.

For many viruses, non-structural proteins are involved in the enzymatic processes of virus replication and/or are responsible for the interference with cellular processes such as abrogation of the host immune response, shutting down host protein synthesis and hijacking host pathways (Lyles 2000; Fontoura, Faria *et al.* 2005; Hengel, Koszinowski *et al.* 2005). For the *Reoviridae* the enzymatic functions required for virus replication i.e. the helicase, guanyltransferase, triphosphatase and RNA-dependent RNA polymerase are performed by structural proteins. The non-structural proteins of viruses within the *Reoviridae* are likely to be involved in modulation of host responses to virus infection. In addition to the role many non-structural proteins play in virus-host

interactions, it is probable that they interact specifically with other viral proteins. Elucidation of these relationships may allow the identification of the role they play in virus replication.

When NS1 was knocked down using a single chain antibody against NS1 (BSR anti-NS1 cells), virus titres were increased in comparison to those produced from normal mammalian cell infection by BTV and the amount of virus released into the culture medium, unusually by budding rather than cell lysis, increased by 10-fold (Owens, Limn *et al.* 2004). During this experiment no tubules were detected, presumably due to the low amounts of free NS1 available to multimerise into tubules. However, it is impossible to confirm whether the change in egress is due to a lack of tubules or a lack of NS1 monomer/dimer. On closer analysis of the data for the BSR anti-NS1 cells, the pulse-chase analysis of protein expression and stability within these cells indicates a reduction in several other proteins, in addition to NS1, including VP1, VP4, VP5 and VP6. It is possible that this is due to the reduced amount of virions within the cell due to increased virus egress, though this is unlikely as the expression and stability of VP2/3 and VP7 appear unchanged. No information on the expression levels of the other two non-structural proteins, NS2 and NS3, is available.

Data from the knock down of NS1, using BSR anti-NS1 cells, also implicated NS1 in the egress of BTV, when BTV NS1 was knocked down there was a change in the mode of virus egress from lytic to non-lytic. However due to the decreased expression/stability of some of the viral structural proteins and lack of data on the expression and stability of the other non-structural proteins this phenotype may not be

due to the reduction of NS1. NS1 is not essential for virus egress and the presence of NS3 is sufficient for the egress of VLP from *Sf* cells (Hyatt, Zhao *et al.* 1993).

The analysis of NS1 interactions with mammalian and insect cell proteins identified a putative interaction of NS1 with ubiquitin activating E1 enzyme, a protein involved in the ubiquitin pathway of *Drosophila melanogaster*, and the small ubiquitin-like modifier of the sumoylation pathway, SUMO-1. NS3 interacts with proteins of the Nedd4 like group of ubiquitin ligases that facilitate ubiquitination of target proteins, but are not involved in the classic ubiquitin pathway (Wirblich, Bhattacharya *et al.* 2006). It is therefore possible that NS1 may have a role that is complementary to that of NS3 and hence the mode of virus egress is different in insect cells and mammalian cells where the ratio of NS1:NS3 is different.

The BTV outer capsid protein VP2, along with NS1, was detected in close association with cellular cytoskeletal fibres (Eaton, Hyatt *et al.* 1987). Recent data identifies a direct interaction of VP2 with the intermediate filament protein vimentin (Bhattacharya, B and Roy, P; personal correspondence). Viruses frequently traffic structural proteins, immature virions and mature virions using the cellular cytoskeleton (Bearer and Satpute-Krishnan 2002). The AcMNPV non-structural protein p10, forms tubules that interact with α-tubulin microtubules of the cytoskeleton, this interaction may be involved in cell lysis for efficient virus egress (Williams, Rohel *et al.* 1989; Patmanidi, Possee *et al.* 2003). It is possible that NS1, like VP2, associates directly with the cytoskeleton and its role in virus replication is linked to this.

This chapter describes the interactions of BTV NS1 with other BTV proteins and the implications of these interactions. It also examines a possible role of NS1 in trafficking and virus assembly via interaction with cytoskeletal proteins. Finally the importance of NS1 in virus replication was investigated using siRNA to knock-down NS1.

6.2: Results

6.2.1: NS1 interactions with Structural Proteins

To identify if NS1 was involved in trafficking of core particles or virus particles the interactions of NS1 with the outer capsid proteins VP2 and VP5, and the outer layer of the core, VP7, were analysed by biochemical methods. The interactions of NS1 with the VP2, VP5 and VP7 were first analysed by immunoprecipitation, using antibodies against both NS1 and the test protein. No co-precipitation occurred for NS1 and VP2 or NS1 and VP5 with either antibody. NS1 and VP7 co-precipitated with beads labelled with both anti-NS1 and anti-VP7; neither protein precipitated with the negative control (Fig 6.1). This experiment gave consistent reproducible results.

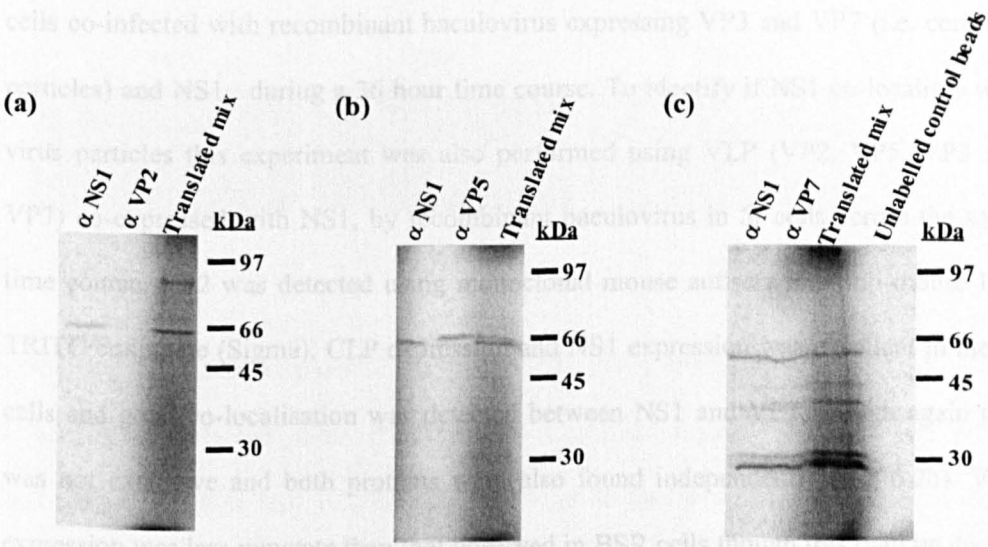

Figure 6.1: Immunoprecipitation of NS1 with BTV structural proteins (a) VP2, (b) VP5 and (c) VP7. Proteins were precipitated with antisera against both NS1 and either anti-VP2, anti-VP5 or anti-VP7 antisera. NS1 was precipitated in all 3 experiments with anti-NS1 antisera and was also precipitated with anti-VP7 antisera. NS1 was not precipitated with either anti-VP2 or anti-VP5 antisera.

To further confirm the interaction identified between NS1 and VP7, co-localisation of NS1 with VP7 was examined by confocal immunofluorescence microscopy. BSR cells were infected with BTV-10 at an MOI of 1 and analysed 24 hours post infection by immunofluorescence. NS1 was detected with polyclonal antisera GP691 and anti-guinea pig IgG FITC conjugate (Sigma), VP7 was detected with monoclonal mouse antisera MAb 11A10 and anti-mouse IgG TRITC conjugate (Sigma) and the nucleus was stained using Hoesch stain. NS1 and VP7 show some co-localisation within BSR infected cells but both proteins are also found independently in other areas of every cell examined, possibly due to a non-synchronous cell population (Fig 6.2a).

A more in depth study was carried out examining co-localisation of NS1 and VP7, in *Sf* cells co-infected with recombinant baculovirus expressing VP3 and VP7 (i.e. core-like particles) and NS1, during a 36 hour time course. To identify if NS1 co-localises with virus particles this experiment was also performed using VLP (VP2, VP5, VP3 and VP7) co-expressed with NS1, by recombinant baculovirus in *Sf* cells across the same time course. VP2 was detected using monoclonal mouse antisera and anti-mouse IgG TRITC conjugate (Sigma). CLP expression and NS1 expression was excellent in the *Sf* cells and good co-localisation was detected between NS1 and VP7, though again this was not exclusive and both proteins were also found independently (Fig 6.2b). VP7 expression was less punctate than that observed in BSR cells though this may be due to the lack of NS2 since VP7 is often found accumulated in the periphery of inclusion bodies. In *Sf* cells expressing VLP and NS1 expression of both VP2 and NS1 was lower than that observed in cells expressing VP7 and NS1. NS1 showed minor co-localisation with VP2; the distribution of NS1 and VP2 is mainly at the outer periphery of the cytoplasm (Fig 6.2b).

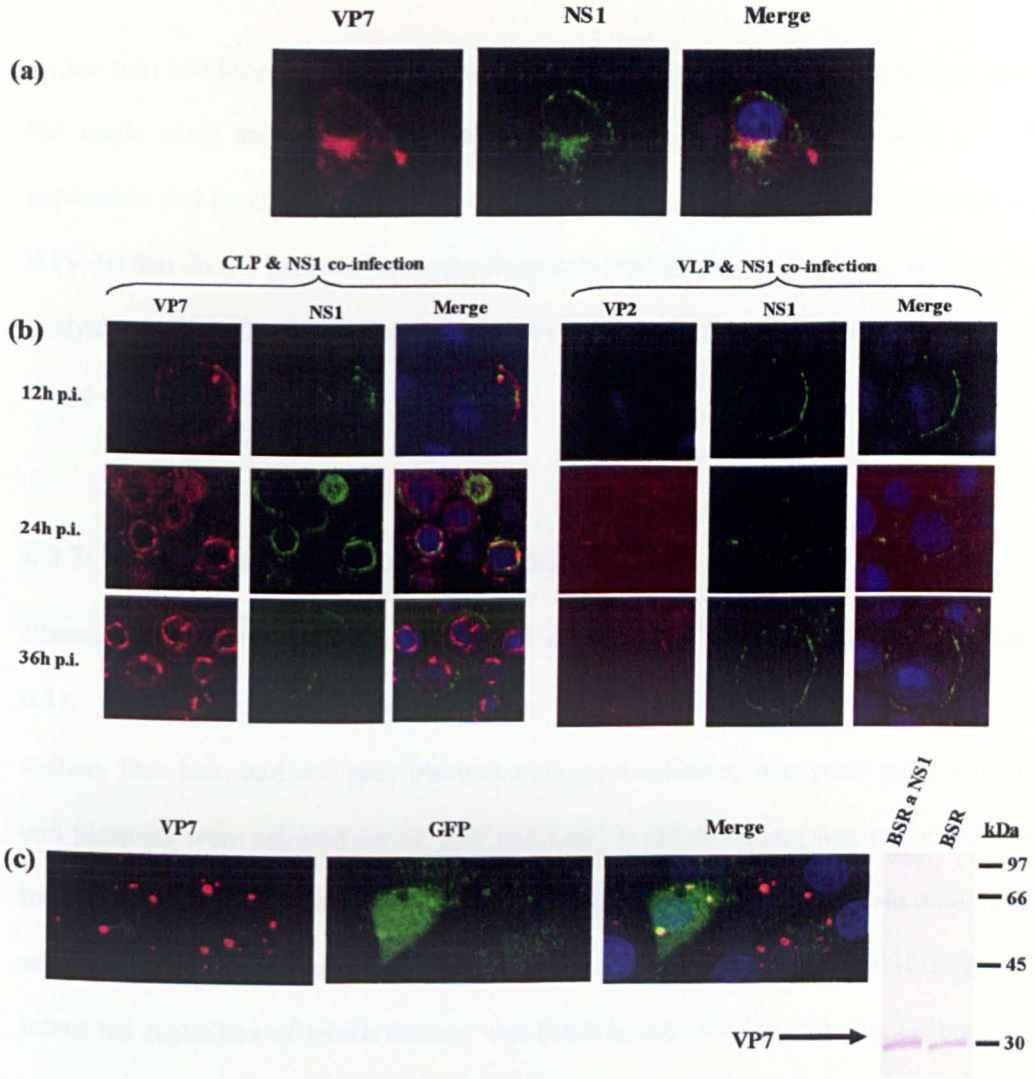

Figure 6. 2: Confocal analysis of NS1 and VP7. (a) Co-localisation of NS1 and VP7 in BSR cells infected with BTV-10. (b) Confocal studies of NS1 and VP7 localisation, and NS1 and VP2 localisation, over 36 hours in *Sf* 21 cells co-infected with recombinant baculovirus expressing VP3, VP7 (i.e. core-like particles) and NS1 or VP2 , VP5 (VLP) and NS1. (c) Expression of VP7 in BSR α NS1 cells expressing a single chain antibody against NS1 at 24 hours post infection with BTV-10 (GFP expression is indicative of NS1 knockdown (Owens *et al.* 2004)).

Expression and localisation of VP7 was also examined in BSR α NS1 cells (expressing the single chain antibody against NS1), 24 hours post infection with BTV-10. VP7 expression and localisation was comparable to that detected in BSR cells infected with BTV-10 that do not express the single chain anti-NS1 antibody (Fig 6.2c). Western blot analysis confirms that VP7 expression is the same in cells that do and do not express the single chain anti-NS1 antibody (Fig 6.2c).

6.2.2: Yeast Two-Hybrid Analysis of NS1 and VP7

Plasmids pAS-NS1, pAS-VP7 , pACT-NS1 and pACT-VP7 (for descriptions see table 6.1), were used to confirm the interactions of NS1 and VP7 in the yeast two-hybrid system. One bait, and one prey plasmid were co-transfected into yeast strain PJ694A and plasmids were selected for on SM Trp^- Leu^-. A single colony was replicated onto media minus all 4 amino acids selecting for a stringent interaction and again onto media selecting for both plasmids proving viability of the yeast colony. NS1 and VP7 interacted regardless of which domain was fused to the proteins, growing on both SM Trp^- Leu^- and SM His^- Ade^- Trp^- Leu^- (Fig 6.3).

Plasmid	Description
pAS-NS1	NS1 with the GAL4 DNA binding domain fused at the C-terminus
pAS-VP7	VP7 with the GAL4 DNA binding domain fused at the N terminus
pACT-NS1	NS1 with the GAL4 DNA activation domain fused at the C terminus
pACT-VP7	VP7 with the GAL4 DNA activation domain fused at the N terminus

Table 6. 1: Descriptions of plasmids used to confirm specific interactions in the yeast two-hybrid system.

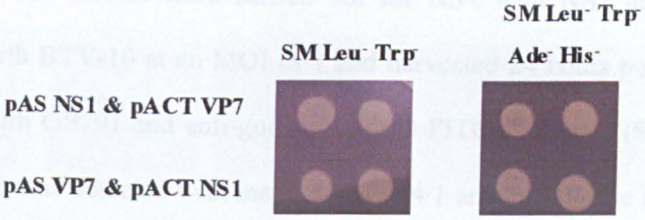

Figure 6. 3: Yeast two-hybrid analysis of VP7/NS1 interaction. pAS-VP7 interacts with pACT-NS1, pACT-VP7 also interacts with pAS-NS1 indicating that the different GAL4 domains have no effect on the interaction. All yeast transformants grow on media selecting for both plasmids (SM Leu- Trp-) proving viability.

6.2.3: NS1 interactions with Non-Structural Proteins

The interactions of NS1 with one of the other two non-structural proteins NS2 was examined by immunoprecipitation. Due to the transmembrane domains within NS3 it was not possible to study its interaction with NS1 using immunoprecipitation as the protein must first be separated from the membrane which may affect both the conformation of NS3 and its interactions. Both NS1 and NS2 precipitated with their respective antibodies but no co-precipitation was detected for NS1 and NS2 indicating that NS1 does not associate with NS2 at the periphery of inclusion bodies (Fig 6.4).

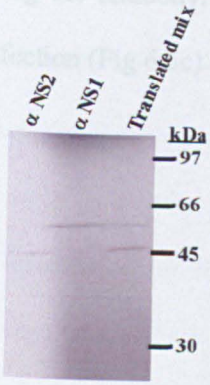

Figure 6. 4: Immunoprecipitation of NS1 and NS2. NS1 was precipitated by polyclonal antisera against NS1; NS2 was precipitated by polyclonal antisera against NS2; neither protein co-precipitated with the other.

Co-localisation studies were carried out for NS1 with NS2 and NS3 in BSR cells infected with BTV-10 at an MOI of 1 and harvested 24 hours post infection. NS1 was detected with GP791 and anti-guinea pig IgG FITC conjugate (Sigma) in studies with NS3, which was detected with monoclonal 444/1 and anti-mouse IgG TRITC conjugate (Sigma). NS2 was detected with GP373 and anti-guinea pig IgG FITC conjugate (Sigma), in this study NS1 was detected with polyclonal R633 and anti-rabbit IgG TRITC conjugate (Sigma). NS1 displayed a normal distribution with disperse punctate pattern throughout the cytoplasm, NS2 also displayed the normal punctate distribution of several large patches within the cytoplasm (Fig 6.5a) with little to no co-localisation with NS1. NS3 displayed a normal distribution with much of it being located at the periphery of the cell; some NS3 staining is visible in the main body of the cell presumably associated with internal membranes (Fig 6.5b), some co-localisation between NS1 and NS3 is visible though this may be due to the excessive cytoplasmic staining of NS1.

Expression and localisation of NS2 and NS3 was also examined in BSR α NS1 cells expressing the single chain antibody against NS1, 24 hours post infection with BTV-10. NS2 expression and distribution was identical to that in cells not expressing the antibody, NS3 expression was lower than that detected in the control cells not expressing the antibody; however the distribution was comparable to that of normal BTV infection (Fig 6.5c).

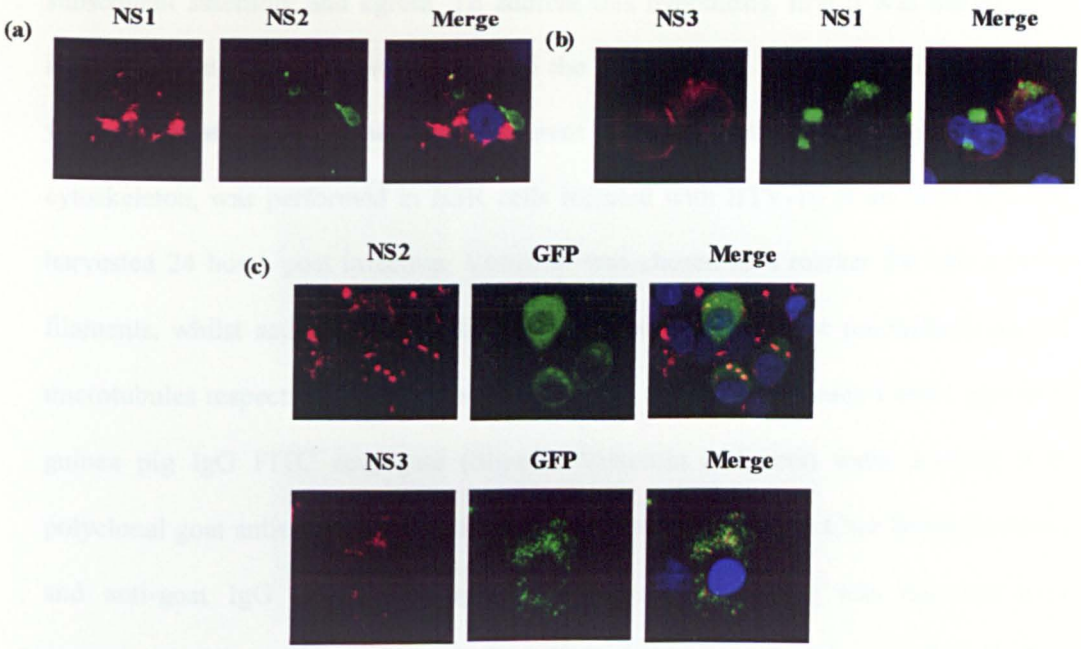

Figure 6.5: Confocal localisation analysis of NS1 with the other non-structural proteins NS2 and NS3. (a) BSR cells 24 hours post infection with BTV-10 stained for NS1 and the distinct inclusions of NS2. (b) BSR cells 24 hours post infection showing NS1 and membrane associated NS3. (c) Distribution of NS2 and NS3 in BSR α NS1 cells expressing the single chain antibody, comparison to (a) and (b) confirms normal localisation though a slight decrease in NS3 levels (GFP expression is indicative of NS1 knockdown (Owens *et al.* 2004)).

6.2.4: NS1 and Interactions with the Cellular Cytoskeleton

From the observation that NS1 interacts with VP7 but does not interact with VP2, and is found in close proximity to VIBs and the cytoskeleton (Eaton, Hyatt et al. 1987; Brookes, Hyatt et al. 1993), where VP2 and virus particles accumulate, it is possible that NS1 may be involved in trafficking virus cores from VIB to the cytoskeleton for

subsequent assembly and egress. To address this hypothesis, first it was necessary to identify an interaction between NS1 and the cytoskeleton. Confocal analysis of NS1 with three proteins of the three different types of filament that make up the cytoskeleton, was performed in BSR cells infected with BTV-10 at an MOI of 1 and harvested 24 hours post infection. Vimentin was chosen as a marker for intermediate filaments, whilst actin and α tubulin were chosen as markers for microfilaments and microtubules respectively. NS1 was detected with polyclonal antisera GP691 and anti-guinea pig IgG FITC conjugate (Sigma), Vimentin and actin were detected with polyclonal goat antisera Sc 7557 and Sc 1616 respectively (Santa Cruz Biotechnology) and anti-goat IgG TRITC conjugate (Sigma) and α tubulin was detected with monoclonal antisera Sc 5286 (Santa Cruz Biotechnology) and anti-mouse IgG TRITC conjugate (Sigma). Vimentin shows an extensive network of staining with a perinuclear distribution, in some cells this is mainly to one side of the nucleus, in others it is throughout the cytoplasm; α tubulin and actin show extensive staining throughout the cytoplasm. Given the diffuse distribution of staining detected for both NS1 and the cytoskeletal markers it was not possible to draw conclusions about possible interactions of the proteins (Fig 6.6).

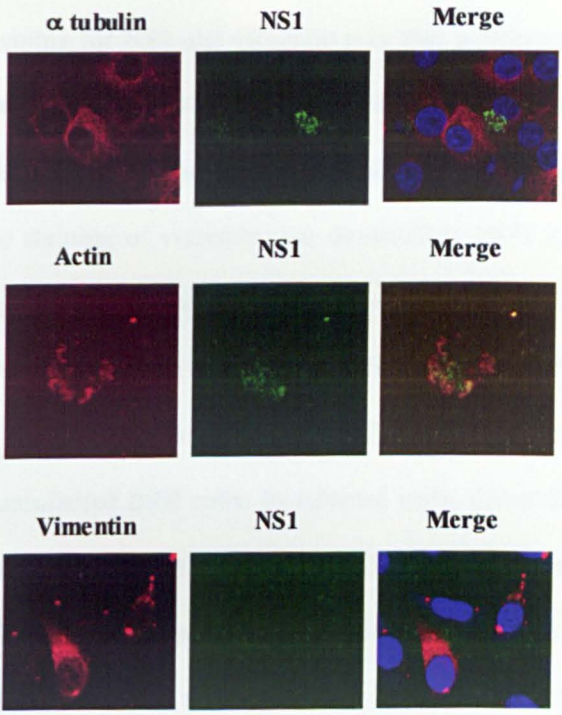

Figure 6. 6: Confocal localisation analysis of NS1 and cytoskeletal components in BSR cells 24 hours post infection with BTV-10. A diffuse and extensive tubular network of staining is visible for all three cytoskeletal markers, vimentin, α tubulin and actin. NS1 shows a normal punctate distribution that extends throughout the cytoplasm.

6.2.5: NS1 co-localises with Intermediate Filament Vimentin

Several drugs exist that allow disruption of each type of filament, the disruption of intermediate filaments, vimentin, is possible using low concentrations of acrylamide

added to the media in cell culture. Since VP2 was shown to interact with only the intermediate filaments and not the microfilaments or microtubules, the interaction of intermediate filaments with NS1 was tested in both 293T cells and BSR cells. A negative control staining for NS2 and vimentin was also performed in BSR cells. Cells were infected and stained as above and examined using confocal microscopy, NS2 was detected using polyclonal antisera GP373 and anti-guinea pig IgG FITC conjugate (Sigma). Very little staining of vimentin was observed in 293T cells, with some cells showing no staining at all, in comparison to the excellent staining observed in BSR cells (Fig 6.7a), therefore the remaining work was completed in BSR cells. Vimentin showed a dense network of fibres that were detected as diffuse staining across the cytoplasm in both infected and uninfected BSR cells. In infected cells, dense foci of vimentin were also visualised. These foci do not correspond to VIB as there was no co-localisation with NS2 (Fig 6.7c). Areas of co-localisation were visible for NS1 and vimentin although, as described previously, staining was so diffuse it was not possible to confirm whether the proteins were co-localised (Fig 6.7bi). However, with the addition of 2mM acrylamide to the media a distinct change is detected in the distribution of both NS1 and vimentin (Fig 6.7bii). Vimentin condensed into small punctate localised patches, these patches showed good, though not complete, co-localisation with NS1. The pattern of NS1 did not alter to the same extent as that of vimentin; some condensation was seen though a significant proportion of NS1 was not co-localised with vimentin, indicating not all NS1 was able to associate with vimentin.

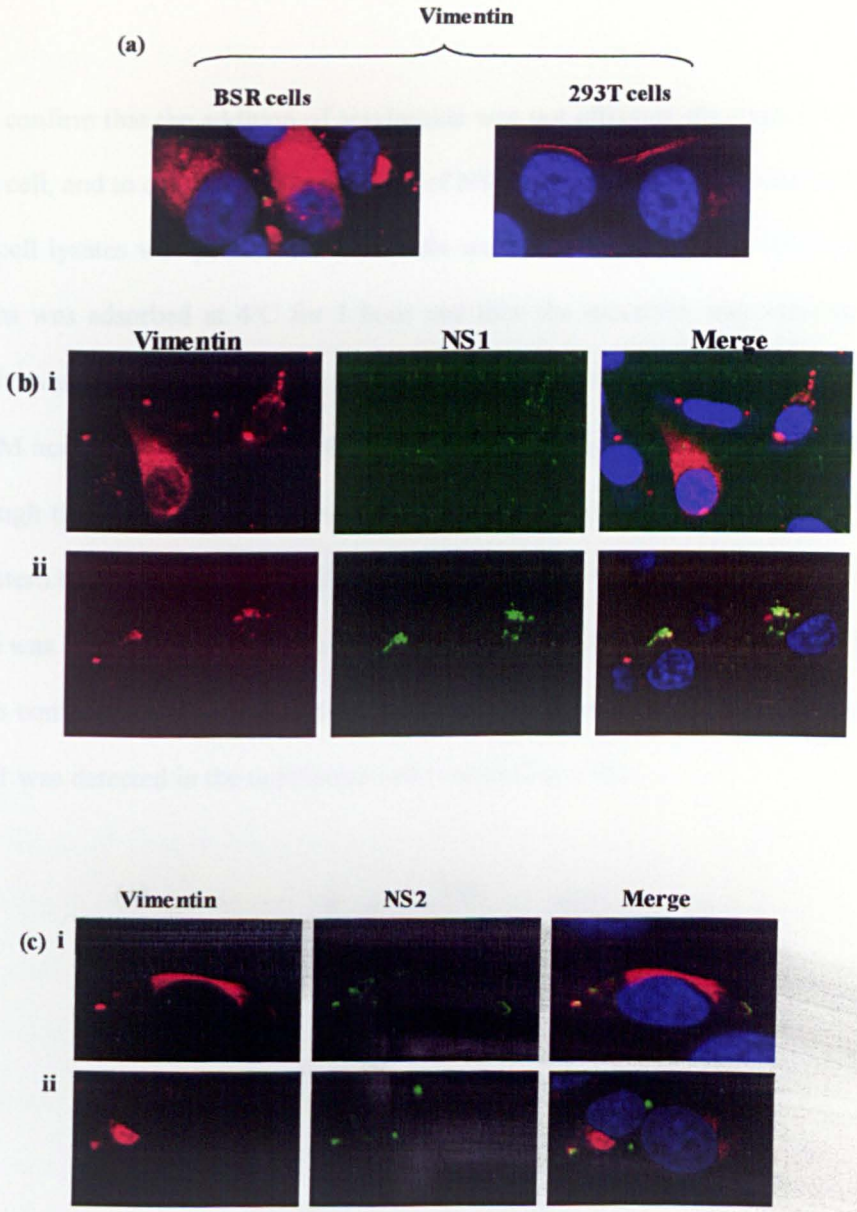

Figure 6. 7: Effect of drug disruption on vimentin networks and NS1 distribution. (a) Expression of vimentin in uninfected 293T cells and BSR cells. (b) Distribution of vimentin and NS1 in BSR cells 24 hours post infection with BTV-10 treated with (i) 0mM acrylamide or (ii) 2mM acrylamide. (c) Distribution of vimentin and NS2 in BSR cells 24 hours post infection with BTV-10 treated with (i) 0 mM acrylamide or (ii) 2 mM acrylamide.

To confirm that the addition of acrylamide was not affecting the amount of vimentin in the cell, and to confirm that expression of NS1 remained the same, western blot analysis of cell lysates was performed. BSR cells were infected with BTV-10 at an MOI of 1, virus was adsorbed at 4°C for 1 hour and then the inoculum was removed. The cells were washed with fresh media and then maintained until harvest in DMEM 2% FCS, 2mM acrylamide at 35°C, 5% CO_2. A negative control was prepared in the same way though the fresh media contained no acrylamide. The amount of vimentin detected by western blot analysis was comparable in both the 2mM acrylamide and un-treated cells, and was also similar in the uninfected un-treated control (Fig 6.8a). NS1 expression was also comparable for both the acrylamide and un-treated control cells. As expected, no NS1 was detected in the uninfected cell control (Fig 6.8b).

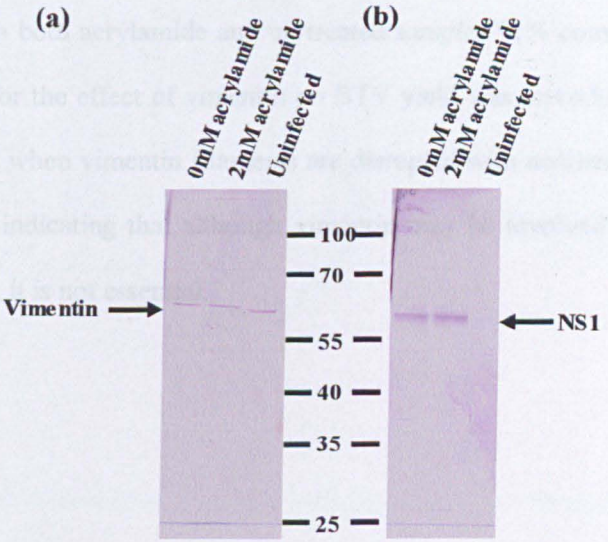

Figure 6. 8: Western blot analysis of expression of (a) vimentin and (b) NS1 in uninfected, infected and infected 2mM acrylamide treated BSR cells.

To analyse the importance of vimentin in BTV infection the titre of virus produced during infection was studied. BSR cells were prepared as above. Samples were harvested at 6, 8 and 24 hours post infection; titres of virus in the supernatant, i.e. released virus, and cell associated virus were measured independently. The total virus yield was similar for both the acrylamide and non-acrylamide treated cells at 6 and 8 hours post infection, at 24 hours post infection the total yield was slightly lower for the acrylamide treated cells (Fig 6.9d). At 6 and 8 hours post infection the percentage of virus in the cell associated sample was higher for the acrylamide treated samples than the un-treated samples, by 16% and 11% respectively (Fig 6.9 a & b), though the difference is not statistically significant. Conversely the percentage of released virus was higher for the un-treated samples than the 2mM treated samples at both 6 and 8 hours post infection, though again not significantly. At 24 hours post infection the percentage of virus in the cell associated sample and released virus sample, was almost identical in both acrylamide and un-treated samples 91% compared to 92% (Fig 6.9c). The data for the effect of vimentin on BTV yield was reproducible. The differences in virus yield when vimentin filaments are disrupted with acrylamide are not significantly increased, indicating that although vimentin may be involved in BTV replication and trafficking, it is not essential.

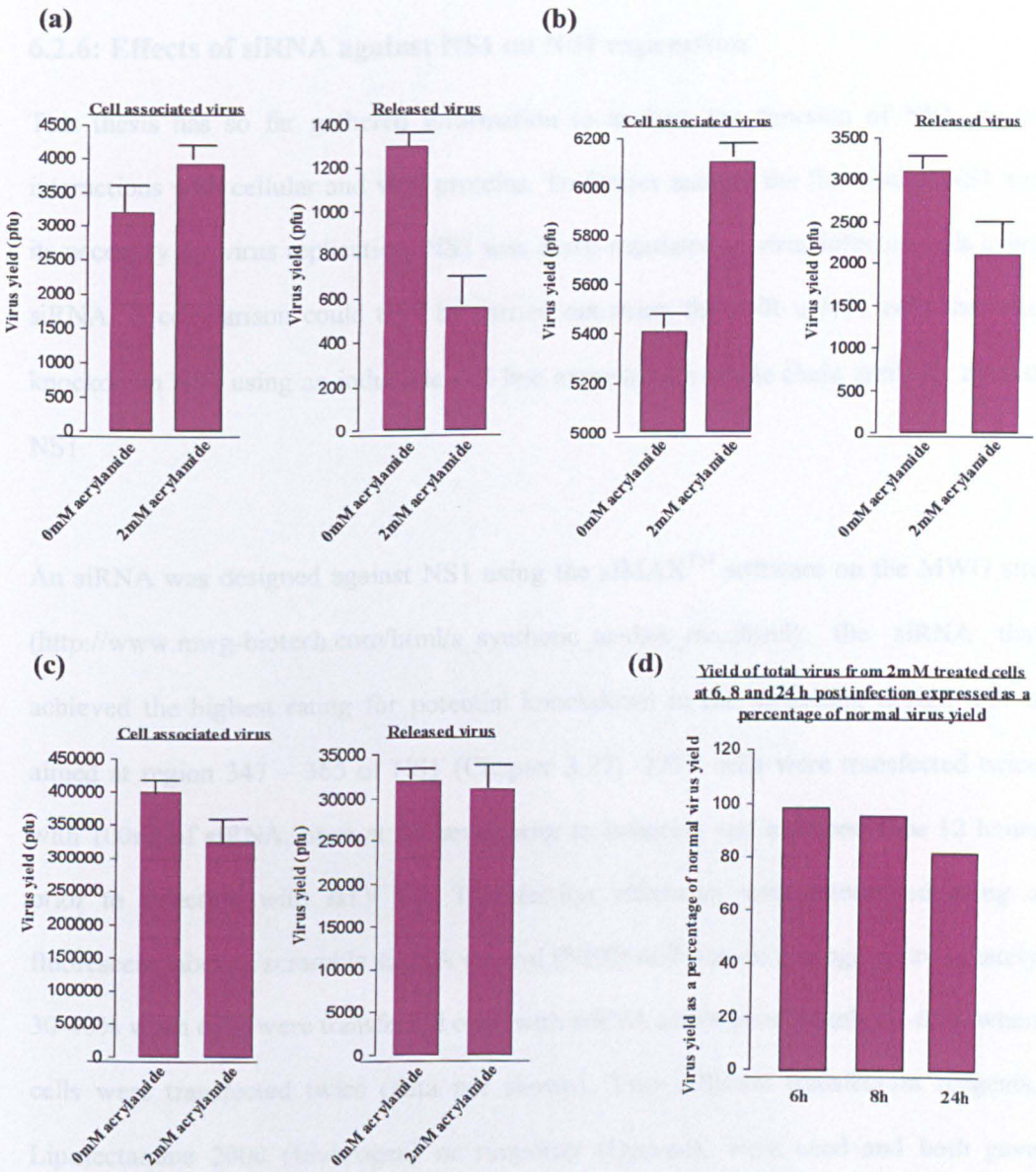

Figure 6. 9: Effect of acrylamide induced vimentin disruption on virus replication and release at (a) 6 hours, (b) 8 hours and (c) 24 hours. (d) Yield of total virus from 2mM acrylamide treated cells expressed as a percentage of normal virus yield. Error bars represent standard deviation where n= 4.

6.2.6: Effects of siRNA against NS1 on NS1 expression

This thesis has so far gathered information to analyse the function of NS1 via its interactions with cellular and viral proteins. To further analyse the function of NS1 and its necessity for virus replication, NS1 was down-regulated in virus infected cells using siRNA. A comparison could then be carried out using the BSR α NS1 cells that also knockdown NS1 using an inducible cell line expressing a single chain antibody against NS1.

An siRNA was designed against NS1 using the siMAX™ software on the MWG site (http://www.mwg-biotech.com/html/s_synthetic_acids/s_rna.shtml), the siRNA that achieved the highest rating for potential knockdown in the modelling design tool is aimed at region 347 – 365 of NS1 (Chapter 3.27). 293T cells were transfected twice with 100ng of siRNA, once at 24 hours prior to infection and a second time 12 hours prior to infection with BTV 10. Transfection efficiency was determined using a fluorescein labelled scramble siRNA control (NEB) and was on average approximately 30-40% when cells were transfected once with siRNA and approximately 50-65% when cells were transfected twice (data not shown). Two different transfection reagents, Lipofectamine 2000 (Invitrogen) or simporter (Upstate), were used and both gave similar results (data not shown).

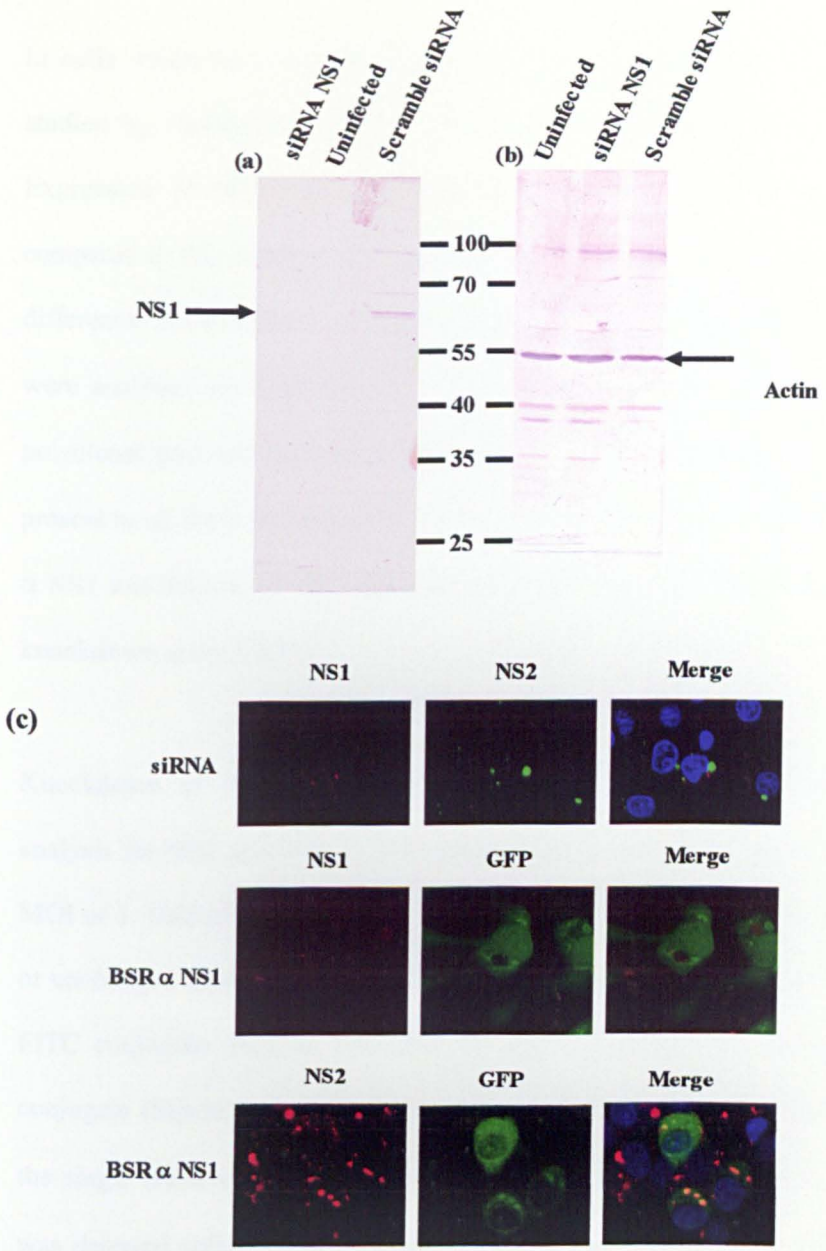

Figure 6. 10: Western blot analyses of (a) NS1 knockdown and (b) actin expression, in 293T cells transfected with NS1 specific siRNA or control scramble siRNA and infected with BTV-10. A negative control of uninfected 293T cells indicates normal actin levels. (c) Confocal analysis of NS1 knockdown and NS2 expression in 293T cells transfected with NS1 specific siRNA and BSR α NS1 cells which were subsequently infected with BTV-10.

In cells where the transfection efficiency exceeded 50% the expression of NS1 was studied by western blot analysis, NS1 was detected with R633 polyclonal antisera. Expression of NS1 was lower in cells transfected with the NS1 specific siRNA compared to the scramble siRNA control (Fig 6.10a) and there was no apparent visual difference in the amount of CPE caused by virus infection. When the same samples were analysed for expression of a cellular protein, actin, as a control, detected with polyclonal goat anti-actin (Santa Cruz Biosciences), comparable amounts of actin were present in all lanes including the uninfected 293T cells (Fig 6.10b). The results for BSR α NS1 knockdown of NS1 and expression of actin were comparable to those of NS1 knockdown using siRNA.

Knockdown of NS1 was confirmed by confocal immunofluorescence microscopy analysis for NS2 and NS1 in 293T cells at 24 hours post-infection with BTV-10 at an MOI of 1. NS2 expression was used to identify infected cells expressing either reduced or unchanged amounts of NS1. NS2 was detected with GP373 and anti-guinea pig IgG FITC conjugate (Sigma), NS1 was detected with R633 and anti-rabbit IgG TRITC conjugate (Sigma). In BSR α NS1 cells GFP expression confirmed the expression of the single chain antibody against NS1. NS1 and NS2 expression in BSR α NS1 cells was detected independently as above, except that both proteins were visualised with TRITC conjugated antibodies. NS1 expression levels were visibly knocked-down in cells expressing the single chain antibody against NS1 whilst NS2 expression and distribution appeared unchanged. In cells treated with siRNA against NS1, NS2 was detected presenting a normal punctate pattern of large cytoplasmic patches and was comparable to cells transfected with scramble control siRNA (data not shown). NS1 was detectable in all cells expressing NS2. However the levels of NS1 expression

relative to NS2 varied significantly from normal to barely detectable; many cells expressed intermediate levels of NS1 (Fig 6.10c).

6.2.7: Presence of Tubules in siRNA treated cells

It was necessary to establish the presence of tubules in cells treated with the NS1 specific siRNA and displaying a reduction in NS1 concentration since it is not known if tubules are the active form of NS1 or not. Cells were transfected and infected as previously (Chapter 6.2.7) giving samples 1) Non-transfected positive control 293T cells, 2) NS1 siRNA transfected cells, 3) scramble siRNA transfected cells and 4) BSR α NS1 cells expressing the single chain antibody specific to NS1. All samples were harvested 40 hours post infection and were examined for tubule presence. NS1 was visible in the cell lysates of all 4 samples though less was visible in the lysate of 293T cells treated with NS1 siRNA (Fig 6.11). In the 293T non-transfected control a little NS1 was detected in sample 5, collected from the top of the gradient; a high amount of NS1 was detected in the mid to lower parts of the gradient, fractions 20 and 30 (Fig 6.11a). The distribution of NS1 within the gradient for the cells transfected with scramble control siRNA was comparable to the positive control with the exception that more NS1 was detected in fractions 10 and 15 (Fig 6.11c). The cells treated with NS1 siRNA showed a different distribution of NS1 throughout the gradient; NS1 was detected only in fractions 5 and 10 and in lesser amounts than in the positive control (Fig 6.11b). This indicated that any NS1 present was assembled as smaller multimers, not particular tubule structures. Similarly, NS1 from the BSR α NS1 cells was distributed more towards the top of the gradient with NS1 detected in samples 5, 10 and a little in fraction 15; no NS1 was detected in fractions 20 and 30 again indicating the presence of NS1 multimers but not particular tubule structures (Fig 6.11d).

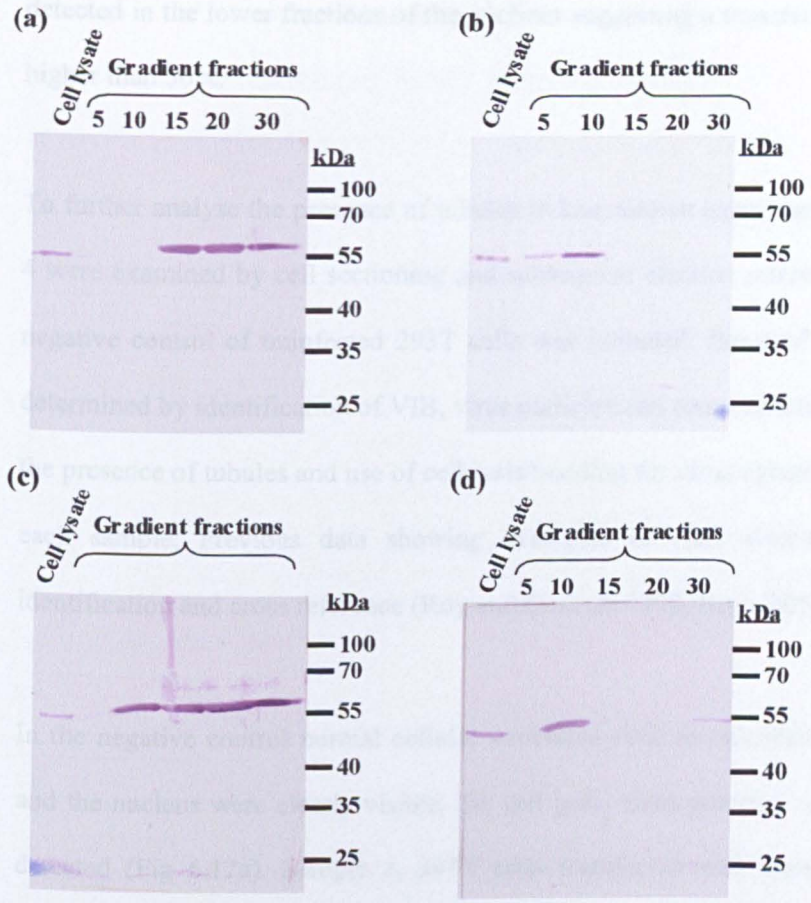

Figure 6. 11: Western blot analysis of NS1 in sucrose gradient fractions from NS1 tubule purification for (a) 293T cells, (b) 293T cells treated with NS1 siRNA, (c) 293T cells treated with control scramble siRNA and (d) BSR α NS1 cells. All samples were infected with BTV-10 and harvested after 40 hours.

It is evident from the western blot data that knockdown levels of NS1 vary from experiment to experiment. In Fig 6.11a no NS1 is detected in the samples treated with siRNA where as in Fig 6.11b NS1 is detected although at lesser levels than detected in control transfections. In addition to this it is probable that the transfection efficiencies also vary, if transfection efficiency was 50% then 50% of the cells would still be producing tubules yet Fig 6.11b indicates that this is not the case since no NS1 is

detected in the lower fractions of the gradient suggesting a transfection efficiency much higher than 50%.

To further analyse the presence of tubules in knockdown experiments samples 2, 3 and 4 were examined by cell sectioning and subsequent electron microscopy. In addition a negative control of uninfected 293T cells was included. Proof of virus infection was determined by identification of VIB, virus particles and core particles; in addition to this the presence of tubules and use of cell lysis/budding for virus egress was determined for each sample. Previous data showing examples of each structure were used for identification and cross reference (Roy and Gorman 1990; Roy 2005).

In the negative control normal cellular structures such as mitochondria, cell junctions and the nucleus were clearly visible. No cell lysis, virus particles or NS1 tubules were detected (Fig 6.12a). Sample 3, 293T cells transfected with control siRNA, clearly showed all signs of virus infection including VIB, virus particles and core particles. Localised patches of NS1 tubules were also detected; many cells showed areas of lysis though no virus egress was visible (Fig 6.12b). Clear evidence of virus infection was also identified in BSR α NS1 cells though no tubules could be detected confirming the knock down of NS1 within these cells. In contrast to previous pictures of these cells (Owens, Limn et al. 2004) no evidence was found of virus budding from the plasma membrane; cells showed amounts of lysis comparable to those with normal levels of NS1, though again no direct evidence of virus egress was observed (Fig 6.12c). The test sample of NS1 siRNA transfected cells was comparable with the BSR α NS1 cells. VIB, virus particles and core particles were all detected as was some cell lysis. No tubules were detected within the cells examined in this sample, though it is possible that

although no tubules were formed, oligomers of NS1 with no distinct structure were not detectable by this method (Fig 6.12d). Again it is probable that transfection efficiencies of siRNA are higher than 50% in this experiment as no NS1 tubules were detected in any of the cells.

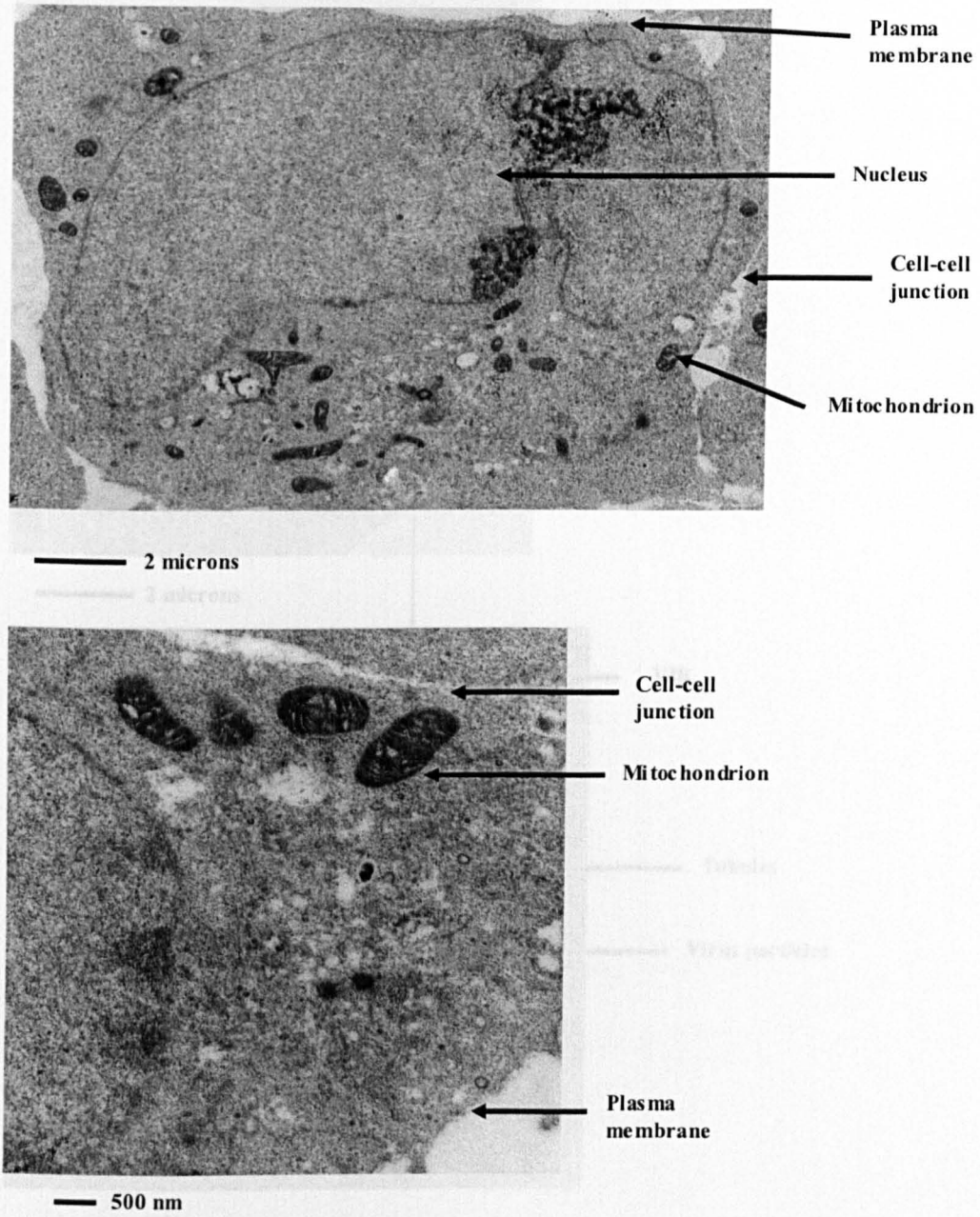

Figure 6. 12: Cell sectioning transmission electron micrographs. NB all samples were analysed 'blind' by the EM operator to ensure that all samples were searched equally for the presence of tubules.

(a) uninfected 293T cells, indicating some cellular structures.

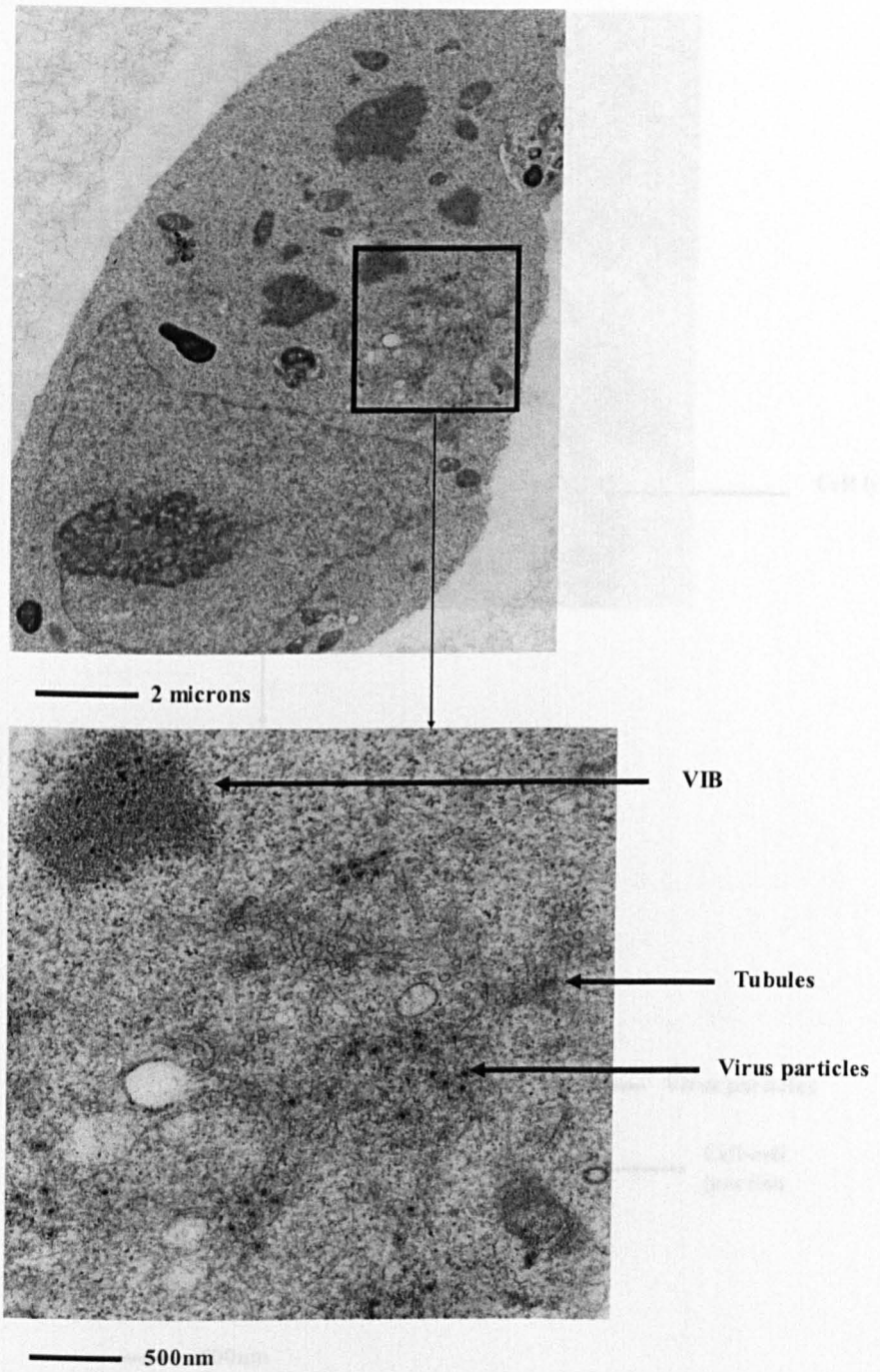

(b) 293T cells treated with control scramble siRNA and infected with BTV-10 indicating NS1 tubules and virus particles.

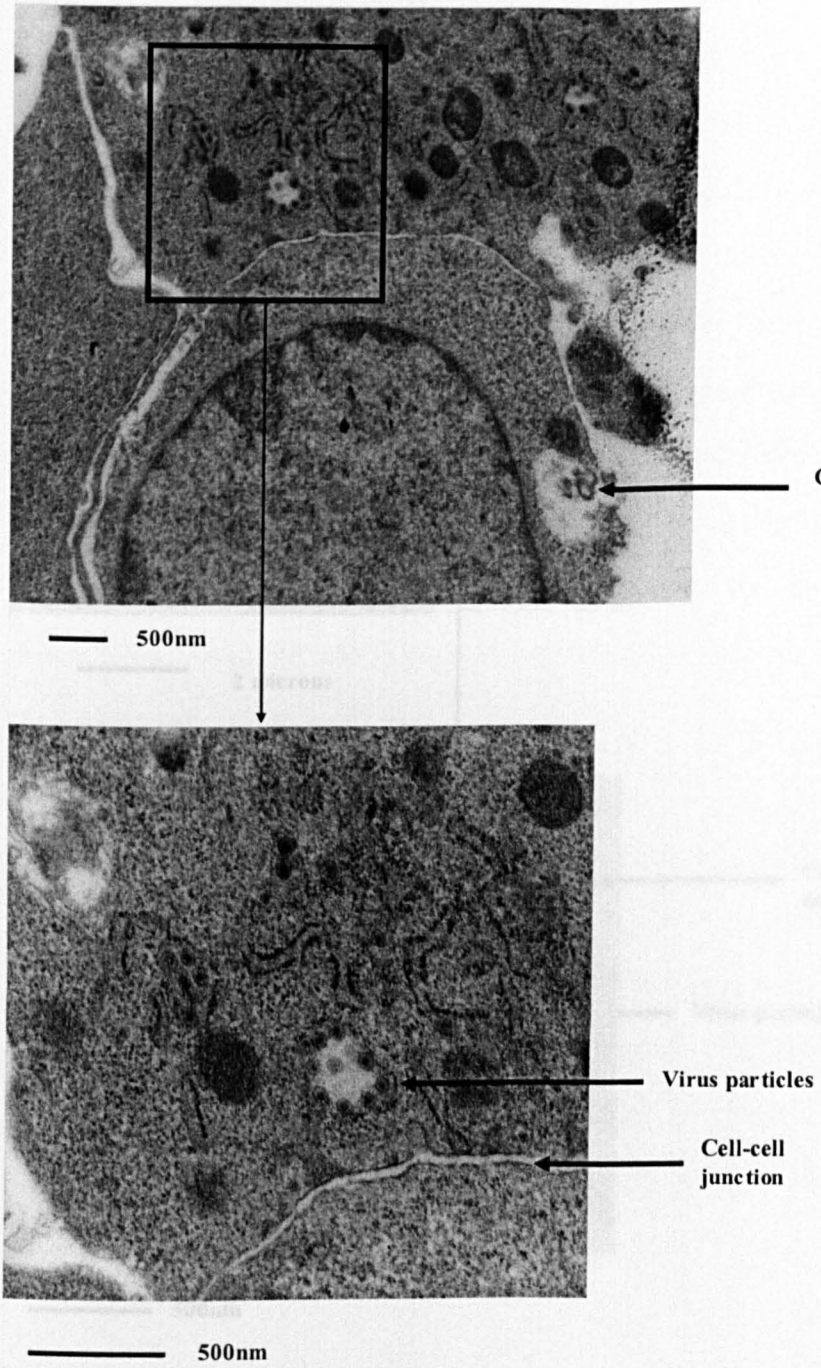

(c) BSR α NS1 cells infected with BTV-10 indicating cell lysis and virus particles. Note no NS1 tubules are detected.

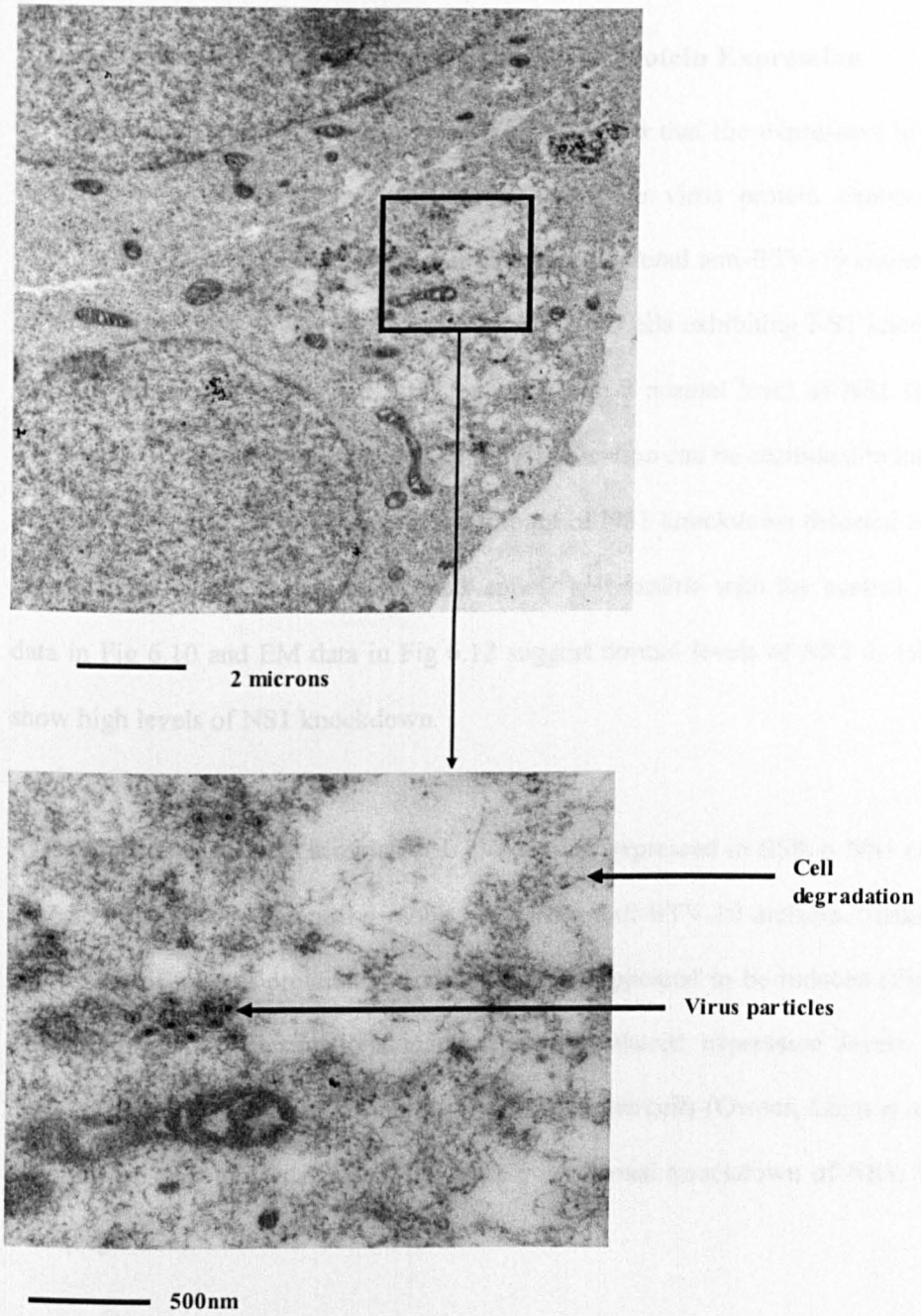

(d) 293T cells treated with NS1 siRNA indicating virus particles and areas of cell degradation. Note no NS1 tubules are detected.

6.2.8: Effects of NS1 specific siRNA on BTV Protein Expression

To confirm that the siRNA was specific to NS1 and that the expression levels of no other BTV protein were affected levels of whole virus protein expression were examined by western blot analysis using rabbit polyclonal anti-BTV-10 antisera. Ratios of all proteins, except NS1, appeared unchanged in cells exhibiting NS1 knockdown in comparison to non-transfected, infected cells with a normal level of NS1 (Fig 6.13). This data indicated that any changes in BTV replication can be attributed to knockdown of NS1. As with other experiments the amount of NS1 knockdown detected is variable and in Fig 6.13 NS1 expression levels appear comparable with the control. Confocal data in Fig 6.10 and EM data in Fig 6.12 suggest normal levels of NS2 in cells which show high levels of NS1 knockdown.

As a comparison, protein samples of BTV proteins expressed in BSR α NS1 cells were analysed by western blot using rabbit polyclonal anti-BTV-10 antisera. Strikingly the expression of several proteins in addition to NS1 appeared to be reduced (Fig 6.13b). This confirms the observations made about the altered expression levels of BTV proteins in the pulse-chase analysis performed on these cells (Owens, Limn *et al.* 2004). Separate western blot analysis of the sample confirmed knockdown of NS3, VP3 and VP5 (Fig 6.13c).

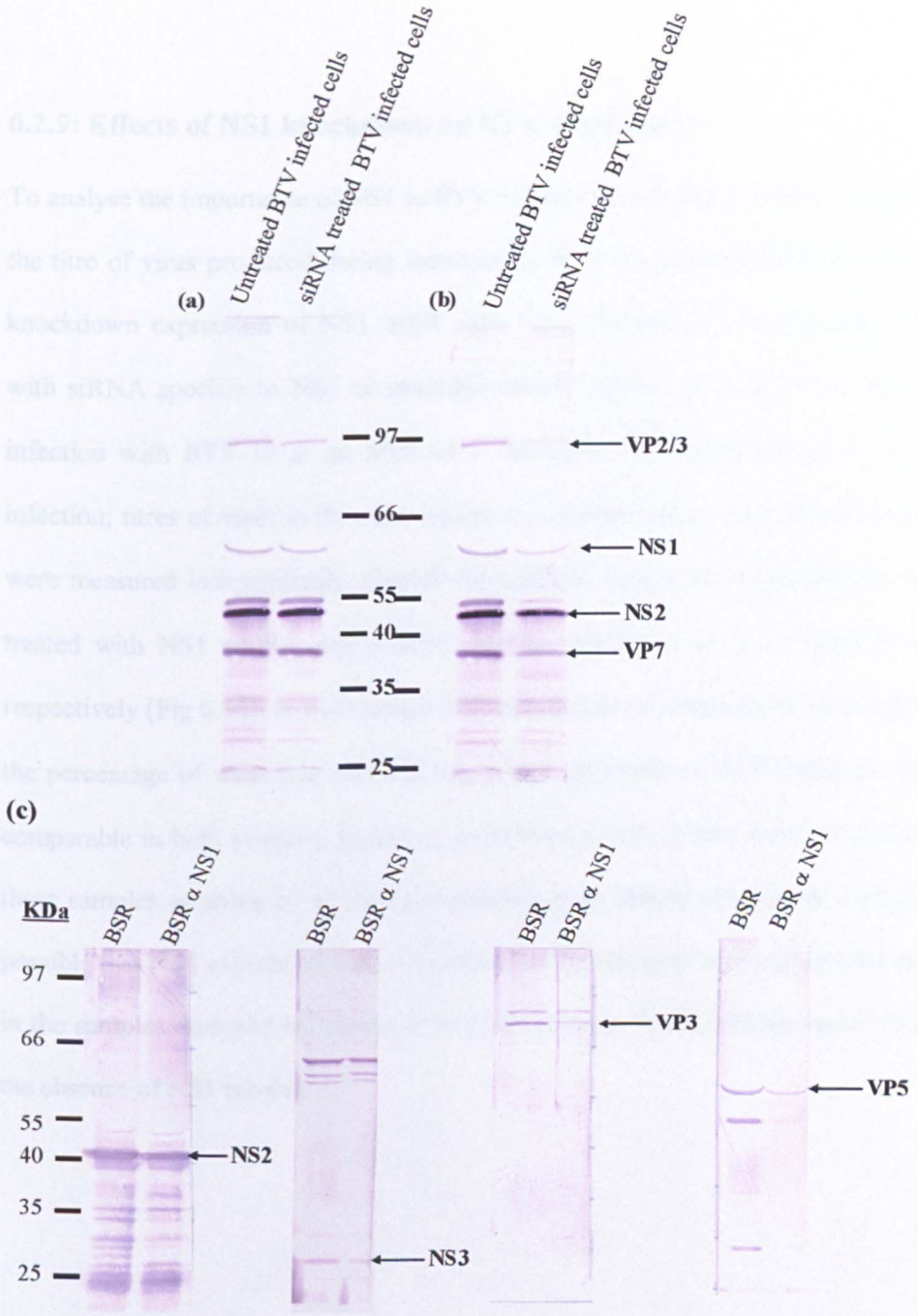

Figure 6. 13: Western blot analysis, using polyclonal anti-BTV-10 antisera, of BTV proteins in (a) NS1 specific siRNA treated cells and (b) BSR α NS1 cells, all infected with BTV-10. (c) Western blot analysis of specific BTV protein expression in BSR α NS1 cells detected with anti-NS2, anti-NS3, anti-VP3 and anti-VP5 polyclonal antisera.

6.2.9: Effects of NS1 knockdown on BTV Replication

To analyse the importance of NS1 in BTV infection and identify potential roles for NS1 the titre of virus produced during infection by BTV-10 was studied under normal and knockdown expression of NS1. BSR cells were transfected as previously described, with siRNA specific to NS1 or scramble control siRNA at 12 and 24 hours prior to infection with BTV-10 at an MOI of 1. Samples were harvested at 24 hours post infection; titres of virus in the supernatant, i.e. released virus, and cell associated virus were measured independently. Overall the yield of virus was comparable for the cells treated with NS1 siRNA and control scramble siRNA, 6.16×10^4 and 4.78×10^4 respectively (Fig 6.14). In both samples the percentage of released virus was higher than the percentage of virus that was cell associated. Amounts of BTV induced CPE were comparable in both samples. However, expression levels of NS1 were not tested for in these samples as doing so would have resulted in an altered virus yield, therefore it is possible that NS1 expression was not reduced as significantly in these samples as it was in the samples analysed by Owens *et al* (2004) where virus yield increased 10-fold in the absence of NS1 tubules.

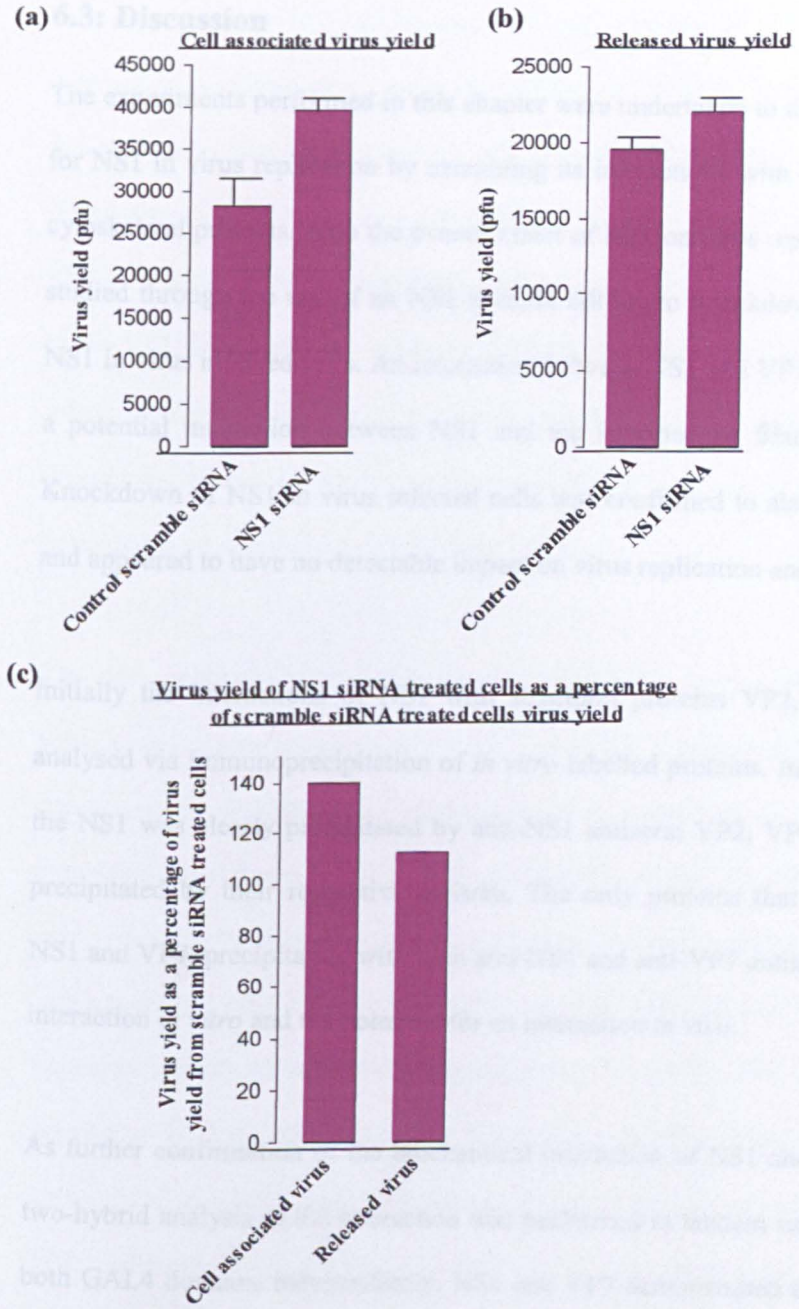

Figure 6. 14: Effect of NS1 specific siRNA on virus replication and release at 24 hours post infection with BTV-10. Yield of (a) cell associated virus and (b) released virus was analysed separately; (c) total virus yield of cells treated with NS1 siRNA expressed as a percentage of scramble siRNA treated cells virus yield. Error bars represent standard deviation where n=3.

6.3: Discussion

The experiments performed in this chapter were undertaken to determine a possible role for NS1 in virus replication by examining its interactions with other viral proteins and cytoskeletal proteins. Also the overall effect of NS1 on virus replication and egress was studied through the use of an NS1 specific siRNA to knockdown expression levels of NS1 in virus infected cells. An interaction between NS1 and VP7 was identified, as was a potential interaction between NS1 and the intermediate filament protein vimentin. Knockdown of NS1 in virus infected cells was confirmed to abrogate tubule assembly and appeared to have no detectable impact on virus replication and release.

Initially the interactions of NS1 with structural proteins VP2, VP5 and VP7 were analysed via immunoprecipitation of *in vitro* labelled proteins. In all three experiments the NS1 was clearly precipitated by anti-NS1 antisera; VP2, VP5 and VP7 were also precipitated by their respective antisera. The only proteins that co-precipitated were NS1 and VP7, precipitating with both anti-NS1 and anti-VP7 antisera thus indicating an interaction *in vitro* and the potential for an interaction *in vivo*.

As further confirmation of the biochemical interaction of NS1 and VP7 *in vitro*, yeast two-hybrid analysis of the interaction was performed in tandem using proteins fused to both GAL4 domains independently. NS1 and VP7 demonstrated interaction regardless of the GAL 4 domain they were fused to confirming the immunoprecipitation data.

To analyse the interactions of VP7 and NS1 *in vivo* in BTV-10 infected cells BSR cells were examined by confocal immunofluorescence microscopy. NS1 and VP7 co-localised with each other, although each protein was also found localised independently.

This may be due to non-synchronous cell and virus populations. In nearly all cases co-localisation was towards the outer edge of the VP7 staining which was in large punctate foci that co-localised perfectly with NS2 (data not shown). This was expected as VP7 is found in high quantities in the periphery of VIB, with core particles detected inside the VIB, and NS1 tubules are frequently detected by electron microscopy in close proximity to the VIB. In *Sf* cells expressing CLP (VP3 and VP7) and NS1 from baculovirus co-infection, the distribution of VP7 was different forming large patches rather than distinct inclusions. However the co-localisation pattern was similar, with localisation occurring on the periphery of VP7 patches.

The data presented within this chapter identifies a robust biochemical interaction between the outer-most core protein, VP7, and NS1. It is unclear from this data what the interaction of NS1 and VP7 contributes to virus replication. In BSR α NS1 cells exhibiting knockdown levels of NS1 and absence of NS1 tubules, VP7 distribution is unchanged. Furthermore in the study performed by Owens *et al*, overall virus yield was increased when NS1 tubules were not present; in the NS1 siRNA studies virus yield appeared unchanged when NS1 tubules were not present. This data suggests that the interaction of VP7 with NS1 does not rely on tubule formation and may even be enhanced by the lack of NS1 tubules, increasing virus replication. Work by Eaton et al 1987, supports this observation that NS1 and VP7 interaction may not involve tubules; anti-NS1 labelled gold particles were detected on the surface of core particles when no tubules were visually detected (Eaton, Hyatt *et al.* 1987).

NS1 does not interact with NS2 in virus infected cells; no co-immunoprecipitation could be detected and confocal data did not show co-localisation of NS1 and NS2. This

was not surprising since NS1 tubules were not detected within the VIB and previous gold labelling electron micrograph studies of VIB showed no staining for NS1 indicating the absence of NS1 monomers/dimers from the VIB (Eaton, Hyatt *et al.* 1987). However, NS1 tubules were found in close proximity to VIBs (Eaton, Hyatt *et al.* 1987; Brookes, Hyatt *et al.* 1993); NS1 interacts with VP7 which is found localised with NS2 in VIBs, and this may explain the close proximity of NS1 to VIBs but lack of interaction with NS2.

Immunoprecipitation was not performed for NS1 and the remaining non-structural protein NS3 due to the membrane spanning nature of NS3. Confocal studies identified areas of co-localisation within the cell cytoplasm though this does not confirm an interaction. Much of the NS3 detected within the virus infected cells is localised at the plasma membrane where NS1 is not routinely localised. NS3 is associated with virus egress and NS1 knockdown has been linked to a change in virus egress (Owens, Limn *et al.* 2004; Wirblich, Bhattacharya *et al.* 2006). Both NS1 and NS3 interact with proteins involved in the ubiquitination and sumoylation of target proteins as discussed in chapter 4 and 5 (Wirblich, Bhattacharya *et al.* 2006). It is possible that an interaction occurs between NS1 and NS3, though this need not be direct, and is possibly most important via a supportive/opposing effect on aspects of ubiquitin and SUMO-1 control of protein expression and distribution.

NS1 tubules are often found in close proximity to the cytoskeleton where both VP2 (Bhattacharya B and Roy, P; personal communication) and virus particles are located (Eaton, Hyatt *et al.* 1987), and in close proximity to VIB (Eaton, Hyatt *et al.* 1988; Brookes, Hyatt *et al.* 1993). In addition to this, the observation that NS1 interacts with

VP7 gives a hypothesis for the role of NS1 in virus infection. BTV core-like particles are soluble and not associated with the cytoskeleton; previous investigations have also demonstrated that CLPs synthesised either in the presence of VP2 or VP5 fail to attach to the cytoskeleton (Hyatt, Zhao *et al.* 1993). This indicated that both the outer coat proteins are required for stable virus-cytoskeletal interaction. One hypothesis for the role of NS1 in virus infection is that NS1 helps core particles to accumulate near to VP2 since NS1 is associated with intermediate filaments. It is possible that NS1 either as tubules or monomers/dimers transports virus cores, from the VIB where they assemble (Kar, Iwatani *et al.* 2005), to the cytoskeleton where VP2 is located thus helping in virus maturation and subsequent egress. It is also possible that NS1 serves merely as an anchor for virus cores allowing the build up of cores in close proximity to VP2 before subsequent maturation and egress. To test this hypothesis the interaction of NS1 with cytoskeletal proteins was first confirmed.

Confocal analysis of NS1 with cytoskeletal markers vimentin, α tubulin and actin was inconclusive. Staining of the cytoskeletal networks was comprehensive and throughout the cytoplasm indicating areas of co-localisation when in fact this may be overlap of localisation due to the cytoskeleton occupying so much of the cell.

Studies were targeted to the intermediate filaments, vimentin, of the cytoskeleton since if the hypothesis is true NS1 would be expected to localise with the same filaments as VP2 as it does not directly interact with VP2. Acrylamide is a known disrupter of vimentin filaments and has been well documented. In PtK2 cells acrylamide causes aggregation of vimentin filaments in a concentration-dependent fashion; these effects occurred at a lower concentration than alterations in other cytoskeletal filaments and

were fully reversible causing no cytoskeletal cross linking (Sager 1989). In LLC-MK2 cells acrylamide specifically disrupts intermediate filaments in a short period of time and cells recover their normal morphology and functionality in only a few hours after the removal of the drug (Arcangeletti, Pinardi *et al.* 1997). A more recent study has also shown that acrylamide disrupts the intermediate filament network and results in the formation of cytoplasmic aggregates of vimentin in the cell, a distinct change from the perinuclear cap distribution (Cordo and Candurra 2003).

Vimentin expression was easily detectable and displayed a normal perinuclear network with some cells showing a cap like distribution and others showing a more diffuse network. The distribution of vimentin in BTV infected cells appeared unchanged in comparison to that in uninfected cells. BTV VIB are not the same as the viral aggresomes, formed by other viruses, whereby vimentin forms a dense area for virus replication and assembly similar to that formed by NS2.

Addition of 2mM acrylamide to BTV-10 infected BSR cells resulted in the expected change in vimentin distribution, vimentin appeared in perinuclear aggregates rather than the network normally detected. NS1 distribution also changed in a similar way, though to a lesser extent than vimentin. This indicates that some NS1 remained unaffected by vimentin distribution indicating that not all NS1 interacts with vimentin. As a negative control NS2 localisation was also studied, no co-localisation was detected for NS2 and vimentin, this further confirms the absence of viral aggresomes and the distinct separate identification of VIB. An earlier investigation using the same concentration of acrylamide showed that cellular protein synthesis was not significantly altered in Vero cells in the presence of the acrylamide (Cordo and Candurra 2003). The distribution of

NS1 and vimentin in the acrylamide treated BSR cells could be explained on the basis of selective primary collapse and disassembly of vimentin in the cells, and not on the drug induced reduction or change in the synthesis of vimentin. Confirmation of this was achieved by western blot analysis indicating that the expression levels of vimentin and NS1 remained comparable to those in cells un-treated with acrylamide.

The effect of vimentin and NS1 distribution, in acrylamide treated cells, on virus replication and egress over a 24 hour time course was examined by a study of virus yield, both cell associated and released virus yield. Total virus yield was comparable for both 0 and 2mM acrylamide treated cells at 6, 8 and 24 hours post-infection. This data indicates that although vimentin may be involved in virus replication and release it is not essential. It is possible that the change in distribution of vimentin and subsequently VP2 and some NS1, has a small effect on virus assembly or trafficking along the cytoskeleton, due to an altered cellular localisation, that is not detectable in this experiment. Also it is important to note that the optimum concentration of acrylamide for disruption of vimentin is 2mM (Sager 1989; Arcangeletti, Pinardi et al. 1997; Cordo and Candurra 2003). This is much higher than the concentration most pharmacological inhibitors are used at, and although cells return to healthy normal morphology after removal of acrylamide it can not be assumed that acrylamide is not having an effect on overall cell health in a way other than disruption of vimentin.

Vimentin is involved in the replication of other viruses from different families; acrylamide has an inhibitory effect on Junin virus replication in a dose dependent manner without modifying the cellular viability (Cordo and Candurra 2003). It does not affect virus entry but significantly decreases virus protein expression and overall titre

indicating that vimentin has a role in the early stages of JUNV replication. Many other viruses such as poxviruses and African swine fever virus (A*SF*V) rearrange vimentin during virus replication to create viral aggresomes. Viral proteins accumulate in the aggresomes before assembly and release of the virus (Heath, Windsor *et al.* 2001; Risco, Rodriguez *et al.* 2002; Stefanovic, Windsor *et al.* 2005).

An siRNA against BTV-10 NS1 was designed to knockdown NS1 in BTV infected cells. This technique was used to identify and analyse any changes lack of NS1 causes in BTV replication and to examine if it was possible to draw conclusions about the function of NS1. Previous data produced using BSR α NS1 cells to knockdown NS1 had indicated that tubules could not be detected in these cells though some NS1 was still present. This data suggested that the lack of, or severe reduction of NS1 tubules causes a change in virus egress.

Western blot analysis determined that NS1 knockdown varied greatly between experiments but was on average NS1 expression was reduced by approximately 50%, in cells treated with siRNA. This was expected since on average 50-65% of cells were transfected and siRNA is not 100% efficient, especially against a protein as highly expressed as NS1. Detection of actin within cells displaying a reduced expression of NS1 indicated that the expression levels of cellular proteins were not affected by siRNA transfection. Confocal immunofluorescence microscopy analysis confirmed that NS1 levels were reduced in 293T cells treated with NS1 siRNA and that NS2 expression and distribution were normal. BSR α NS1 cells were confirmed by western blot and confocal analysis to have comparable levels of NS1 as cells treated with NS1 siRNA.

To address the study of knockdown with regards to lack/reduction of tubules it was necessary to confirm that NS1 tubules were absent or reduced. Biochemical analysis of tubule presence by sucrose gradient purification indicated that less NS1 was present overall and that the majority of NS1 was detected in the upper quarter of the gradient as is the case for BSR α NS1 cells NS1 purification. NS1 tubules are normally detected in the mid to lower fractions of the gradient, with lesser amounts towards the top. This indicates that in cells treated with NS1 siRNA there are no particular tubule structures and NS1 exists as oligomers of an undetermined size. The absence of NS1 in the lower fractions also indicates a much higher transfection efficiency than achieved in some experiments; the absence of detectable tubules suggests a transfection rate of higher than 70%.

NS1 tubules were easily detectable by electron microscopy of BTV infected cells and the cellular distribution was comparable to previous studies (Eaton, Hyatt *et al.* 1988; Brookes, Hyatt *et al.* 1993; Monastyrskaya, Gould *et al.* 1995; Owens, Limn *et al.* 2004). To confirm the absence of tubules in NS1 siRNA treated cells and BSR anti-NS1 cells EM studies were performed. Positive signs of virus infection were identified; these included the presence of VIB, virus particles and core particles. NS1 tubules were not detectable in cells displaying knocked down expression of NS1, again this indicates a transfection efficiency much higher than 50%. In this experiment no virus particles could be detected egressing from the cell membrane via budding as was seen in the previous study of BSR α NS1 cells (Owens, Limn et al. 2004), though this may be due to different methods of analysis.

To ensure that any changes detected in virus replication were due to knockdown of NS1 and not due to an effect on another BTV protein, expression of BTV-10 proteins was examined by western blot analysis in 293T cells treated with NS1 siRNA. As expected less NS1 was visible though knockdown was not as successful as in previous experiments, although all other proteins appeared present in the same ratios and amounts as in the control. As a cross reference this experiment was also carried out in BSR α NS1 cells. Previous data on these cells indicated a decreased stability/expression of certain proteins (Owens, Limn *et al.* 2004); western blot analysis confirmed reproducibly lower expression levels of VP3, VP5 and NS3. The knockdown of other BTV proteins may have serious consequences regarding virus infection; effects previously attributed to NS1 knockdown must be reconsidered in this cell line. This may explain the apparent differences in virus egress between cells displaying NS1 knockdown due to siRNA and knockdown due to internally expressed single chain anti-NS1. However, it is also possible that the differences detected between the two cell lines may be due to differences in the levels of NS1 knockdown or differences in analysis methods.

Finally the effect of reduced NS1 expression and absence of tubules were analysed with respect to the ability of the virus to replicate and release to normal titres. Previous western blot analysis indicated that viral protein expression was normal, thus any changes detected in virus yield may be due to changes in virus assembly and the later stages of virus maturation. Cell associated and released virus yield were measured separately providing information on virus egress, the total yield gives an indication of overall virus fitness. Total virus yield in NS1 siRNA treated cells was comparable to the control yield, indicating that viral fitness was not detectably affected by NS1

knockdown and tubule absence. In BSR α NS1 the knockdown of NS1 gave a 10-fold increase in virus yield. Differences in methodologies and knockdown levels of NS1 between the two experiments may explain this difference.

7: Conclusion

This thesis set out to identify cellular proteins from mammals and insects that interact with NS1 and to investigate the role of NS1 in BTV replication by its interactions with these cellular proteins and other BTV proteins.

BTV NS1 was identified as interacting with aldolase A, NUBP1, pyruvate kinase M2, cathespin B and peptide TY7 from mammalian cells and ubiquitin activating E1 enzyme from insect cells. The interaction of NS1 with SUMO-1 was confirmed and the importance of SUMO-1 in BTV infection was established. Knockdown of NS1 in mammalian cell BTV infection indicated a possible role for NS1 monomers/dimers in BTV infection as absence of NS1 tubules did not result in a detectable change in virus replication and yield.

Expression of peptide FLAGTY7 and NS1 in 293T cells resulted in extensive cell death within 16 hours of plasmid transfection, which was not apoptosis. Proteomic analysis of FLAGTY7 detected a high level of hydrophobicity; no other features were identified. The virus yield of cells treated with FLAGTY7/NS1 before infection with BTV-10 was 63% of normal virus yield, a 3-fold reduction. The decrease in BTV yield is likely to be due to the rapid cell death and consequently less virus progeny are synthesised. It can be assumed that if no programmed response is occurring upon the co-expression of NS1 and FLAGTY7 from either plasmid or virus expressed NS1, the subsequent cell death may be caused by a toxic effect of the two proteins and not due to a specific effect on part of the BTV replication cycle or cellular response to infection.

Two main roles have been identified for NS1 in virus replication; one involves the interaction of NS1 with cellular proteins involved in control of protein expression and degradation. The other involves the interaction of NS1, probably in free monomer/dimer form, with BTV core protein, VP7, and vimentin intermediate filaments of the cellular cytoskeleton.

BTV NS1 interacts with human SUMO-1. BTV-10 infection, but not NS1 alone, was sufficient to induce SUMO-1 expression in mammalian cells. When SUMO-1 expression in BTV infected cells was knocked-down by specific siRNA, a dramatic reduction in virus yield was observed. Only 27% of the normal virus yield was detected. SUMO-1 has diverse roles within the cell including regulation of transcription, chromatin structure, DNA repair and differential protein localisation.

It is possible that the interaction of NS1 with SUMO-1 leads to a modulation of host response to BTV infection in one of two ways. NS1 may be binding sumoylated transcription factors and retarding their translocation to the nucleus, thus NS1 would be preventing induction of BTV induced gene expression in a way that was advantageous for the virus. It is more probable that NS1, like many other viral proteins, forms part of an E3 ligation complex and is involved in the targeting of SUMO-1 onto specific cellular targets. This would also allow modification and control of host responses to BTV infection creating a more advantageous environment for BTV replication. Knockdown of SUMO-1 would prevent NS1 targeting specific proteins for sumoylation, altering the expression levels of various cellular proteins, which may account for the significant reduction in virus yield.

NS1 also putatively interacts with the ubiquitin activating E1 enzyme of *Culicoides*. A *Culicoides* protein with homology to the *Drosophila melanogaster* E1 protein was identified as interacting with BTV NS1 *in vitro*. E1 is one of three essential genes necessary for the activation of ubiquitin for ubiquitination of proteins in the cell cycle and degradation pathways. Many viruses interact with enzymes from the ubiquitin pathway to degrade cellular proteins that interfere with virus replication such as factors of the immune response or to affect the cell cycle in a way which is advantageous for virus replication. It is possible that NS1 interacts with E1 to target specific cellular factors for ubiquitination, thus effecting the degradation of cellular factors, again modulating the host response to BTV infection.

Knockdown of NS1 is variable between experiments due to apparent differences in transfection and knockdown levels; this system therefore requires further standardisation for continutaion of this work. Knockdown of NS1 inhibits tubule formation with no apparent effect on virus replication, indicating that NS1 in its monomeric or oligomeric form may interact with SUMO-1 and ubiquitin activating E1 to modulate the host response to BTV infection. It is possible that NS1 tubules are more important in BTV replication and transmission *in vivo* where these processes are more complex.

The interaction of BTV NS1 with proteins involved in the ubiquitin pathway and sumoylation pathway, and the interaction of BTV NS3 with Nedd4 like ubiquitin ligases, gives rise to a number of interesting possibilities for virus release and pathogenicity. It is possible that NS1 and NS3 function synergistically, either

dependently or independently, to regulate virus replication and egress; NS1 by its interactions with proteins that modulate host protein expression, targeting and degradation, and NS3 by its interaction with host proteins that effect budding of virus particles by targeting host proteins for ubiquitination. Furthermore, given the differences in the ratio of NS1: NS3 between insect and mammalian cell infections, it is possible that more budding is seen during insect cell infection due to the relative balance of interactions with cellular proteins via NS1 and NS3.

BTV NS1 interacts reproducibly with VP7 *in vitro*. In BSR α NS1 cells exhibiting knockdown levels of NS1 and absence of NS1 tubules, VP7 distribution is unchanged. Further more in the siRNA NS1 studies inhibition of tubule formation did not detectably effect virus replication. This data suggests that the interaction of VP7 with NS1 does not rely on tubule formation. Work by Eaton *et al* 1988, supports this observation that NS1 and VP7 interaction may not involve tubules; anti-NS1 labelled gold particles were detected on the surface of core particles when no tubules were visually detectable (Eaton, Hyatt *et al.* 1988).

NS1 interacts to some extent with vimentin intermediate filaments. When vimentin fibres were disrupted with acrylamide a change was detected in the distribution of NS1 which mirrors, but to a lesser extent, the change in vimentin distribution, indicating that not all NS1 within the cell interacted with vimentin. Disruption of vimentin filaments did not significantly alter virus replication or release indicating that vimentin is not essential. It is possible that the change in distribution of vimentin and subsequently VP2 and some NS1, has some effect on virus assembly or trafficking along the cytoskeleton due to an altered cellular localisation that was not detectable.

NS1 tubules are often found in close proximity to the cytoskeleton where both VP2 (Bhattacharya, B and Roy, P; personal communication) and virus particles are located (Eaton, Hyatt *et al.* 1987) and in close proximity to VIB where VP7 is located in high quantities (Eaton, Hyatt *et al.* 1988; Brookes, Hyatt *et al.* 1993). One hypothesis for the role of NS1 in virus infection is that NS1 helps core to accumulate near to VP2 since NS1 is associated with intermediate filaments. It is possible that NS1 either as tubules or monomers/oligomers transports virus cores, from the VIB where they assemble, to the cytoskeleton where VP2 is located thus helping in virus maturation and subsequent egress. It is also possible that NS1 serves merely as an anchor for virus cores allowing the build up of cores in close proximity to VP2 before subsequent maturation and egress.

Down regulation of BTV NS1 in mammalian cell infection has no apparent effect on virus replication *in vitro*. Down regulation of SUMO-1 leads to a huge reduction in virus yield *in vitro*. Absence of NS1 tubules, but presence of NS1 monomer/oligomer, does not lead to a change in VP7 or SUMO-1 distribution and expression, therefore it is probable that the function of NS1 does not rely on the formation of tubules and that NS1 tubules are a form of storage for the active monomer/dimer form of NS1. NS1 may be more essential during BTV infection *in vivo* where transmission and propagation are more complex.

This project has generated some interesting data much of which is incomplete and requires further studying. The most promising aspects of this work involve NS1 interactions with host cell environment regulators, SUMO-1 and possibly UBA-1. More

work is required into this area to confirm the interaction of NS1 and UBA-1 and to identify the mechanisms and outcomes of these interactions. Also further analysis of the involvement of NS3 with a similar set of proteins including TSG101 and Nedd4, in addition to the role of NS1 with SUMO-1 and UBA-1 may help to identify cumulative/antagonistic affects of these two non-structural proteins in BTV infection.

The interaction of NS1 with pFLAGTY7 produces an extremely interesting effect during BTV-10 infection. Further study in this area may elucidate how the addition of a peptide with no defining characteristics has such a large impact on cellular health when expressed in conjunction with NS1. However it is unlikely that this interaction occurs during BTV-10 infection since peptide FLAGTY7 is not a naturally expressed protein and is therefore unlikely to be studied further. It is also unlikely that the interactions of Aldolase A and NUBP1 with NS1 will be studied further due to a lack of literature suggesting their possible importance, it is not clear why NS1 would interact with these two proteins and it is possible that they are yeast two-hybrid artefacts rather than true positives.

References

Alaoui-Ismaili, M. H. and C. D. Richardson (1996). "Identification and characterization of a filament-associated protein encoded by Amsacta moorei entomopoxvirus." J Virol **70**(5): 2697-705.

Aminev, A. G., S. P. Amineva, et al. (2003). "Encephalomyocarditis viral protein 2A localizes to nucleoli and inhibits cap-dependent mRNA translation." Virus Res **95**(1-2): 45-57.

Aminev, A. G., S. P. Amineva, et al. (2003). "Encephalomyocarditis virus (EMCV) proteins 2A and 3BCD localize to nuclei and inhibit cellular mRNA transcription but not rRNA transcription." Virus Res **95**(1-2): 59-73.

Arcangeletti, M. C., F. Pinardi, et al. (1997). "Modification of cytoskeleton and prosome networks in relation to protein synthesis in influenza A virus-infected LLC-MK2 cells." Virus Res **51**(1): 19-34.

Attoui, H., F. Mohd Jaafar, et al. (2005). "Expansion of family Reoviridae to include nine-segmented dsRNA viruses: Isolation and characterization of a new virus designated aedes pseudoscutellaris reovirus assigned to a proposed genus (Dinovernavirus)." Virology **343**(2): 212-23.

Baker, T. S., N. H. Olson, et al. (1999). "Adding the third dimension to virus life cycles: three-dimensional reconstruction of icosahedral viruses from cryo-electron micrographs." Microbiol Mol Biol Rev **63**(4): 862-922, table of contents.

Banerjee, R., M. K. Weidman, et al. (2005). "Modifications of both selectivity factor and upstream binding factor contribute to poliovirus-mediated inhibition of RNA polymerase I transcription." J Gen Virol **86**(Pt 8): 2315-22.

Bearer, E. L. and P. Satpute-Krishnan (2002). "The role of the cytoskeleton in the life cycle of viruses and intracellular bacteria: tracks, motors, and polymerization machines." Curr Drug Targets Infect Disord **2**(3): 247-64.

Beaton, A. R., J. Rodriguez, et al. (2002). "The membrane trafficking protein calpactin forms a complex with bluetongue virus protein NS3 and mediates virus release." Proc Natl Acad Sci U S A **99**(20): 13154-9.

Boutell, C., M. Canning, et al. (2005). "Reciprocal activities between herpes simplex virus type 1 regulatory protein ICP0, a ubiquitin E3 ligase, and ubiquitin-specific protease USP7." J Virol **79**(19): 12342-54.

Bowman, V. D., E. S. Chase, et al. (2002). "An antibody to the putative aphid recognition site on cucumber mosaic virus recognizes pentons but not hexons." J Virol **76**(23): 12250-8.

Boyce, M., J. Wehrfritz, et al. (2004). "Purified Recombinant Bluetongue Virus VP1 Exhibits RNA Replicase Activity." J Virol **In Press**.

Brookes, S. M., A. D. Hyatt, et al. (1993). "Characterization of virus inclusion bodies in bluetongue virus-infected cells." J Gen Virol **74 (Pt 3)**: 525-30.

Brussaard, C. P., A. A. Noordeloos, et al. (2004). "Discovery of a dsRNA virus infecting the marine photosynthetic protist Micromonas pusilla." Virology **319**(2): 280-91.

Caton, A. J. and J. S. Robertson (1980). "Structure of the host-derived sequences present at the 5' ends of influenza virus mRNA." Nucleic Acids Res **8**(12): 2591-603.

Chang, L. K., Y. H. Lee, et al. (2004). "Post-translational modification of Rta of Epstein-Barr virus by SUMO-1." J Biol Chem **279**(37): 38803-12.

Chare, E. R. and E. C. Holmes (2004). "Selection pressures in the capsid genes of plant RNA viruses reflect mode of transmission." J Gen Virol **85**(Pt 10): 3149-57.

Chiou, C. T., C. C. Hu, et al. (2003). "Association of Japanese encephalitis virus NS3 protein with microtubules and tumour susceptibility gene 101 (TSG101) protein." J Gen Virol **84**(Pt 10): 2795-805.

Choe, S. S., D. A. Dodd, et al. (2005). "Inhibition of cellular protein secretion by picornaviral 3A proteins." Virology **337**(1): 18-29.

Cordo, S. M. and N. A. Candurra (2003). "Intermediate filament integrity is required for Junin virus replication." Virus Res **97**(1): 47-55.

Dhar, R., R. M. Chanock, et al. (1980). "Nonviral oligonucleotides at the 5' terminus of cytoplasmic influenza viral mRNA deduced from cloned complete genomic sequences." Cell **21**(2): 495-500.

Diamond, M. S. (2003). "Evasion of innate and adaptive immunity by flaviviruses." Immunol Cell Biol **81**(3): 196-206.

DiPerna, G., J. Stack, et al. (2004). "Poxvirus protein N1L targets the I-kappaB kinase complex, inhibits signaling to NF-kappaB by the tumor necrosis factor

superfamily of receptors, and inhibits NF-kappaB and IRF3 signaling by toll-like receptors." J Biol Chem **279**(35): 36570-8.

Eaton, B. T., A. D. Hyatt, et al. (1987). "Association of bluetongue virus with the cytoskeleton." Virology **157**(1): 107-16.

Eaton, B. T., A. D. Hyatt, et al. (1988). "Localization of the nonstructural protein NS1 in bluetongue virus-infected cells and its presence in virus particles." Virology **163**(2): 527-37.

Eichwald, V., L. Daeffler, et al. (2002). "The NS2 proteins of parvovirus minute virus of mice are required for efficient nuclear egress of progeny virions in mouse cells." J Virol **76**(20): 10307-19.

Espagne, E., V. Douris, et al. (2005). "A virus essential for insect host-parasite interactions encodes cystatins." J Virol **79**(15): 9765-76.

Fauquet, C. (2005). Virus taxonomy : classification and nomenclature of viruses : eighth report of the International Committee on the Taxonomy of Viruses. San Diego, Calif. ; London, Elsevier Academic Press.

Fillmore, G. C., H. Lin, et al. (2002). "Localization of the single-stranded RNA-binding domains of bluetongue virus nonstructural protein NS2." J Virol **76**(2): 499-506.

Fontoura, B. M., P. A. Faria, et al. (2005). "Viral interactions with the nuclear transport machinery: discovering and disrupting pathways." IUBMB Life **57**(2): 65-72.

Forzan, M., C. Wirblich, et al. (2004). "A Capsid Protein of Nonenveloped Bluetongue Virus exhibits Membrane Fusion Activity." Proc Natl Acad Sci U S A **101**(7): 2100-2105.

French, T. J., S. Inumaru, et al. (1989). "Expression of two related nonstructural proteins of bluetongue virus (BTV) type 10 in insect cells by a recombinant baculovirus: production of polyclonal ascitic fluid and characterization of the gene product in BTV-infected BHK cells." J Virol **63**(8): 3270-8.

Garrus, J. E., U. K. von Schwedler, et al. (2001). "Tsg101 and the vacuolar protein sorting pathway are essential for HIV-1 budding." Cell **107**(1): 55-65.

Ghosh, M. K., M. V. Borca, et al. (2002). "Virus-derived tubular structure displaying foreign sequences on the surface elicit CD4+ Th cell and protective humoral responses." Virology **302**(2): 383-92.

Ghosh, M. K., E. Deriaud, et al. (2002). "Induction of protective antiviral cytotoxic T cells by a tubular structure capable of carrying large foreign sequences." Vaccine **20**(9-10): 1369-77.

Goff, S. P. (2004). "Genetic reprogramming by retroviruses: enhanced suppression of translational termination." Cell Cycle **3**(2): 123-5.

Gorlich, D. and I. W. Mattaj (1996). "Nucleocytoplasmic transport." Science **271**(5255): 1513-8.

Gouet, P., J. M. Diprose, et al. (1999). "The highly ordered double-stranded RNA genome of bluetongue virus revealed by crystallography." Cell **97**(4): 481-90.

Granzow, H., C. Birghan, et al. (1997). "A second form of infectious bursal disease virus-associated tubule contains VP4." J Virol **71**(11): 8879-85.

Gray, S. and F. E. Gildow (2003). "Luteovirus-aphid interactions." Annu Rev Phytopathol **41**: 539-66.

Gray, S. M. and N. Banerjee (1999). "Mechanisms of arthropod transmission of plant and animal viruses." Microbiol Mol Biol Rev **63**(1): 128-48.

Grimes, J. M., J. N. Burroughs, et al. (1998). "The atomic structure of the bluetongue virus core." Nature **395**(6701): 470-8.

Grimes, J. M., J. Jakana, et al. (1997). "An atomic model of the outer layer of the bluetongue virus core derived from X-ray crystallography and electron cryomicroscopy." Structure **5**(7): 885-93.

Guha, S., T. K. Manna, et al. (1998). "Chaperone-like activity of tubulin." J Biol Chem **273**(46): 30077-80.

Guirakhoo, F., J. A. Catalan, et al. (1995). "Adaptation of bluetongue virus in mosquito cells results in overexpression of NS3 proteins and release of virus particles." Arch Virol **140**(5): 967-74.

Hassan, S. H., C. Wirblich, et al. (2001). "Expression and functional characterization of bluetongue virus VP5 protein: role in cellular permeabilization." J Virol **75**(18): 8356-67.

Hassan, S. S. and P. Roy (1999). "Expression and functional characterization of bluetongue virus VP2 protein: role in cell entry." J Virol **73**(12): 9832-42.

He, Y., S. L. Tan, et al. (2001). "Regulation of mRNA translation and cellular signaling by hepatitis C virus nonstructural protein NS5A." J Virol **75**(11): 5090-8.

Heath, C. M., M. Windsor, et al. (2001). "Aggresomes resemble sites specialized for virus assembly." J Cell Biol **153**(3): 449-55.

Hengel, H., U. H. Koszinowski, et al. (2005). "Viruses know it all: new insights into IFN networks." Trends Immunol **26**(7): 396-401.

Hernandez, R., D. Ferreira, et al. (2005). "Single amino acid insertions at the junction of the sindbis virus E2 transmembrane domain and endodomain disrupt virus envelopment and alter infectivity." J Virol **79**(12): 7682-97.

Hewat, E. A., T. F. Booth, et al. (1992). "Structure of bluetongue virus particles by cryoelectron microscopy." J Struct Biol **109**(1): 61-9.

Hewat, E. A., T. F. Booth, et al. (1992). "3-D reconstruction of bluetongue virus tubules using cryoelectron microscopy." J Struct Biol **108**(1): 35-48.

Hill, C. L., T. F. Booth, et al. (1999). "The structure of a cypovirus and the functional organization of dsRNA viruses." Nat Struct Biol **6**(6): 565-8.

Ho, L. J., L. F. Hung, et al. (2005). "Dengue virus type 2 antagonizes IFN-alpha but not IFN-gamma antiviral effect via down-regulating Tyk2-STAT signaling in the human dendritic cell." J Immunol **174**(12): 8163-72.

Huang, Z., V. M. Andrianov, et al. (2001). "Identification of arabidopsis proteins that interact with the cauliflower mosaic virus (CaMV) movement protein." Plant Mol Biol **47**(5): 663-75.

Huang, Z., Y. Han, et al. (2000). "Formation of surface tubules and fluorescent foci in Arabidopsis thaliana protoplasts expressing a fusion between the green fluorescent protein and the cauliflower mosaic virus movement protein." Virology **271**(1): 58-64.

Huismans, H. (1979). "Protein synthesis in bluetongue virus-infected cells." Virology **92**(2): 385-96.

Hyatt, A. D. and B. T. Eaton (1988). "Ultrastructural distribution of the major capsid proteins within bluetongue virus and infected cells." J Gen Virol **69 (Pt 4)**: 805-15.

Hyatt, A. D., B. T. Eaton, et al. (1987). "The grid-cell-culture technique: the direct examination of virus-infected cells and progeny viruses." J Microsc **145 (Pt 1)**: 97-106.

Hyatt, A. D., Y. Zhao, et al. (1993). "Release of bluetongue virus-like particles from insect cells is mediated by BTV nonstructural protein NS3/NS3A." Virology **193**(2): 592-603.

Izumiya, Y., T. J. Ellison, et al. (2005). "Kaposi's sarcoma-associated herpesvirus K-bZIP represses gene transcription via SUMO modification." J Virol **79**(15): 9912-25.

Jennings, D. M. and P. S. Mellor (1987). "Variation in the responses of Culicoides variipennis (Diptera, Ceratopogonidae) to oral infection with bluetongue virus." Arch Virol **95**(3-4): 177-82.

Kar, A. K., N. Iwatani, et al. (2005). "Assembly and intracellular localization of the bluetongue virus core protein VP3." J Virol **79**(17): 11487-95.

Kar, A. K. and P. Roy (2003). "Defining the structure-function relationships of bluetongue virus helicase protein VP6." J Virol **77**(21): 11347-56.

Kibenge, F. S., B. Qian, et al. (1997). "Infectious bursal disease virus polyprotein processing does not involve cellular proteases." Arch Virol **142**(12): 2401-19.

Kikonyogo, A., F. Bouamr, et al. (2001). "Proteins related to the Nedd4 family of ubiquitin protein ligases interact with the L domain of Rous sarcoma virus and are required for gag budding from cells." Proc Natl Acad Sci U S A **98**(20): 11199-204.

Kobayashi, K., S. Tsuge, et al. (2002). "The cauliflower mosaic virus virion-associated protein is dispensable for viral replication in single cells." J Virol **76**(18): 9457-64.

Kuyumcu-Martinez, N. M., M. E. Van Eden, et al. (2004). "Cleavage of poly(A)-binding protein by poliovirus 3C protease inhibits host cell translation: a novel mechanism for host translation shutoff." Mol Cell Biol **24**(4): 1779-90.

Larke, N., A. Murphy, et al. (2005). "Induction of human immunodeficiency virus type 1-specific T cells by a bluetongue virus tubule-vectored vaccine prime-recombinant modified virus Ankara boost regimen." J Virol **79**(23): 14822-33.

Lazarowitz, S. G. and R. N. Beachy (1999). "Viral movement proteins as probes for intracellular and intercellular trafficking in plants." Plant Cell **11**(4): 535-48.

Lee, B. H., K. Yoshimatsu, et al. (2003). "Association of the nucleocapsid protein of the Seoul and Hantaan hantaviruses with small ubiquitin-like modifier-1-related molecules." Virus Res **98**(1): 83-91.

Lee, J. W. and P. Roy (1986). "Nucleotide sequence of a cDNA clone of RNA segment 10 of bluetongue virus (serotype 10)." J Gen Virol **67 (Pt 12)**: 2833-7.

Leh, V., E. Jacquot, et al. (2001). "Interaction between the open reading frame III product and the coat protein is required for transmission of cauliflower mosaic virus by aphids." J Virol **75**(1): 100-6.

Lejal, N., B. Da Costa, et al. (2000). "Role of Ser-652 and Lys-692 in the protease activity of infectious bursal disease virus VP4 and identification of its substrate cleavage sites." J Gen Virol **81**(Pt 4): 983-92.

Lepault, J., I. Petitpas, et al. (2001). "Structural polymorphism of the major capsid protein of rotavirus." Embo J **20**(7): 1498-507.

Lewandowski, D. J. and S. Adkins (2005). "The tubule-forming NSm protein from Tomato spotted wilt virus complements cell-to-cell and long-distance movement of Tobacco mosaic virus hybrids." Virology **342**(1): 26-37.

Li, Y., Y. M. Bao, et al. (2004). "Rice dwarf phytoreovirus segment S6-encoded nonstructural protein has a cell-to-cell movement function." J Virol **78**(10): 5382-9.

Lin, R. J., C. L. Liao, et al. (2004). "Blocking of the alpha interferon-induced Jak-Stat signaling pathway by Japanese encephalitis virus infection." J Virol **78**(17): 9285-94.

Ludwig, G. V., J. P. Kondig, et al. (1996). "A putative receptor for Venezuelan equine encephalitis virus from mosquito cells." J Virol **70**(8): 5592-9.

Lyles, D. S. (2000). "Cytopathogenesis and inhibition of host gene expression by RNA viruses." Microbiol Mol Biol Rev **64**(4): 709-24.

Lymperopoulos, K., C. Wirblich, et al. (2003). "Sequence specificity in the interaction of Bluetongue virus non-structural protein 2 (NS2) with viral RNA." J Biol Chem **278**(34): 31722-30.

Maeda, A., B. H. Lee, et al. (2003). "The intracellular association of the nucleocapsid protein (NP) of hantaan virus (HTNV) with small ubiquitin-like modifier-1 (SUMO-1) conjugating enzyme 9 (Ubc9)." Virology **305**(2): 288-97.

Manna, T., T. Sarkar, et al. (2001). "Chaperone-like activity of tubulin. binding and reactivation of unfolded substrate enzymes." J Biol Chem **276**(43): 39742-7.

Martin-Serrano, J., T. Zang, et al. (2001). "HIV-1 and Ebola virus encode small peptide motifs that recruit Tsg101 to sites of particle assembly to facilitate egress." Nat Med **7**(12): 1313-9.

Martinez-Costas, J., G. Sutton, et al. (1998). "Guanylyltransferase and RNA 5'-triphosphatase activities of the purified expressed VP4 protein of bluetongue virus." J Mol Biol **280**(5): 859-66.

Mikhailov, M., K. Monastyrskaya, et al. (1996). "A new form of particulate single and multiple immunogen delivery system based on recombinant bluetongue virus-derived tubules." Virology **217**(1): 323-31.

Miller, C. L. and D. J. Pintel (2002). "Interaction between parvovirus NS2 protein and nuclear export factor Crm1 is important for viral egress from the nucleus of murine cells." J Virol **76**(7): 3257-66.

Mishra, R. K., S. S. Jatiani, et al. (2004). "Dynamin interacts with members of the sumoylation machinery." J Biol Chem **279**(30): 31445-54.

Monastyrskaya, K., T. Booth, et al. (1994). "Mutation of either of two cysteine residues or deletion of the amino or carboxy terminus of nonstructural protein NS1 of bluetongue virus abrogates virus-specified tubule formation in insect cells." J Virol **68**(4): 2169-78.

Monastyrskaya, K., E. A. Gould, et al. (1995). "Characterization and modification of the carboxy-terminal sequences of bluetongue virus type 10 NS1 protein in relation to tubule formation and location of an antigenic epitope in the vicinity of the carboxy terminus of the protein." J Virol **69**(5): 2831-41.

Mortola, E., R. Noad, et al. (2004). "Bluetongue Virus Outer Capsid proteins are Suffcient to Trigger Apoptosis in Mammalian Cells." J Virol **78**(6): 2875-2883.

Munoz-Jordan, J. L., G. G. Sanchez-Burgos, et al. (2003). "Inhibition of interferon signaling by dengue virus." Proc Natl Acad Sci U S A **100**(24): 14333-8.

Munoz, M. L., A. Cisneros, et al. (1998). "Putative dengue virus receptors from mosquito cells." FEMS Microbiol Lett **168**(2): 251-8.

Nakata, T., K. Sobue, et al. (1990). "Conformational change and localization of calpactin I complex involved in exocytosis as revealed by quick-freeze, deep-etch electron microscopy and immunocytochemistry." J Cell Biol **110**(1): 13-25.

Nason, E. L., R. Rothagel, et al. (2004). "Interactions between the inner and outer capsids of bluetongue virus." J Virol **78**(15): 8059-67.

Noah, D. L., K. Y. Twu, et al. (2003). "Cellular antiviral responses against influenza A virus are countered at the posttranscriptional level by the viral NS1A protein via

its binding to a cellular protein required for the 3' end processing of cellular pre-mRNAS." Virology **307**(2): 386-95.

Ono, A. and E. O. Freed (2004). "Cell-type-dependent targeting of human immunodeficiency virus type 1 assembly to the plasma membrane and the multivesicular body." J Virol **78**(3): 1552-63.

Owens, R., C. Limn, et al. (2004). "Role of an Arboviral Nonstructural Protein in Cellular Pathogenesis and Virus Release." J Virol **In Press**.

Palacios, I., M. Drucker, et al. (2002). "Cauliflower mosaic virus is preferentially acquired from the phloem by its aphid vectors." J Gen Virol **83**(Pt 12): 3163-71.

Palukaitis, P., M. J. Roossinck, et al. (1992). "Cucumber mosaic virus." Adv Virus Res **41**: 281-348.

Patmanidi, A. L., R. D. Possee, et al. (2003). "Formation of P10 tubular structures during AcMNPV infection depends on the integrity of host-cell microtubules." Virology **317**(2): 308-20.

Perbal, M. C., C. L. Thomas, et al. (1993). "Cauliflower mosaic virus gene I product (P1) forms tubular structures which extend from the surface of infected protoplasts." Virology **195**(1): 281-5.

Pornillos, O., J. E. Garrus, et al. (2002). "Mechanisms of enveloped RNA virus budding." Trends Cell Biol **12**(12): 569-79.

Prasad, B. V., R. Rothnagel, et al. (1996). "Visualization of ordered genomic RNA and localization of transcriptional complexes in rotavirus." Nature **382**(6590): 471-3.

Precious, B., K. Childs, et al. (2005). "Simian virus 5 V protein acts as an adaptor, linking DDB1 to STAT2, to facilitate the ubiquitination of STAT1." J Virol **79**(21): 13434-41.

Precious, B., D. F. Young, et al. (2005). "In vitro and in vivo specificity of ubiquitination and degradation of STAT1 and STAT2 by the V proteins of the paramyxoviruses simian virus 5 and human parainfluenza virus type 2." J Gen Virol **86**(Pt 1): 151-8.

Protopopova, E. V., A. D. Khusainova, et al. (1996). "[Preparation and study of properties of anti-idiotypic antibodies, carrying hemagglutinating paratopes of tick-borne encephalitis virus on their surface]." Vopr Virusol **41**(2): 50-3.

Purse, B. V., P. S. Mellor, et al. (2005). "Climate change and the recent emergence of bluetongue in Europe." Nat Rev Microbiol **3**(2): 171-81.

Quant-Russell, R. L., M. N. Pearson, et al. (1987). "Characterization of baculovirus p10 synthesis using monoclonal antibodies." Virology **160**(1): 9-19.

Raiborg, C., T. E. Rusten, et al. (2003). "Protein sorting into multivesicular endosomes." Curr Opin Cell Biol **15**(4): 446-55.

Ramadevi, N., N. J. Burroughs, et al. (1998). "Capping and methylation of mRNA by purified recombinant VP4 protein of bluetongue virus." Proc Natl Acad Sci U S A **95**(23): 13537-42.

Ramadevi, N. and P. Roy (1998). "Bluetongue virus core protein VP4 has nucleoside triphosphate phosphohydrolase activity." J Gen Virol **79 (Pt 10)**: 2475-80.

Reyes-del Valle, J. and R. M. del Angel (2004). "Isolation of putative dengue virus receptor molecules by affinity chromatography using a recombinant E protein ligand." J Virol Methods **116**(1): 95-102.

Risco, C., J. R. Rodriguez, et al. (2002). "Endoplasmic reticulum-Golgi intermediate compartment membranes and vimentin filaments participate in vaccinia virus assembly." J Virol **76**(4): 1839-55.

Rodriguez-Lecompte, J. C., R. Nino-Fong, et al. (2005). "Infectious bursal disease virus (IBDV) induces apoptosis in chicken B cells." Comp Immunol Microbiol Infect Dis **28**(4): 321-37.

Roy, P. (2005). "Bluetongue virus proteins and particles and their role in virus entry, assembly, and release." Adv Virus Res **64**: 69-123.

Roy, P. and B. M. Gorman (1990). Bluetongue virus. Berlin ; London, Springer-Verlag.

Sager, P. R. (1989). "Cytoskeletal effects of acrylamide and 2,5-hexanedione: selective aggregation of vimentin filaments." Toxicol Appl Pharmacol **97**(1): 141-55.

Salas-Benito, J. S. and R. M. del Angel (1997). "Identification of two surface proteins from C6/36 cells that bind dengue type 4 virus." J Virol **71**(10): 7246-52.

Stauber, N., J. Martinez-Costas, et al. (1997). "Bluetongue virus VP6 protein binds ATP and exhibits an RNA-dependent ATPase function and a helicase activity that catalyze the unwinding of double-stranded RNA substrates." J Virol **71**(10): 7220-6.

Stavolone, L., M. E. Villani, et al. (2005). "A coiled-coil interaction mediates cauliflower mosaic virus cell-to-cell movement." Proc Natl Acad Sci U S A **102**(17): 6219-24.

Stefanovic, S., M. Windsor, et al. (2005). "Vimentin rearrangement during African swine fever virus infection involves retrograde transport along microtubules and phosphorylation of vimentin by calcium calmodulin kinase II." J Virol **79**(18): 11766-75.

Szczepanowski, R. H., R. Filipek, et al. (2005). "Crystal structure of a fragment of mouse ubiquitin-activating enzyme." J Biol Chem **280**(23): 22006-11.

Thepparit, C. and D. R. Smith (2004). "Serotype-specific entry of dengue virus into liver cells: identification of the 37-kilodalton/67-kilodalton high-affinity laminin receptor as a dengue virus serotype 1 receptor." J Virol **78**(22): 12647-56.

Thomas, C. P., T. F. Booth, et al. (1990). "Synthesis of bluetongue virus-encoded phosphoprotein and formation of inclusion bodies by recombinant baculovirus in insect cells: it binds the single-stranded RNA species." J Gen Virol **71 (Pt 9)**: 2073-83.

Ulmanen, I., B. A. Broni, et al. (1981). "Role of two of the influenza virus core P proteins in recognizing cap 1 structures (m7GpppNm) on RNAs and in initiating viral RNA transcription." Proc Natl Acad Sci U S A **78**(12): 7355-9.

Urakawa, T., D. G. Ritter, et al. (1989). "Expression of largest RNA segment and synthesis of VP1 protein of bluetongue virus in insect cells by recombinant baculovirus: association of VP1 protein with RNA polymerase activity." Nucleic Acids Res **17**(18): 7395-401.

Urakawa, T. and P. Roy (1988). "Bluetongue virus tubules made in insect cells by recombinant baculoviruses: expression of the NS1 gene of bluetongue virus serotype 10." J Virol **62**(11): 3919-27.

van den Heuvel, J. F., S. A. Hogenhout, et al. (1999). "Recognition and receptors in virus transmission by arthropods." Trends Microbiol **7**(2): 71-6.

Van Oers, M. M., J. T. Flipsen, et al. (1994). "Specificity of baculovirus p10 functions." Virology **200**(2): 513-23.

Van Regenmortel, M. H. V. (2000). Virus taxonomy : classification and nomenclature of viruses : seventh report of the International Committee on Taxonomy of Viruses. San Diego, Calif. ; London, Academic.

Wang, K. S., R. J. Kuhn, et al. (1992). "High-affinity laminin receptor is a receptor for Sindbis virus in mammalian cells." J Virol **66**(8): 4992-5001.

Wang, X., M. Li, et al. (2000). "Influenza A virus NS1 protein prevents activation of NF-kappaB and induction of alpha/beta interferon." J Virol **74**(24): 11566-73.

Whetter, L. E., D. H. Gebhard, et al. (1990). "Temporal appearance of structural and nonstructural bluetongue viral proteins in infected cells, as determined by immunofluorescence staining and flow cytometry." Am J Vet Res **51**(8): 1174-9.

Williams, G. V., D. Z. Rohel, et al. (1989). "A cytopathological investigation of Autographa californica nuclear polyhedrosis virus p10 gene function using insertion/deletion mutants." J Gen Virol **70 (Pt 1)**: 187-202.

Wirblich, C., B. Bhattacharya, et al. (2006). "Nonstructural Protein 3 of Bluetongue Virus Assists Virus Release by Recruiting ESCRT-I Protein Tsg101." J Virol **80**(1): 460-73.

Ye, Y., Y. Shibata, et al. (2005). "Inaugural Article: Recruitment of the p97 ATPase and ubiquitin ligases to the site of retrotranslocation at the endoplasmic reticulum membrane." Proc Natl Acad Sci U S A **102**(40): 14132-8.

Young, M. J. and S. A. Filichkin (1999). "Luteovirus interactions with aphid vector cellular components." Trends Microbiol **7**(9): 346-7.

Zhao, Y., C. Thomas, et al. (1994). "Deletion and mutational analyses of bluetongue virus NS2 protein indicate that the amino but not the carboxy terminus of the protein is critical for RNA-protein interactions." J Virol **68**(4): 2179-85.